The 11th Conference
on Functional and Nanostructured Materials

FNMA'14

1–5 September 2014
Camerino, Italy

ABSTRACT BOOK

TITLE

The 11th Conference on Functional and Nanostructured Materials – FNMA'14

1–5 September 2014, Camerino, Italy – Abstract Book

EDITORS

Roberto Gunnella and Jarosław Rybicki

TYPESETTING USING TEX

BOP, www.bop.com.pl

TASK PUBLISHING 2014
GDAŃSK

ISBN 978-83-937979-0-5

FNMA'14 – The 11th Conference on Functional and Nanostructured Materials

Organizers

University of Camerino, Italy
Department of Solid State Physics, Faculty of Physics, University of Athens, Greece
Department of Solid State Physics, Gdansk University of Technology, Poland
Institute of Molecular Physics, Polish Academy of Sciences, Poznan, Poland
Institute of Physics, Faculty of Mechanical Engineering and Mechatronic, West Pomeranian University of Technology, Szczecin, Poland
Lublin University of Technology, Poland
University of Zielona Gora, Poland
PWSZ im. Prezydenta St. Wojciechowskiego, Kalisz, Poland

In cooperation with:

TASK – Academic Computer Centre in Gdansk, Poland
Poznan Supercomputing and Networking Center, Poland
Intel Corporation Polish Physical Society

Honorary Chairmen

R. Marassi (Camerino, Italy)
G. J. Papadopoulos (Athens, Greece)

Scientific Committee

A. Alderson (Bristol, UK) • F. J. Baltá-Calleja (Madrid, Spain) • J. Barnaś (Poznan, Poland) • J. Bernholc (Raleigh, USA) • X. M. Duan (Beijing, China) J. Felba (Wroclaw, Poland) • J. Grima (Msida, Malta) • B. Grzybowski (Evanston, USA) • R. Gunnella (Camerino, Italy) – Chairman • W. G. Hoover (Ruby Valley, USA) A. B. Kolomeisky (Houston, USA) • A. A. Kornyshev (London, UK) • V. Likodimos (Athens, Greece) • H. Mizuta (Southampton, UK) • A. Morawski (Szczecin, Poland) S. Mudry (Lviv, Ukraine) • B. Padlyak (Lviv, Ukraine) • V. Radmilovic (Berkeley, USA) • W. Sadowski (Gdansk, Poland) • F. Scarpa (Bristol, UK) K. Schulte (Hamburg, Germany) • T. Tsuboi (Kyoto, Japan) • K. W. Wojciechowski (Poznan, Poland) – Co-Chairman • N. I. Zheludev (Southampton, UK)

Programme Committee

A. Cricenti (Rome, Italy) • A. Di Cicco (Camerino, Italy) • M. Dudek (Zielona Gora, Poland) • N. Gouskos (Athens, Greece) – Co-Chairman • R. Gunnella (Camerino, Italy) – Co-Chairman • W. Kempinski (Poznan, Poland) S. Kruchinin (Kiev, Ukraine) • A. Marcelli (Frascati, Italy) • B. Maruszewski (Poznan, Poland) • U. Narkiewicz (Szczecin, Poland) • J. Olchowik (Lublin, Poland) • J. Rybicki (Gdansk, Poland) – Co-Chairman • J. Typek (Szczecin, Poland)

Organizing Committee

R. Gunnella (Camerino, Italy) – Chairman • N. Gouskos (Athens, Greece) M. Nakonieczny (Gdansk, Poland) • F. Nobili (Camerino, Italy) • A. Rybicka (Gdansk, Poland) • J. Rybicki (Gdansk, Poland) • Sz. Winczewski (Gdansk, Poland) – Secretary • K. W. Wojciechowski (Poznan, Poland)

CONTENTS

LECTURES

POSTERS

LECTURES

Molecular dynamics study on shock-wave simulations in porous media

W. Alda

AGH University of Science and Technology, Department of Computer Science
Al. Mickiewicza 30, 30-050 Krakow, Poland

It is commonly known that porous materials can absorb energy and efficiently attenuate shock waves resulting from explosions. In this study such behavior of porous materials is examined at the nano-structure level. The molecular dynamics method was adopted to simulate a classical system with a setup including a moving piston, gas volume, porous material and a solid target. Gas particles interact via the short range Lennard-jones type potential, while porous materials assume more realistic interactions with the embedded atom method. The results of the simulations show how the presence of a porous material in front of the target, as well as its thickness and porosity structure can reduce the force magnitude applied to the wall. Space-time distributions of temperature, velocity, density and pressure are presented and analyzed.

An investigation of the mechanical properties of a high pressure silica polymorph

K. M. Azzopardi[1], J.-P. Brincat[1], J. N. Grima[1,2], R. Gatt[1]

[1] *Metamaterials Unit, Faculty of Science, University of Malta Msida MSD 2080, Malta*

[2] *Chemistry Department, Faculty of Science, University of Malta Msida MSD 2080, Malta*

The current theoretical study makes use of DFT methods to investigate the anomalous behaviour of a high pressure silica polymorph. In the initial analysis we note that the crystal has a negative Poisson's ratio in the (001) plane under relatively low pressure, while also providing a strong validation for the method by comparing the off-axis Poisson's ratio with data available from literature. We also outline the mechanisms responsible for this anomalous property.

In the second part of our study, the changes in Poisson's ratio upon increasing pressure are investigated. Through our calculations, we have found that the auxeticity in the (001) plane tends to decrease, i.e. becomes more positive. Concurrently the Poisson's ratio in both the (100) and the (010) planes tends to decrease in specific off-axis directions, ultimately achieving significantly negative Poisson's ratios at elevated pressures. We have also measured the geometrical changes which result in the negative Poisson's ratio at elevated pressures to enable a description of the underlying mechanism.

Self-sustaining α-ε phase transition in iron triggered by small magnetic perturbation

F. Baudelet[1], L. Nataf[1], S. Pascarelli[2], O. Mathon[2], J. P. Itié[1]

[1] *Synchrotron SOLEIL – L'Orme des Merisiers Saint-Aubin 91192 Gif-sur-Yvette, France*

[2] *E.S.R.F. 6 Rue Jules Horowitz, 38000 Grenoble, France*

After decades of controversies about the role of magnetism in the martensitic transition of iron [1], we present experimental evidence that a small change of the magnetic order, induced by pressure, is sufficient to induce a structural change. Magnetic driven reversible transition under pressure for α-ε phases in iron is investigated by X-ray absorption spectroscopy.

We have investigated the bcc to hcp phase transition in iron metal for increasing and decreasing pressure by XAS and XMCD. Both structural and magnetic transitions are sharp and present an hysteresis, in agreement with the first order nature of the transition. We confirm the triggering role of magnetism for the bcc to hcp transition and also for the reverse transition. In addition, by tuning the pressure just at the transition onset, we were able to follow the time-dependence evolution of the magnetic and structural transitions. At constant pressure and as a function of time, the XMCD signal fist decreases slightly, triggering the bcc-hcp structural transition. The structural transition then evolves very rapidly (faster than the magnetic transition) within the first two hours, and is achieved after 21 hours without any additional pressure, in agreement with a self-sustaining transition scheme [2]. After an abrupt decrease followed by a slower attenuation, a residual XMCD signal continues to persist, corresponding to a reduced ferromagnetic component in agreement with the theoretically predicted role of complex magnetic structures for some transition paths [3]. In the pure hcp phase, a small ferromagnetic component survives at least 2 days at fixed pressure, and is killed by a small pressure increase.

References

[1] A. Monza, A. Meffre, F. Baudelet, J. P. Rueff, M. D'Astuto, P. Munsch, S. Huotari, S. Lachaize, B. Chaudret, A. Shukla 2011 *Phys. Rev. Lett.* **106**, 247201

[2] B. Dupé, B. Amadon, Y. P. Pellegrini, C. Denoual 2013 *Phys. Rev. B* **87**, 024103

[3] S. Mankovsky, S. Polesya, H. Ebert, W. Bensch, O. Mathon, S. Pascarelli, J. Minar 2013 *Phys. Rev. B* **88**, 184108

Electrical conductivity and relaxation in oxide glasses

R. J. Barczyński, L. Murawski

Department of Solid State Physics, Faculty of Applied Physics and Mathematics
Gdansk University of Technology
Narutowicza 11/12, 80-233 Gdansk, Poland

A concise survey of electrical conductivity and relaxation processes in glasses exhibiting electronic and electronic-ionic conductivity mechanisms is presented. DC and AC electrical conductivity data on a range of transition metal oxide (TMO) glasses shows that a polaronic model of conductivity is generally applicable. It is shown that both AC and DC conductivity processes are due to the same mechanism. By applying a scaling procedure it is possible to obtain a universal conductivity curve and find the relation between AC and DC activation energy. A complex plot of an electric modulus gives a simple scaling analysis method.

A classification of mixed electronic-ionic behavior in a TMO containing alkali ions was performed on the basis of impedance spectroscopy. A deep minimum of conductivity at a certain content of alkali ions was observed in glasses where TMO was a glass former. Two different behaviors could be distinguished in glasses where TMO was a glass network modifier. In glasses containing iron oxide electrical properties were only slightly influenced by alkali ions. A mixed electronic-ionic conduction was observed in glasses containing copper oxides.

It is shown that internal friction is closely related to the electrical properties. In electronic and ionic conducting glasses internal friction spectra reveal a peak the activation energy of which is identical as for the DC conductivity. In mixed electronic-ionic conducting glasses the internal friction spectra reveal two peaks, which are attributed to the electronic hopping and the alkali ion migration.

Statistical physics of complexity by scanning nano X-ray diffraction: a new method probing mixed k-space real space unveiling functional scale free distributions in complex matter

A. Bianconi[1,2], G. Campi[2]

[1] *Rome International Center for Materials Science Superstripes, RICMASS*
Via dei Sabelli 119/A, 00185 Roma, Italy

[2] *Istituto di Cristallografia, Consiglio Nazionale delle Ricerche CNR*
Via Salaria, Roma, Italy

There has been a growing interest to investigate the idea that the lack of a scientific agreement on the mechanism of high temperature superconductivity is due to the lack of information on the lattice structure. While it is known that lattice complexity due to disorder and strain induces exceptional electronic and magnetic functionality in transition metal oxides [1] (like in colossal magnetoresistance oxides, and on the two dimensional electron gas at the oxides interface) its role in the emergence of high temperature superconductivity has been neglected by the majority of authors for more than 25 years. There exists ample evidence from local bulk probes that the local lattice structure in cuprates exhibits significant local deviations from the average crystal structure [2] making them a particular case of nanostructured materials which require novel experimental approaches to unveil features of inhomogeneity at multiple scales

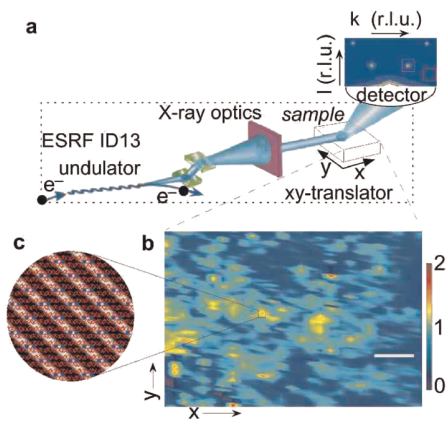

Figure 1: Scanning nano XRD set up to unveil scale free fluctuations in doped perovskites; from [5]

from nanoscale to micron-scale [3]. Recently there has been growing evidence that superconducting, magnetic, charge ordered phases form intertwined complex architectures [4]. In this new paradigm superconductivity emerges in a percolation regime of nanoscale puddles with density fluctuation up to the micron scale as observed by scanning micro X-ray diffraction [5–7]. There is a high interest in the search for information on the spatial statistical distribution of superconducting units since it is needed to test theories of percolative superconductivity [8]. We will discuss the case of both LSCO [9] and Hg1201 [10]. We present unique information on the variation of the statistical distribution of local lattice fluctuations in particular for the prediction of an increasing fat tail of the distribution with increasing critical temperature.

References

[1] P. B. Littlewood 2012 *Disorder and Strain-Induced Complexity in Functional Materials* Springer, Berlin Heidelberg, 95
[2] T. Egami and S. J. L. Billinge 2003 *Underneath the Bragg peaks: structural analysis of complex materials* Elsevier
[3] S. J. L. Billinge *et al.* 2007 *Science* **316**, 561
[4] A. Bianconi 2013 *Nature Phys.* **9**, 536
[5] M. Fratini *et al.* 2010 *Nature* **466**, 841
[6] N. Poccia *et al.* 2012 *Proc. Nat. Acad. Scie.* **109**, 15685
[7] A. Ricci *et al.* 2013 *Scientific Reports* **3**, 238
[8] G. Bianconi 2013 *Europhys. Lett.* **101**, 26003
[9] A Bianconi *et al.* 1996 *Phys. Rev. Lett.* **76**, 3412
[10] A.Lanzara *et al.* 1999 *Phys. Rev. B* **59**, 3851

Metal–oxide glass composites as potential materials for thermoelectric devices

B. Bochentyn, J. Karczewski, M. Gazda, B. Kusz

Department of Solid State Physics, Faculty of Applied Physics and Mathematics
Gdansk University of Technology
Narutowicza 11/12, 80-233 Gdansk, Poland

The continuously increasing world demand for energy drives various investigations in the field of effective energy management. One of them is the scavenging of waste heat with thermoelectric generators. In general, every thermoelectric device consists of two types of conducting materials. One of them is a p-type conductor (containing holes) and the other is an n-type conductor (containing electrons). They are wired electrically in series and thermally in parallel. When electric current is applied to the junction, the free carriers move away from the junction and cool it, what is known as the Peltier effect. If a temperature gradient is applied, the mobile charge carriers at the hot end tend to diffuse to the cold end producing an electrostatic potential (V). This is known as the Seebeck effect.

Certain parameters should be determined to estimate the thermoelectric material usability for both heat generation and cooling: the Seebeck coefficient (α), electrical conductivity (δ) and thermal conductivity (κ). Thus, the dimensionless figure of merit is defined: $ZT = \alpha^2 T\delta/\kappa$ [1]. The higher the Seebeck coefficient and electrical conductivity of the material and the lower the thermal conductivity, the better is the material from the point of view of thermoelectric applications. Glasses exhibit some of the lowest lattice thermal conductivities. In order to make glasses useful for thermoelectric devices, they should be modified to obtain a kind of 'phonon-glass electron-crystal [2]. Such composite materials can be obtained by heating oxide glasses in a hydrogen atmosphere (reduction process). This procedure causes reduction of metal ions and formation of metal grains both in an amorphous glass matrix and on the glass surface. If a certain critical grain concentration is achieved, electron tunneling between grains becomes possible. Further reduction leads to the connecting of metal grains and to formation of a continuous, metallic layer on the surface of the glass. Thus, an increase in the surface electrical conductivity, even of several orders of magnitude, is observed [3]. In this work some results indicating a possibility of applying reduced oxide glasses in thermoelectric devices will be shown.

Acknowledgements
This work was partially supported by the National Science Center under grant No. NCN2012/05/B/ST3/02816/

References

[1] DiSalvo F J 1999, *Science* **285** 703
[2] Snyder J, Toberer J S 2008, *Nature Materials* **7** 105
[3] Gackowska J, Gazda M, Trzebiatowski K, Kusz B 2008, *J. Non-Cryst. Solids* **354** 4319

Electrospun electrolytes and electrodes for Li-ion batteries

F. Croce

Università "G.d'Annunzio" Chieti-Pescara, Italy

The quest for more efficient and low environmentally impacting energy conversion and storage technologies has become a priority for modern society. In particular, rechargeable, high capacity and high power electric energy storage systems, if developed, would play a central role in accelerating the transition toward an electric transportation economy, which, in turn, would dramatically reduce the risks associated with the burning of fossil fuels. To this purpose, 'ad hoc' engineered functional materials that join improved electrochemical properties with a scalable preparation process for electrodes and electrolytes are needed. The most promising of such materials are those with nanometric-scale dimensions, including nanoparticles and nanofibers. These materials, having a very high surface to volume ratio, show enhanced bulk charge transport and faster electrodic reaction rates. Nowadays, new methods have emerged for manipulation, assembly and characterization of nanostructured materials, particularly regarding functional electrodes and electrolytes based on nanofibers. Among the methods for generating nanofibrous structures, electrospinning is a top-down approach proved to be simple, cost effective and versatile allowing the fabrication of polymeric and inorganic nanofibers in a scalable process. Electrospinning is based on the application of an electric field to a drop of a viscous solution on the tip of a spinneret. The electric field elongates the drop to form a conical shape known as the Taylor cone. For an electric field critical value, the repulsive electrical

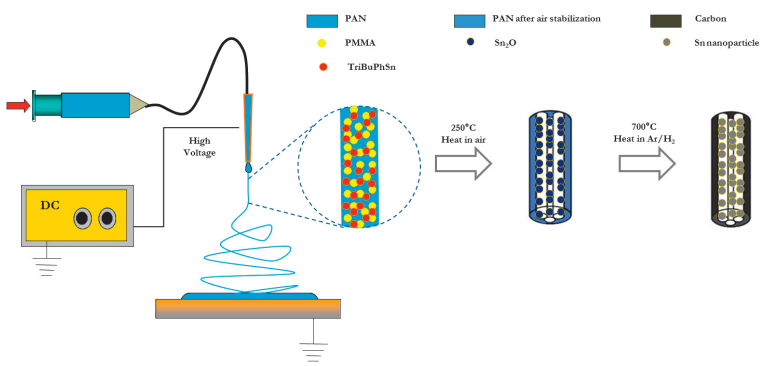

Figure 1: Scheme of experiment

forces between the charges in the fluid overcome the surface tension of the drop and a charged jet of the solution is ejected from the tip of the Taylor cone. The jet becomes unstable and rapidly whipping leading to the evaporation of the solvent and the formation of dry, continuous, ultra-thin fibers on the collector (Figure 1). The collected electrospun mats present peculiar properties, such as a very high surface to volume ratio, low density, high pore volume and remarkable mechanical strength.

In this presentation, the electrospinning technique will be illustrated particularly regarding the optimization of the system and process parameters, which mostly influence the electrospun nanofibers. The characteristics of some gel electrolytes formed by electrospun polymeric separators will be discussed. Finally, the preparation by co-electrospinning followed by air stabilization and carbonization of nanosized tin particles embedded in electrically conducting porous multichannel carbon microtubes (Sn-PMCMT) will be described (Figure 1). Composite electrodes prepared using Sn-PMCMT powders exhibit a superior rate capability and cycle life in cell tests at room temperature.

Influence of substrate morphology in pentacene thin films grown on Si(100) modified surfaces

F. D'Amico[1], M. Passacantando[2], L. Ottaviano[2], R. Gunnella[3]

[1] *Sincrotrone Trieste*
Strada Statale 14 km 163.5, Area Science Park, I-34012 Trieste, Italy

[2] *CNISM – Department of Physics, L'Aquila University*
Via Vetoio 67010 Coppito, L'Aquila (AQ), Italy

[3] *CNISM – Universita' di Camerino*
Via Madonna delle Carceri 62032 Camerino (MC), Italy

Pentacene (Pn), a chain-like aromatic molecule composed of five fused aromatic rings, is one of the most promising organic semiconducting materials [1]. This is due to its ability to pack into a highly ordered crystal structure, with an optimal π orbital overlap, which leads to high electrical mobility [2]. Since the first interfacial layer plays an important role in the growth of Pn on inorganic substrates, most research is directed to understand the adsorption of the first monolayer and its influence on the subsequent growth of the Pn multilayer film. A recent work has demonstrated that on metallic surfaces Pn molecules interact strongly with the surface valence charge density near the Fermi level, leading to a planar adsorption geometry, while, when such valence charge density is reduced, the molecule-molecule interaction becomes stronger than the molecule-substrate interaction [3]. As a consequence, Pn molecules lie perpendicular to the surface forming several dendritic layers [4]. Several experiments were performed to study the growth of Pn on Si(100)-2×1 surfaces [2,5,6], finding that a similar mechanism is operating on semiconductors, with the first pentacene layer lying flat on the surface, while further layers, about 1.5 nm high, pack themselves vertically forming a molecular solid, as measured by diffraction experiments [7,8].

It is interesting to investigate if modified Si(100)-2×1 surfaces are able to lead to different results with respect to the clean Si surface. For instance, we wonder if a Pn film could grow more ordered on a Si surface kept at temperatures higher (70°C) than RT. Moreover, it must be recognized if the morphology of the buffered substrate can influence the film morphology. It is reasonably expected that the morphology is deeply influenced in the growth of a Pn thin film with a thickness comparable with the superficial roughness. However it is intriguing to investigate what happens when the substrate roughness results to be negligible with respect to the Pn film thickness.

Modifications of the growth behavior using a buffered substrate were found by Meyer et al. [4]. They observed that a dead-time before nucleations of Pn dendritic layers, due to chemisorption with Si dimers, was strongly reduced if one ML of cyclohexene was used to saturate the Si dimer dangling bonds before the Pn deposition. It would be interesting to know if similar interactions of Pn molecules with unsaturated C=C bonds are useful to grow a smoother, or less distorted, interface with Si

and consequently to attain a higher degree of order on the molecular film. In fact, in a recent work, Wakatsuchi et al. [9] demonstrated that a different morphology (factor ten larger islands with respect to the growth on SiO_2) occurred, if Pn films were grown on a Si(100) surface previously functionalized with a 1,4-Cyclohexadiene (CHD) monolayer. However, the reasons for such behavior were not explained.

The molecule of 1,4-CHD is composed of a hexagonal C ring with two double C=C bonds on the opposite sides of the molecule. Several experimental works have confirmed that the CHD molecule chemisorbs on the Si(100)-2×1 surface forming di-σ bonding to the silicon dimers using one of the two π bonds [10–13] leaving the remaining π bond available for further manipulation.

With the purpose of understanding how modifications in the substrate can influence the film characteristics we have studied the Pn growth on Si(100) surfaces clean (2×1 reconstruction), oxidized and saturated with 1,4-CHD. This study was performed using Auger electron spectroscopy, corroborated by AFM and XRD measurements. We have verified how the substrate can influence the morphology of a Pn thin film. This was obtained analyzing the morphology of Pn films grown on SiO_2/Si(100) (pristine native silicon oxide) and on a passivated CHD/Si(100) substrate.

The growth of the Pn films and the subsequent AES analysis were performed in an ultrahigh (UHV) vacuum chamber with a base pressure of 3×10^{-10} Torr. A Si(100) sample was carefully outgassed and resistively heated in the UHV chamber up to 1200°C to remove the silicon oxide and all the contaminants from the surface. Pn was dosed in vacuum by sublimation from a quartz crucible. A tungsten wire was used to resistively heat the crucible and the temperature was monitored by an internal thermocouple. By tuning the electric current intensity in the tungsten wire, it was possible to keep the Pn deposition rate in the range of 0.4 Å/s. During the procedure the base pressure in the evaporation chamber was kept below 2×10^{-9} Torr. Pn thin film thickness was monitored by a quartz microbalance placed close to the sample. Functionalization of the Si surface is obtained trough pre-deposition of 1,4-CHD, following the procedure performed on [12]. Briefly, commercial 1,4-CHD was purified by several freeze-pump-taw cycles. After this treatment, gaseous molecules were introduced into the UHV chamber using a leak valve, with the chamber pressure in the range of $1 \div 2 \times 10^{-8}$ Torr. Saturation is obtained after a $1 \div 2$ L dose.

The AES and EELS spectra were recorded using a single pass cylindrical mirror analyzer (CMA) in the first derivative mode, 2 V peak-to-peak modulation and a primary electron beam energy of 1000 eV and 500 eV, respectively.

XRD measurements were performed in air using a Siemens 5000 diffractometer with an unmonochromatized source (CuK_α radiation, $\lambda = 1.5406$ Å). The measurements were performed in reflection geometry using symmetrical 2θ scans (Bragg-Brentano geometry).

The morphology of the Pn film was analyzed with an Atomic Force Microscope (Veeco 5000 Dimension), working in the tapping mode with a cantilever frequency of 80 kHz. The quantitative morphological analysis was performed using WS×M 4.0 software [15].

It is known in literature that a Pn thin film grown on a SiO_2 substrate shows a terrace structure with planes spaced by 1.54 nm between each other [16,17]. This behavior was confirmed also in our films grown on the first oxidized layer of a pristine Si(100) surface. Figure 1 shows the Bragg Brentano XRD spectra collected on

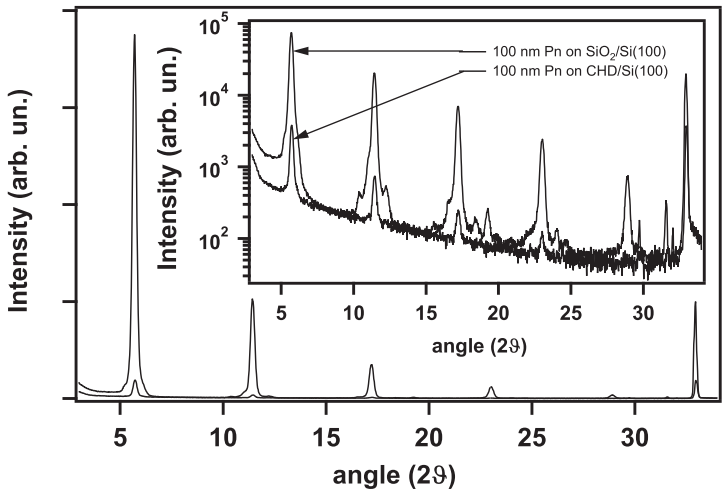

Figure 1: XRD spectra (Bragg Brentano geometry) of a 100 nm Pn thin film grown on SiO_2/Si(100) and on CHD/Si(100) substrates; in the inset the same spectra are reported in a logarithmic scale

a 100 nm Pn thin film grown on pristine SiO_2/Si and on a passivated CHD/Si(100) surface. As clearly evidenced in Figure 1, diffraction peaks are present at 2θ equals to 5.70, 14.42, 17.20 and 23.02 degrees that can be interpreted as the (001), (002), (003) and (004) peaks of the well-known Pn thin film phase [16,17]. Using the formula

$$2d\sin(\theta) = n\lambda$$

and considering $\lambda = 1.5406$ Å (CuK_α) we have found a interplanar distance of 15.5 Å, as previously found [7,16].

It is possible to observe that after depositing 100 nm Pn on a passivated CHD/ Si(100) substrate, the diffraction peaks previously mentioned are still present but their intensity is reduced drastically with respect to the same peaks in the spectrum collected on 100 nm Pn grown on a SiO_2 substrate (see Figure 1). Since both the Pn thin films have the same thickness, the reasons for this different behavior must be found on the morphological and configurational structure of the thin film or in a different conformation of the molecule due to the interaction with the substrate.

To investigate such a morphological structure in both cases we performed an AFM analysis starting from the substrates and gradually growing Pn films. The corresponding topographical maps are reported in Figure 2 and 3, respectively. At the first visual analysis it is shown how the 20 nm Pn thin film grown on a SiO_2/Si(100) (Figure 2 c) presents a terrace morphology. This conformation is also evidenced if we focus our attention on the corresponding line profile. In such a profile steps with a height of about 1.5 nm are clearly visible, in accordance with the XRD results.

An analogue 20 nm Pn film deposited on the CHD/Si(100) surface (Figure 2 d) presents some differences with respect to the film deposited on SiO_2/Si(100). The surface seems to be covered by small clusters of tens of nm in size, missing in the

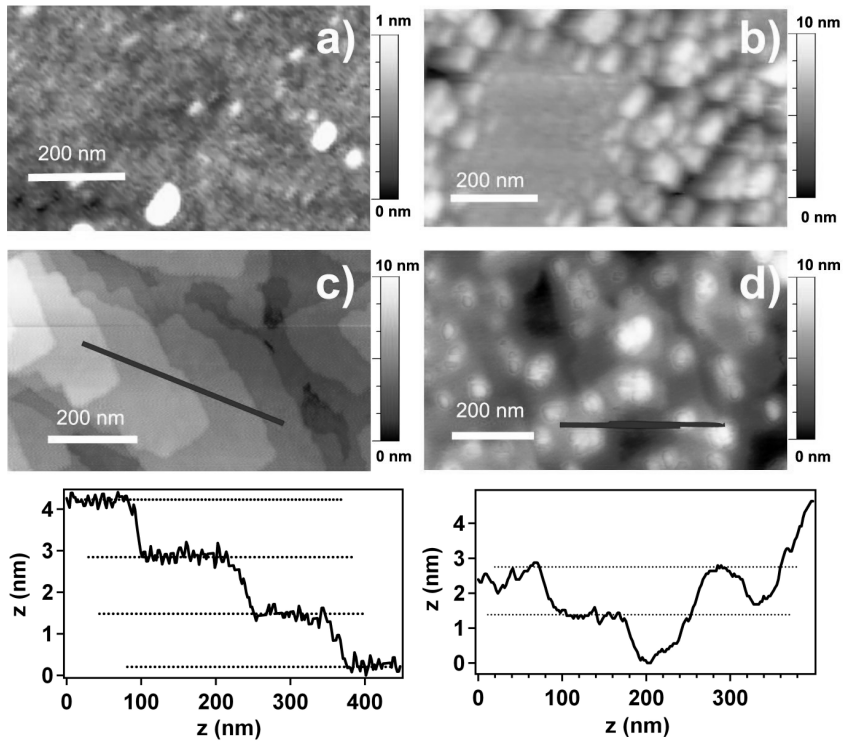

Figure 2: AFM topographical maps of: (a) pristine SiO_2/Si(100) surface; (b) CHD/Si(100) surface; (c) 20 nm Pn on SiO_2/Si(100) surface; (d) 20 nm Pn on CHD/Si(100) surface; the line profiles caught from map c (left) and from map d (right) are reported on the bottom; the position of the line profiles is indicated in the corresponding maps with a black line

previous sample, laying on a background resembling a terrace structure. However, through analysis of the maps it is not possible to establish unambiguously the real presence of terraces. The hypothesis is that these terraces were really present, they were less ordinate and not as well defined as in the film deposited on SiO_2/Si(100).

Since the Pn deposition parameters were identical in both cases, the reason for these differences must be dependent on the substrates. From an AFM analysis of both the substrates (Figure 2 (a) and (b)) it is clearly evident that strong differences are present. While the SiO_2/Si(100) surface presents a roughness mean square (RMS) of 0.27 nm and the presence of few impurities, the CHD/Si(100) surface seems to be covered by a great number of small clusters, and presents an RMS of 1.49 nm. As we will show below with the AES analysis, a layer of CHD is present on the surface after the deposition and we can be sure of the formation of such a buffer.

It is interesting to observe how the different substrate morphology influences the Pn growth also when a ticker film is deposited. The topographical maps of Figure 3 show what happens when 100 nm of Pn (100 times greater than the initial roughness) are deposited on SiO_2/Si(100) and on CHD/Si(100) substrates.

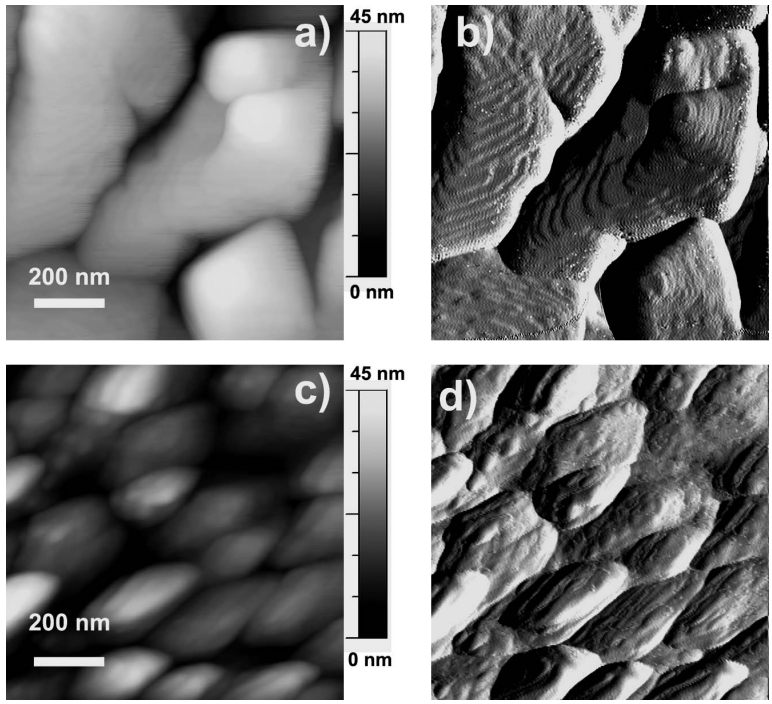

Figure 3: AFM topographical maps (a and c) and corresponding amplitude maps (b and d) of 100 nm Pn grown on a SiO_2/Si(100) substrate (a and b) and on a CHD/Si(100) substrate (c and d)

As evidenced in the amplitude signal of the topographical maps (Figure 3 (c) and 3 (d)), while in the Pn grown on SiO_2/Si(100) the terrace structure is already preserved (the steps of the terraces are clearly visible), the Pn film grown on the CHD/Si(100) evidences the presence of clusters hundreds nm in size, and the complete lack of a terrace structure. This result evidences how the Pn film growth depends on the substrate morphology even at a thickness much larger than the substrate roughness (1.5 nm).

Here, we focus our attention on the growth of a Pn film on a Si(100)-2×1 substrate. Such a system has been already quite well studied and the behavior of the growth and of the morphology is well known in the literature [2,5,8]. As explained above, the first Pn layer chemisorbs flat on the substrate while the subsequent layers grow perpendicular to the substrate forming dendritic morphology.

Figure 4 shows the wide range Auger spectra collected on a Si(100)-2×1 substrate during the growth of a Pn film. It was possible to calibrate the absolute value of the Pn film thicknesses from the quartz microbalance measurements by the peak intensity ratio of the Si LVV and C KVV Auger spectra, corrected by the respective sensitivity factors, 0.35 and 0.2, and the electron attenuation lengths. Moreover, the Auger signal from the saturated 1,4-CHD/Si(100) surface with a well known saturation coverage of about 0.6÷0.7 ML [14] was used as an additional constraint in the calibration.

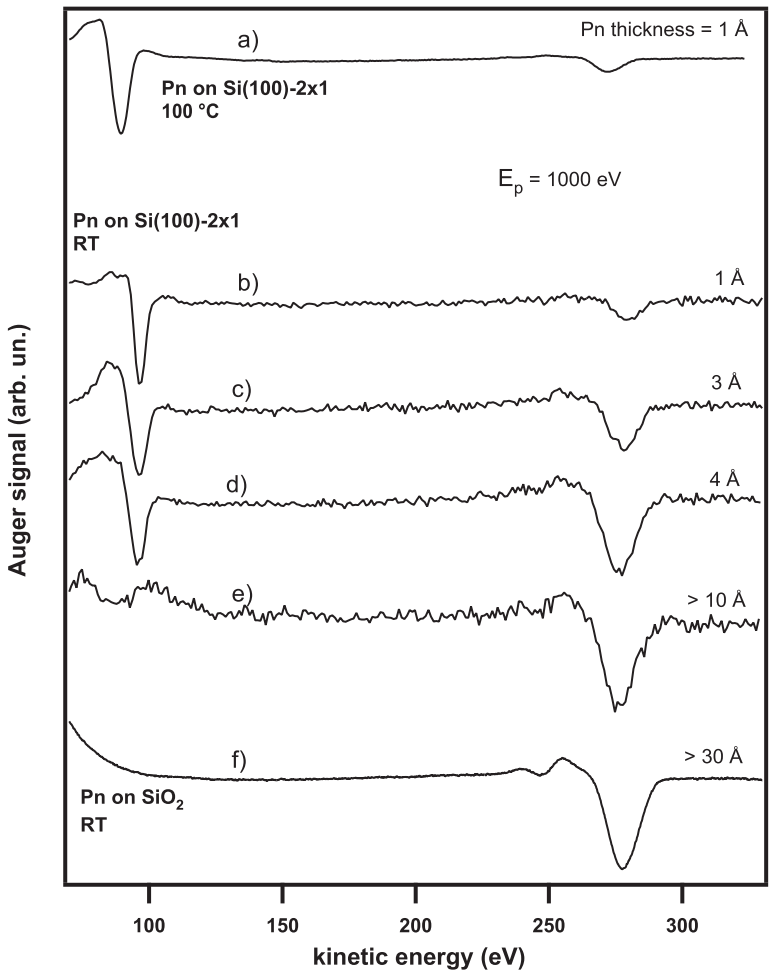

Figure 4: Auger wide scan spectra reported in the first derivative mode at the primary electron beam energy $E_p = 1000$ eV of Pn film grown with different thicknesses (ranging from 1 to more than 10 Å) and conditions: (a) reported the AES of the saturated Si(100)-2×1 surface kept at 100°C. The spectra of films grown at RT from (b) to (e) are reported. Finally, the thick film grown on the SiO_2 surface is shown in (f)

Looking more into details, the ratio between the Si LVV Auger and C KLL Auger peak-to-peak intensity was

$$\frac{I_{\mathrm{Si}}}{I_{\mathrm{C}}} = \frac{S_{\mathrm{C}} \cdot \lambda_{\mathrm{C}}}{S_{\mathrm{Si}} \cdot \lambda_{\mathrm{Si}}} e^{-\frac{nd}{\lambda_{\mathrm{Si}}}}$$

where λ_{C} and λ_{Si} are the electron mean free paths of carbon and silicon, S_{C} and S_{Si} the corresponding sensitivity factor, d is the distance between the atomic layers and n is the number of carbon atomic layers. From this equation we obtained the values of thickness (nd) reported in Figure 4. When the film is grown with the substrate kept at 100°C we find that (1.0 ± 0.5) Å of Pn is the maximum thickness achievable.

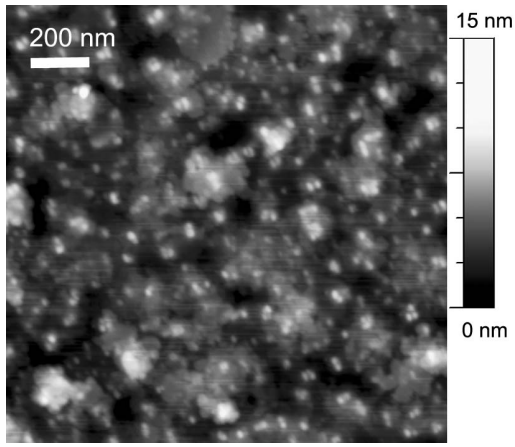

Figure 5: AFM topographical map of 15 nm Pn grown on a Si(100)-2×1 surface

In the case of a thicker molecular film, the rotation of the molecular plane occurs from planar to vertical due to the molecule-molecule interaction; the missing feature at 268 eV in the Auger spectra indicates a multidomain film without a particular orientation of the molecular π orbitals [4]. We performed AFM on the Pn film to verify the achievement of the above conformation. The AFM topographical map so obtained is reported in Figure 5. In this map it is possible to observe typical dendrimer structures present when a Pn thin film is grown on a Si surface. However it is also possible to see an important presence of clusters, several nanometers large, that are typically missing in these kinds of films. If previously it has been shown that the substrate morphology can influence the growth, we can imagine that clusters similar of those found in Figure 2 (b) were present on the substrate. At this point we can propose that the origin of such clusters is due to the thermal process that remove the native oxide layer to generate the clean Si(100)-2×1 surface.

As a result of this work we showed that a 100 nm Pn thin film grown on a pristine SiO_2/Si(100) surface crystallized better with respect to a 100 nm Pn thin film grown on passivated CHD/Si(100) surfaces suggesting that the morphology of the substrate influences the growth on a Pn film even at thicknesses larger compared to the substrate roughness. Furthermore, we find hints that a more ordered monolayer is obtained by higher temperature growth but the morphology is affected by the substrate treatment.

References

[1] G. Witte and C. Woll *J. Mater. Res.* 197 (2004) 1889
[2] K. P. Weidkamp, C. A. Hacker, M. P. Schwartz, X. Cao, R. Tromp and R. H. Hamers *J. Phys. Chem.* 107 (2003) 11142–11148
[3] G. E. Thayer, J. T. Sadowski, F. M. zu Heringdorf and R. M. Tromp *Phys. Rev. Lett.* 95 (2005) 256106
[4] F. J. Meyer zu Heringdorf, M. C. Reuter and R. M. Tromp *Nature* 412 (2001) 517–520
[5] D. Choudhary, P. Clancy and D. R. Bowler *Surf. Sci.* 578 (2005) 20–26
[6] L. Tsetseris and S. T. Pantelides *Appl. Phys. Lett.* 87 (2005) 233109
[7] R. Ruiz, A. C. Mayer, G. G. Malliaras, B. Nickel, G. Scoles et al. *App. Phys. Lett.* 85,21 (2004) 4926

[8] B. Nickel, R. Barabash, R. Ruiz, N. Koch, A. Kahn, L. C. Feldman, R. F. Haglunds and G. Scoles *Phys. Rev. B* 70 (2004) 125401
[9] M. Wakatsuchi, H. S. Kato, H. Fujisawa and M. Kawai *J. Electr. Spectr. Rel. Phen.* 137–140 (2004) 217–221
[10] K. Hamaguchi, K. Mukai, Y. Yamashita, J. Yoshinobu, T. Sato and M. Iwatsuki *Surf. Sci.* 531 (2003) 199
[11] K. Hamaguchi, S. Machida, K. Mukai, Y. Yamashita and J. Yoshinobu *Phys. Rev. B* 62 (2000) 7576–7580
[12] F. D'Amico, R. Gunnella, M. Shimomura, T. Abukawa and S. Kono *Phys. Rev. B* 76 (2007) 165315
[13] R. Gunnella, M. Shimomura, F. D'Amico, T. Abukawa and S. Kono *Phys. Rev. B* 73 (2006) 235435
[14] K. Akagi, S. Tsuneyuki, Y. Yamashita, K. Hamaguchi, J. Yoshinobu *Appl. Surf. Sci.* 234 (2004) 162
[15] I. Horcas, R. Fernández, J. M. Gómez-Rodríguez, J. Colchero, J. Gómez-Herreroand and A. M. Baro *Rev. Sci. Instrum.* 78 (2007) 013705 457–460
[16] H. Yoshida, K. Inaba and N. Sato *Appl. Phys. Lett.* 90 (2007) 181930
[17] S. D. Wang, X. Dong, C. S. Lee and S. T. Lee *J. Phys. Chem. B* 109 (2005) 9892–9896

Thin film solar cells are real competitors for polycrystalline Si-based solar cells

I. Davoli[1], M. Lucci[1], I. Colantoni[2]

[1] *Dipartimento di Fisica, Università di Roma "Tor Vergata" Via della Ricerca Scientifica 1, 00133 Roma, Italy*

[2] *Dipartimento di Fisica, Sapienza Università di Roma P.le Aldo Moro 2, 00133 Roma, Italy*

In the last few decades the photovoltaic research has lived an impressive booming, especially due to the discovery of new materials with very high photon absorbing power. This characteristic favors the building of flexible solar cells and consequent development of new technological application. Here we report the status of art of the new research trends on thin solid films, moving from the amorphous Si film to the organic film, up to the use of semiconductor compounds with a direct gap (kesterite). At the end we will present some recent results reported studying CZTS via chemical process.

Divide-and-Conquer Learn-on-the-Fly: a hybrid quantum-classical approach for simulating the nanomechanical properties of metallic systems

J. Dziedzic, J. Rybicki

Department of Solid State Physics, Faculty of Applied Physics and Mathematics
Gdansk University of Technology
Narutowicza 11/12, 80-233 Gdansk, Poland

Molecular dynamics (MD) simulations constitute an important tool in the study of the mechanical properties of nanoscale systems. The MD method is classical in nature and its main limitations stem from the empirical nature of the employed potentials, whose functional form is postulated a priori, and from not taking the electronic effects explicitly into account. In consequence it does not correctly model physical reality in all cases, particularly for systems that are far from equilibrium, such as nanostructures undergoing plastic deformation; i.e. classical potentials are said to lack *transferability*.

The explicit inclusion of electronic effects offered by first-principles approaches does yield a transferable description of the interatomic interactions, albeit at a cost of significant computational complexity, which prevents these approaches from being directly applied to systems involving more than several hundred atoms, and even then in practice the performed simulations are usually not dynamical.

Hybrid (quantum-classical) approaches seek a compromise, whereby a subset of the system (such as a region where bond-reorganization is taking place) is treated with a first-principles approach, whilst the remainder undergoes classical MD. The Learn-on-the-Fly (LOTF) technique (Csanyi et al., PRL 93 (17), 2004) offers a particularly elegant way of embedding the results of quantum-mechanical calculations within an MD simulation, by periodically, locally re-parametrizing the empirical potential so that it reproduces the accurate forces obtained from first principles in the region of interest. In its original formulation it has been successfully applied to the fracture of silicon, where the classical Stillinger-Weber potential is known to give qualitatively wrong predictions.

We present Divide-and-Conquer Learn-on-the-Fly (Dziedzic et al., PRB 83 (22), 2011) – a generalization of LOTF, which is suitable for systems where the interaction range is longer, such as d-shell metals. We show how the force-matching stage can be recast to make the problem of simultaneously optimizing thousands of parameters in situ to match thousands of atomic forces computationally tractable. We demonstrate the feasibility of our approach on several examples: simulating nanoindentation and nanoscratching of Cu monocrystals, calculating the structure and properties of liquid metals and alloys, and the structure of selected AuCu nanoclusters at finite temperature.

Acknowledgements
JD would like to acknowledge the support of Polish National Science Centre and the Ministry of Science and Higher Education (grants N N519 577838 and IP2012 043972). We would like to thank the TASK Academic Computer Centre for access to the galera cluster.

Nano- and micro-sized silver particles for electronic packaging

J. Felba[1], T. Falat[1], A. Moscicki[2]

[1] *Faculty of Microsystem Electronics and Photonics, Wroclaw University of Technology Janiszewskiego 11/17, 50-372 Wroclaw, Poland*

[2] *Amepox Microelectronics Ltd. Jaracza 6, 90-268 Lodz, Poland*

Production of modern microelectronic devices needs advanced materials and packaging technologies oriented towards miniaturization and high reliability of systems. Micro-and nano-sized silver can be treated as such an advanced material and it is used in advanced packaging technologies, especially for high-density packaging electronics and flexible electronics. The paper presents information about the practical use of silver particles with sizes ranging from 4 nanometers to several micrometers in electronic packaging technologies, such as:

- Ink-jet printing electrically conductive structures (especially on flexible substrates which are temperature sensitive). The technology needs a special liquid (ink) which contains silver nanoparticles. After the final technological step, the resistivity of printed structures is close to the resistivity of bulk silver.
- Creating conductive layers of microvias joining both sides of flexible substrates. Holes with diameters from 30 to 60 μm were laser beam drilled in flexible substrates with a thickness of 100 μm and then filled by ink-jet printing with the use of ink containing nanosilver particles.
- Formulating thermal interface materials (TIM) based on nano-and micro-sized silver particles for effective heat transfer from electronic devices.
- Joining of electronic components to the substrate instead of traditional soldering, by the use of sintered pastes contacting nano-and micro-sized silver particles.

Acknowledgements
All the presented achievements are a result of the work carried out in the Laboratory of Interconnecting and Packaging Electronics Circuits at the Wroclaw University of Technology.

Proton conducting ceramics – structure and properties

M. Gazda[1], A. Mielewczyk-Gryń[1,2], K. Gdula-Kasica[1], S. Wachowski[1], K. Zagórski[1], P. Jasinski[3]

[1] *Department of Solid State Physics, Faculty of Applied Physics and Mathematics Gdansk University of Technology Narutowicza 11/12, 80-233 Gdansk, Poland*

[2] *Peter A.Rock Thermochemistry Laboratory and NEAT ORU, University of California Davis, USA*

[3] *Biomedical Engineering Department, Faculty of Electronics Telecommunication and Informatics, Gdansk University of Technology Narutowicza 11/12, 80-233 Gdansk, Poland*

Introduction

High temperature proton conductors (HTPCs) are materials which have very interesting properties but are not widely known. They may be applied in solid oxide fuel cells, hydrogen separators, hydrogen pumps and gas sensors [1]. Ceramic proton conductors may also work as catalysts for internal methane reforming for oxygen ion conducting solid oxide fuel cells (SOFCs). In view of these applications the most required properties of proton-conducting ceramics include high proton or mixed proton-electron conductivity, catalytic activity, and mechanical and chemical stability at temperatures of about 600–700°C in H_2, H_2O and CO_2. So far, an ideal material has not been found. Examples of most widely studied materials are acceptor-doped solid solutions of barium cerate and zirconate [e.g. 1,2] and acceptor-doped lanthanum niobates [e.g. 3,4]. Acceptor doped barium cerates and zirconates of the perovskite structure [2,5] have the highest reported proton conductivity among HTPCs but they exhibit poor chemical and mechanical stability, especially in carbon dioxide- and sulfur-rich atmospheres. On the other hand, materials from the lanthanum niobate group have lower proton conductivity but higher mechanical and chemical stability at high temperature. For example, lanthanum orthoniobate doped with 1% of Ca has proton conductivity of about 10^{-3} S/cm at 900°C [4].

Both barium cerate-zirconates and lanthanum niobates undergo structural phase transitions at high temperature. A crystal structure of higher symmetry is stable at temperatures above the transition temperature. What is important, the crystal structure symmetry influences the mobility of protons, thus, it also influences proton conductivity. In both cases, higher symmetry corresponds to higher mobility.

In this work examples of proton conducting ceramics belonging to barium cerate-zirconates and lanthanum niobates are reported. Special attention is devoted to the relations between structural phase transitions and proton conductivity of materials.

Experimental

Experimental details of the sample preparation are presented elsewhere [5,6]. Crystal structure and phase composition of the materials were determined with the X-ray diffraction method using Phillips X'Pert Pro MPD with CuKα radiation. The patterns were analysed with the Rietveld refinement method using the Highscore program. The pseudo-Voigt profile function was applied. High temperature XRD measurements were carried out between room temperature and 700°C.The sample microstructure was studied by Scanning Electron Microscope Quanta 250FEG with the Bruker Energy-dispersive X-ray spectroscopy system. The electrical conductivity of the samples was determined from impedance spectroscopy using a Novocontrol Alpha-A analyzer.

Results and discussion

Examples of high temperature X-ray diffraction results obtained for lanthanum niobates and barium cerate are presented in Figures 1 and 2. Figure 1 shows clearly a structural phase transition in lanthanum niobate. On the other hand, structural modifications of the barium cerate-zirconate are much more subtle. They can be seen through a very small modification of the XRD reflection at 2θ about 41°. Nevertheless, in both materials structural changes influence various materials properties.

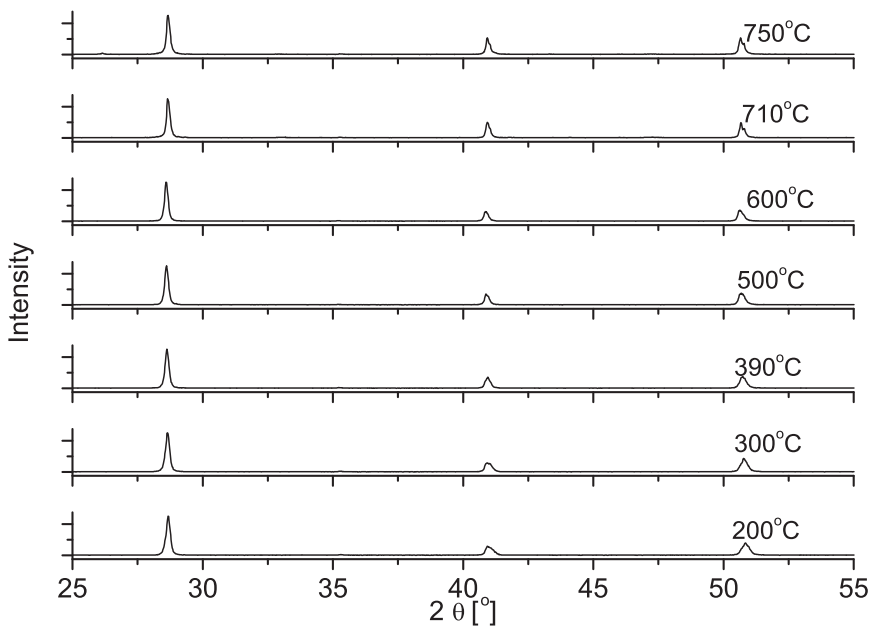

Figure 1: X-ray diffraction patterns obtained for lanthanum niobate.

The properties which are very important from the point of view of such applications like SOFC or hydrogen separators are, for example:

- The rate of the unit cell volume temperature dependence, which may result in a change of the temperature expansion coefficient (TEC);
- Activation energy of proton conductivity.

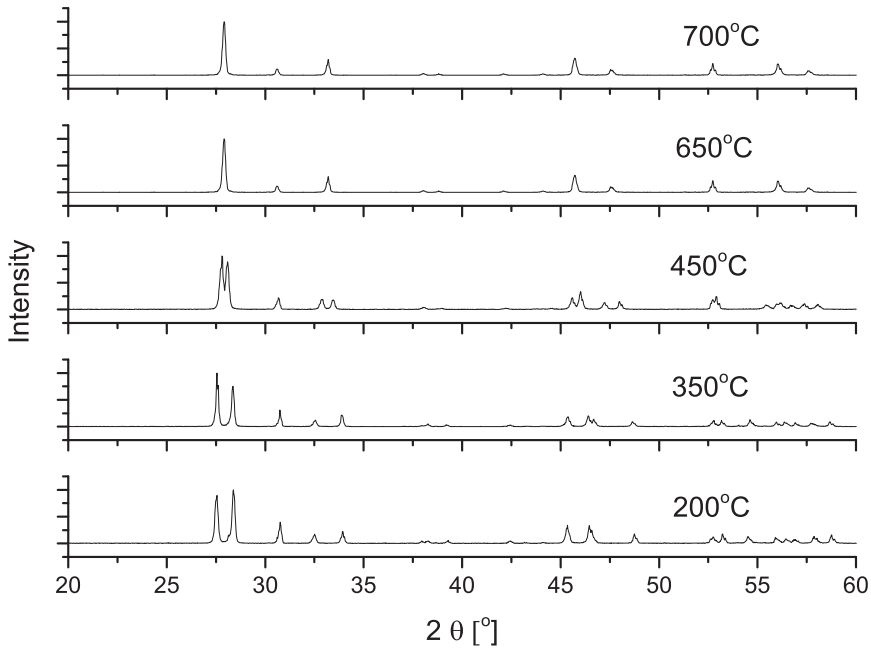

Figure 2: X-ray diffraction patterns obtained for barium cerate.

In the case of lanthanum niobates, both the temperature expansion coefficient and the activation energy of conductivity are lower above the transition temperature. On the other hand, barium cerate-zirconates have almost constant TEC, whereas the activation energy of conductivity is higher above the transition temperature.

Conclusions

The ceramic proton conductors exhibit complex structural properties. Both the families of materials presented here show structural phase transitions. The influence of the phase transition on the properties of materials depends on the material.

References

[1] H. Iwahara, Y. Asakura, K. Kotahira and M. Tanaka 2004 *Solid State Ionics* **168**, 299
[2] S. Nikodemski, J. Tong and R. O'Hayre 2013 *Solid State Ionics* **253**, 201
[3] R. Haugsrud and T. Norby 2006 *Solid State Ionics* **177**, 1129
[4] M. Ivanova, S. Ricote, W. A. Meulenberg, R. Haugsrud and M. Ziegner 2012 *Solid State Ionics* **213**, 45
[5] K. Gdula-Kasica, A. Mielewczyk-Gryń, T. Lendze, S. Molin, B. Kusz and M. Gazda 2010 *Crystal Research and Technology* **45**, 1251
[6] A. Mielewczyk-Gryn, K. Gdula-Kasica, B. Kusz and M. Gazda 2013 *Ceramics International* **39**, 4239

X-rays and electron diffraction imaging to study smart nano/bio materials

C. Giannini, L. De Caro

Institute of Crystallography, National Research Council
Via Amendola 122/O Bari, Italy

Smartness is a typical feature of biological systems that are able to adaptively interact with the environment. Indeed, more or less complex biological systems are able to modify themselves on the basis of the information they get from the surrounding environment in order to respond to such stimuli.

Widely known examples of Smart Nano/Bio Materials include:

- Healthcare: nanoparticle suspensions or solutions to be injected into living tissues to help diagnostics or drug delivery;
- Energy: large-scale nanostructured materials/devices, thanks to their high surface to volume ratio, are potentially superior triggers to enhance every type of surface- or interface-based chemical reaction, i.e., reactions for energy generation, conversion and storage;
- Automotive/infrastructure: composite materials (ex: polymers) containing nano-objects with extraordinary mechanical properties can result in novel outstanding performances, enabling for instance the application of novel coatings with unprecedented resistances.

The synthesis of nano/bio materials is a pivotal research field towards the development of nanotechnology. Presently, a variety of techniques are used to grow or fabricate nanomaterials of different size and shape, including physical and chemical methods in the vapour and liquid phase.

To exploit the full potential that smart nanomaterials offer, a non-destructive and effective structural and morphological characterisation is required.

In the realm of the most known X-ray Imaging techniques, lens-less imaging techniques in diffraction regimes, such as SAXS/WAXS scanning microscopy and Coherent Diffraction Imaging will be described together with some relevant applications, mainly related to the nano-bio world.

References

[1] C. Giannini, D. Siliqi, M. Ladisa, D. Altamura, A. Diaz, A. Beraudi, T. Sibillano, L. De Caro, S. Stea, F. Baruffaldi and O. Bunk 2014 *J. Appl. Cryst.* **47**, 110

[2] Y. Chushkin, F. Zontone, E. Lima, L. De Caro, P. Guardia, L. Manna and C. Giannini 2014 *J. Synch. Rad.* **21**, 594

[3] C. Giannini, D. Siliqi, O. Bunk, A. Beraudi, M. Ladisa, D. Altamura, S. Stea and F. Baruffaldi 2012 *Sci. Rep.* **2**, 435; DOI:10.1038/srep00435

[4] L. De Caro, E. Carlino, G. Caputo, P. D. Cozzoli and C. Giannini 2010 *Nature Nanotechnology* **5**, 360

Computer simulations of mechanical and structural properties of graphene

J. N. Grima[1], J. Rybicki[2], Sz. Winczewski[2], K. W. Wojciechowski[3], L. Mizzi[1], M. C. Grech[1], R. Gatt[1], R. Cauchi[1], D. Attard[1]

[1] *Metamaterials Unit, Faculty of Science, University of Malta Msida MSD 2080, Malta*

[2] *Faculty of Applied Physics and Mathematics, Gdansk University of Technology Narutowicza 11/12, 80-233 Gdansk, Poland*

[3] *Institute of Molecular Physics, Polish Academy of Sciences M. Smoluchowskiego 17, 60-179 Poznan, Poland*

A series of extensive simulations with AIREBO force-field of the mechanical properties of graphene were performed. Many interesting and sometimes surprising results were obtained which will be presented and discussed in detail. When possible, the results of the simulations will be compared with experimental results obtained by other authors.

Acknowledgements

This work has been funded by the Malta Council for Science and Technology through the R&I-2012-061 Project (SMESH). This research was also supported in part by PL-Grid Infrastructure. The authors gratefully acknowledge the TASK Academic Computer Centre in Gdansk (CI TASK) and Poznan Supercomputing and Networking Center (PCSS) for providing the computer time and the facilities. JR acknowledges the support of the Ministry of Science and Higher Education (grant IP2012 043972). Equipment procured through the European Regional Development Fund, Project ERDF-080 'A Supercomputing Laboratory for the University of Malta' was also used.

EPR spectroscopic and photocatalytic properties of TiO_2 subjected to different annealing and rinsing processes

N. Guskos[1,2], A. Guskos[2], G. Zolnierkiewicz[2], J. Typek[2], P. Berczynski[2], D. Dolat[3], S. Mozia[3], A. W. Morawski[3]

[1] *Department of Solid State Physics, Faculty of Physics, University of Athens Panepistimiopolis, 15 784, Greece*

[2] *Institute of Physics, West Pomeranian University of Technology Al. Piastow 48, 70-311 Szczecin, Poland*

[3] *Institute of Chemical and Environmental Engineering West Pomeranian University of Technology Al. Piastow 17, 70-310 Szczecin, Poland*

Samples of TiO_2, annealed at 600°C and 650°C in an ammonia atmosphere, were prepared without and with water rinsing. The materials consisted of a crystalline anatase (95%) and a rutile (5%) phase and their crystallite sizes were determined to be smaller than 50 nm for the anatase and 90 nm for the rutile phase for all types of samples. The temperature dependences of the magnetic resonance spectra (EPR) of the obtained samples were investigated. EPR spectra of samples were recorded before and after rinsing with water showing signals attributed to free radicals that were centered between $g_{eff} = 2.0027(3)$ and $g_{eff} = 2.0032(3)$ with linewidths $\Delta H_{pp} = 5(1)G$ and

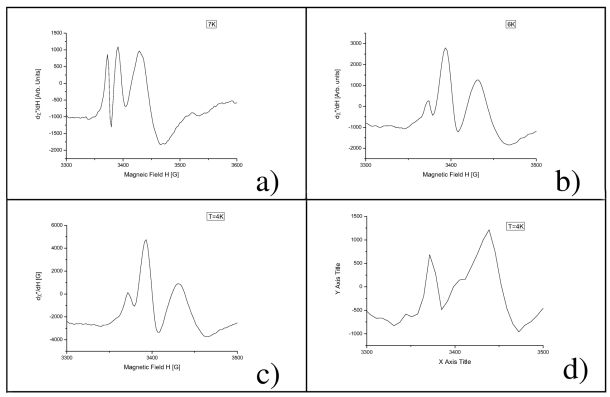

Figure 1: EPR spectra of TiO_2 registered in a low temperature range for the sample annealed at 600°C before rinsing (a), after water rising (b), and the sample annealed at 650 °C before rinsing (c), and the same sample after water rising (d)

$\Delta H_{pp} = 8(1)G$, and additionally a resonance line centered at $g_{eff} = 1.988(1)$. Moreover, a resonance line at $g_{eff} = 1.972(2)$ was detected that could arise from complexes of trivalent titanium ions. The intensities of spectroscopic lines strongly depended on processes of thermal annealing and water rinsing (Figure 1). The concentration of the localized magnetic moments had essential influence on the photocatalytic properties of the investigated samples.

Acknowledgements
This work was supported by the National Centre for Science of Poland under project No. DEC-2012/06/A/ST5/00226.

Magnetic properties of molecular magnets

N. Guskos[1,2], J. Typek[2], G. Zolnierkiewicz[2], C. Aidinis[3], A. Guskos[2], P. Berczynski[2], D. Petridis[4]

[1] *Department of Solid State Section, Faculty of Physics, University of Athens Panepistimiopolis, 15 784 Zografos, Athens, Greece*

[2] *Institute of Physics, West Pomeranian University of Technology Al. Piastow 48, 70-311 Szczecin, Poland*

[3] *Department of Electronics, Faculty of Physics, University of Athens Panepistimiopolis, 15 784 Zografos, Athens, Greece*

[4] *Institute of Materials Science, National Centre for Scientific Research "Demokritos" 153 10 Aghia Paraskevi, Attikis, Athens, Greece*

Two composites consisting of γ-Fe_2O_3 (maghemite) nanoparticles covered by two different molecular magnets were prepared and investigated by detailed DC magnetization measurements and SQUID method in the 2–300 K range. Both composites displayed very intense magnetic response mainly originated from γ-Fe_2O_3 agglomerated nanoparticles. Different kinds of magnetic interactions were evidenced for all the nanocomposites depending essentially on the kind of molecular magnets. The coexistence of superparamagnetic, paramagnetic and antiferromagnetic phases was identified. Strong antiferromagnetic interactions were observed below 30 K, where some parts of the nanocomposites entered a long range antiferromagnetic state.

Magnetic properties of co-modified (Co,N)-TiO_2 nanocomposites

N. Guskos[1,2], G. Zolnierkiewicz[2], A. Guskos[2], J. Typek[2], P. Berczynski[2], D. Dolat[3], B. Grzmil[3], B. Ohtani[4], A. W. Morawski[3], C. Aidinis[5]

[1] *Department of Solid State Physics, Faculty of Physics, University of Athens Panepistimioupolis, GR-157 84 Athens, Greece*

[2] *Department of Physics, West Pomeranian University of Technology Al. Piastow 48, 70-311 Szczecin, Poland*

[3] *Department of Chemical and Environmental Engineering West Pomeranian University of Technology Al. Piastow 17, 70-310 Szczecin, Poland*

[4] *Catalysis Research Center, Hokkaido University Sapporo 001-0021 Japan*

[5] *Department of Electronics, Faculty of Physics, University of Athens Panepistimioupolis, GR-157 84 Athens, Greece*

Cobalt and nitrogen co-modified titanium dioxide, (nCo,N)-TiO_2 ($n = 1$, 5 and 10 wt.%), nanocomposites were investigated by detailed dc magnetization measurements. Different kinds of magnetic interactions were evidenced for all studied nanocomposites depending essentially on cobalt concentration. The coexistence of superparamagnetic, paramagnetic and ferromagnetic phases was identified at high temperatures. Strong antiferromagnetic interactions were observed, with parts of the nanocomposites having entered a long range antiferromagnetic phase. Antiferromagnetic interactions were attributed to the cobalt magnetic agglomerates.

Acknowledgements
This work was partially supported by National Centre for Science and the Ministry of Science and Higher Education of Poland under Project No. MNiSW/DPN/4878/TD/2010.

Determination of ionic conductivity in (Pb,Bi)-(Si,Ge)-O oxide glasses

J. Karczewski, B. Bochentyn, M. Gazda, B. Kusz

Department of Solid State Physics, Faculty of Applied Physics and Mathematics
Gdansk University of Technology
Narutowicza 11/12, 80-952 Gdansk, Poland

Inorganic amorphous materials, such as oxide glasses, are widely used in commercial technical applications. There have been many papers about crystallization discussing this phenomenon in the micro scale. There is a direct relation between the nucleation process and the mobility of ions in glass. It has been found that Bi^{3+} ions are not mobile in bismuth-silicate and bismuth-germanate glasses and it is rather O^{2-} ions that are responsible for ionic transport. Similarities of Pb and Bi ions suggest that the same mechanism of conductivity should exist in other glasses containing Pb or Bi ions. Determination of the charge carriers which take part in ionic conduction will help to avoid some errors in the interpretation of ionic transport in glasses containing bismuth or lead ions. The electrical properties of glass materials were studied by the open circuit voltage (OCV) technique and electrochemical impedance spectroscopy (EIS) under different atmospheres. The OCV technique was used to determine the transport number of all charge carriers. The open circuit voltage (OCV) measurements were carried out to determine the type of conductivity based on the Nernst equation.

Acknowledgements
This work was partially supported by the National Science Center under grant No. NCN2012/05/B/ST3/02816.

White light emission from $Eu^{3+}/Tb^{3+}/Tm^{3+}$ triply-doped GeO_2-PbO-Bi_2O_3-SrF_2 glass

B. Kościelska[1], A. M. Kłonkowski[1,2], W. Sadowski[1], M. Łapiński[1], W. Wiczk[2], I. Bylińska[2], M. Walas[2]

[1] *Department of Solid Stat Physics, Faculty of Applied Physics and Mathematics Gdansk University of Technology Narutowicza 11/12, 80-233 Gdansk, Poland*

[1] *Faculty of Chemistry, Gdansk University Wita Stwosza 63, 80-308 Gdansk, Poland*

In recent years much attention has been paid to white LEDs which are considered to be the next generation of solid state lighting devices, capable of replacing traditional incandescent and fluorescent lamps. Rare-earth ion doped glasses can be proposed as novel materials for white LED applications. These materials should play the role of phosphors that emit white light of high intensity under excitation of UV radiation. Additionally, phosphors based on a glassy matrix have especially attractive attributes such as efficient luminescence, easy fabrication and molding into any shape. White light generation from simultaneous emissions of blue, green and red light under UV-light excitation was attained for the first time in borate-based glasses containing Ce^{3+}, Tb^{3+} and Mn^{2+} as activators [1]. Since that time various types of glasses with rare earth ions have been studied. A very good host material for white LED applications seems to be the GeO_2-PbO-Bi_2O_3-SrF_2 glass. It is a glass with low phonon energy providing less non-radiative relaxation rates and high quantum efficiencies of dopant ions [2,3,4].

In this work preliminary results of white light emission from $Eu^{3+}/Tb^{3+}/Tm^{3+}$ triply-doped GeO_2-PbO-Bi_2O_3-SrF_2 glass excited by UV light are presented.

References

[1] J. C. Zhang, C. Parent, G. Le Flem, P. Hagenmuller 1991 *J. Solid State Chem.* **93**, 17
[2] H. Nii, K. Ozaki, M. Herren, M. Morita 1998 *J. Lumin.* **76–77**, 116
[3] A. Mori, Y. Ohishi, S. Sudo 1997*Electron. Lett.* **33**, 863
[4] B. Kukliński, D. Wileńska, S. Mahlik, K. Szczodrowski, M. Grinberg, A. M. Kłonkowski 2014 *Optical Materials* **36**, 633

Dynamical properties of water embedded in reverse micelles – computer simulation study

D. Makieła, K. Górny, Z. Dendzik, Z. Gburski

Institute of Physics, University of Silesia
Uniwersytecka 4, 40-007 Katowice, Poland

We performed a series of fully atomistic simulations of water embedded in reverse micelles composed of DMPC (1,2-dimyristoyl-sn-glycero-3-phosphocholine) phospholipide.

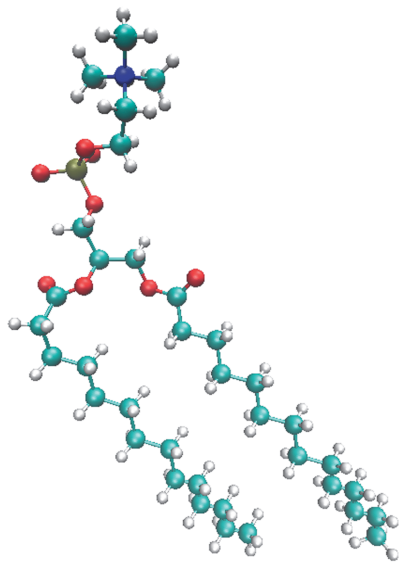

Figure 1: Model of DMPC molecule

Water molecules were modeled using the TIP3P CHARMM adapted model [1].All interactions were modeled using the CHARMM27 potential [2].

The molecular dynamics (MD) simulations were performed using the NAMD 2.9 [3] program in an NVT (constant number of particles, constant volume and constant temperature) ensemble for 5 temperatures: 280, 290, 300, 310 and 320 K. The classical equations of motion were integrated using the Brunger-Brooks-Karplus (BBK) method implemented in NAMD, with the time step of integration of equations of motion of 0.5 fs, which ensured sufficient energy conservation. The temperature was

controlled using a Langevin thermostat. All trajectories were produced over 4 ns (8 000 000 time steps) after 2.0 ns (4 000 000 time steps) of equilibration. Spherical boundary conditions were applied to simulated reverse micelles. For reference purposes we also simulated bulk water modeled as 1981 water molecules in a simulation box, $3.8 \times 3.8 \times 3.8$ nm in size.

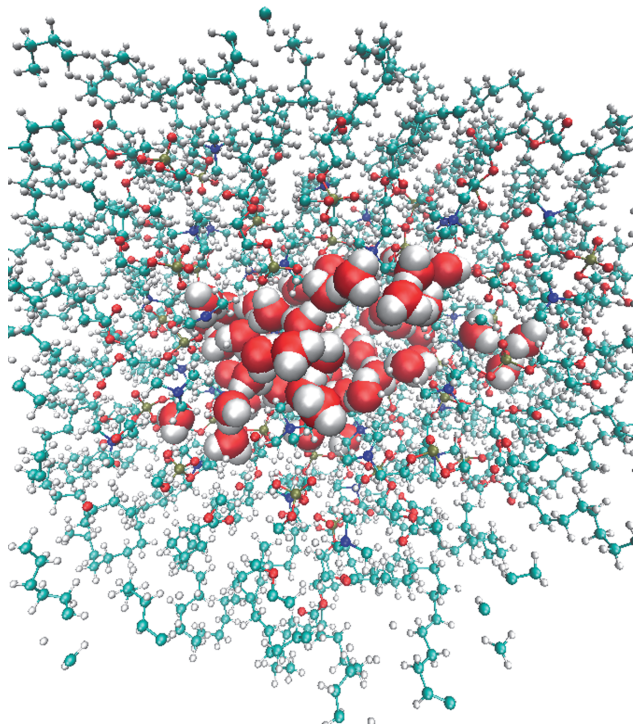

Figure 2: Final configuration of simulated system at 300 K

Dynamics of water molecules in reverse micelles was studied in terms of the MSD, self diffusion coefficient and orientational autocorrelation functions. We applied the Arrhenius equation to describe the activation process of self diffusion of water molecules. The activation energy was estimated to be equal to $E_A = 12.025$ kJ/mol for water encapsulated in a micelle with the inner diameter of 2.2 nm and $E_A = 5.14$ kJ/mol for bulk water. We observed significant slowing down of dynamics of water embedded in reverse micelles and a rise in the diffusion activation energy.

Designing an electro-opto-mechanical device with SiN micro membranes

N. Malossi, I. M. Haghighi, P. Piergentili, M. Baway, F. Bonfigli, M. Asjad, C. Biancofiore, M. Karuza, C. Molinelli, M. Galassi, P. Tombesi, R. Natali, G. Di Giuseppe, D. Vitali

Physics Division, School of Science and Tecnology, University of Camerino
Via Madonna delle Carceri 9, I-62032 Camerino (MC), Italy

Optomechanics is a fast growing field where the knowledge and specialties from different fields are mixing and merging, while new physical phenomena and breakthrough technologies are emerging. An interfacing micro-and nano-electro-mechanical resonator with light is gaining increasing attention of the scientific community. On the one hand, mechanical resonators provide unique opportunities in a disparate field of applications, such as detection of forces, displacements and masses at the ultimate limits imposed by the Heisenberg principle, the realization of quantum information architectures acting as a universal quantum bus, and for fundamental tests of the quantum theory. On the other hand, an electro-optomechanical transducer opens the possibility of interfacing different regimes (frequency from MHz to THz) and interfacing different quantum systems, opening the development of a hybrid quantum system. Here we present a fast review of the status of our opto-mechanical experiment and the preliminary results of the designing of an electro opto-mechanical transducer.

The first step for operating in the quantum regime is to reduce as much as possible the thermal noise effect, while cooling the mechanical resonator close to its quantum ground state. The investigated system consists of a micro mechanical oscillator (SiN membrane 50nm thick) placed inside a high finesse optical cavity (membrane in the middle set-up).

We show here both the experimental study of dynamical back-action cooling of the fundamental vibrational mode of a thin semitransparent membrane and the demonstration at room temperature of analogous electromagnetically induced transparency (EIT).

In the case of fundamental vibration mode cooling, we observe cooling by a factor of $\approx$350 and a mechanical frequency shift due to the quadratic term in the expansion of the cavity mode frequency versus the effective membrane position, which is typically negligible in other cavity optomechanical devices.

In the case of the EIT, a weak probe field is completely reflected by the cavity when the pump beam is resonant with the motional red sideband of the cavity thanks to the interference effect. Under this condition we infer significant slowing down of light of hundreds of microseconds, which is easily tuned by shifting the membrane along the cavity axis. We also observe the associated phenomenon of electromagnetically induced amplification which occurs due to constructive interference when the pump is resonant with the blue sideband.

L21

Our experimental efforts are focused on two different lines: placing the present system in a cryogenic environment in order to reach a quantum regime; building an electro-optomechanical transducer to coherently transfer information between the optical frequency and radio or microwave frequencies.

Here we show the status of the development of the transducer and the preliminary results.

Nanoscale phase separations in correlated materials by μ-XANES

A. Marcelli[1,2,3]

[1] *INFN – Laboratori Nazionali di Frascati*
Via E. Fermi 40, I-00044 Frascati, Italy

[2] *RICMASS, Rome International Center for Materials Science Superstripes*
Via dei Sabelli 119A, 00185 Rome, Italy

[3] *University of Science and Technology of China*
Hefei, Anhui 230026, China

Being a fast and local probe of a selected atomic species, XANES spectroscopy represents a powerful spectroscopic technique suited to investigate the element distribution of different polymorphs down to the micrometer scale using extremely small spots [1]. However, this technique is much more powerful when applied to investigate the nature of multi-scale correlated systems. The definition of the latter is not easy although they can be considered systems with a multi-scale structure and dynamics, unavoidably entangled among them well beyond the manifold nature of a disordered system.

Complex lattice architectures can be associated to transition metal and rare earth oxides and to many superconductors such as cuprates or pnictides, all systems where a rich variety of nanoscale structural, electronic and magnetic phases may coexist. The interplay of nano-and micrometer-scale factors is typically at the origin of the macroscopic behavior of these systems, hence the capability to probe morphology and phase distribution in complex systems at multiple length scales is mandatory.

Many standard experimental probes in such electron microscopy, provide information only on the surface and from a limited number of layers below the surface, therefore they are not able to recognize the competition among different nano-scale phases. Other experimental probes looking at the k-space such as X-ray diffraction (XRD), neutron diffraction, and angular resolved photoemission, provide only non-local and space averaged information. At variance, the study of the multiscale phase separation from nanoscale to the micron scale, demands powerful bulk experimental methods without any time or spatial averaging. Local structural probes with micrometer size spots such the Pair Distribution Function (PDF) or micro-X-ray Absorption Near Edge structure (μ-XANES) may investigate nanoscale structures and these methods have been successfully applied to different cuprates [2,3]. The available data provide information on local electronic and lattice fluctuations, complementary to other techniques such as scanning μ-XRD [4,5].

Nowadays, thanks to the new optical layouts, X-ray imaging at high spatial resolution can be combined with μ-XANES spectroscopy to reconstruct two-dimensional and

three-dimensional morphological and chemical changes in large volumes with a resolution of tens of nanometers [6–8]. In addition to these opportunities we will present μ-XANES data of La_2CuO_{4+y}, the simplest cuprate superconductor with mobile oxygen interstitials that exhibits a bulk multiscale structural phase separation observed also with the μ-X-ray diffraction. We investigated this system by means of scanning La L_3-edge μ-XANES and provided support to a percolative superconductivity scenario in copper oxides and other high temperature cuprate superconductors [3]. Indeed, the percolation phenomenon has strong influence on the superconducting properties within different frameworks that consider the intrinsic percolative nature of the superconductivity phenomenon.

References

[1] D. Andrault, M. Muñoz, N. Bolfan-Casanova, N. Guignot, J.-P. Perrillat, G. Aquilanti, S. Pascarelli, *Experimental evidence of perovskite and post-perovskite coexistence throughout the whole D" region*, Earth Plan. Sci. Lett. 293, 90–96 (2010)

[2] A. Bianconi, N. Saini, A. Lanzara, M. Missori, T. Rossetti, H. Oyanagi, H. Yamaguchi, K. Oka, T. Ito, *Determination of the Local Lattice Distortions in the CuO_2 Plane of $La_{1.85}Sr_{0.15}CuO_4$*, Phys. Rev. Lett. 76, 3412 (1996)

[3] N. Poccia, M. Chorro, A. Ricci, Wei Xu, A. Marcelli, G. Campi, A. Bianconi, *Percolative superconductivity in $La_2CuO_{4.06}$ by lattice granularity patterns with μ-XANES scanning*, Appl. Phys. Lett. 104, 221903-1/221903-5 (2014)

[4] M. Fratini, N. Poccia, A. Ricci, G. Campi, M. Burghammer, G. Aeppli, A. Bianconi, *Scale-free structural organization of oxygen interstitials in La_2CuO_{4+y}*, Nature 466, 841 (2010)

[5] N. Poccia, A. Ricci, G. Campi, M. Fratini, A. Puri, D. Di Gioacchino, A. Marcelli, M. Reynolds, M. Burghammer, N. L. Saini, G. Aeppli, A. Bianconi, *Optimum inhomogeneity of local lattice distortions in La_2CuO_{4+y}*, Proc. Nat. Acad. Sci. 109, 15685–15690 (2012)

[6] F. Meirer, J. Cabana, Yijin Liu, A. Mehta, J. C. Andrews, P. Pianetta, *Three-dimensional imaging of chemical phase transformations at the nanoscale with full-field transmission X-ray microscopy*, J. Synchrotron Rad. 18, 773–781 (2011)

[7] Yijin Liu, F. Meirer, Junyue Wang, G. Requena, P. Williams, J. Nelson, A. Mehta, J. C. Andrews, P. Pianetta, *3D elemental sensitive imaging using transmission X-ray microscopy*, Anal. Bioanal. Chem. 404, 1297–1301 (2012)

[8] Yijin Liu, Junyue Wang, M. Azuma, W. L. Mao, Wenge Yang, *Five-dimensional visualization of phase transition in $BiNiO_3$ under high pressure*, Appl. Phys. Lett. 104, 043108 (2014)

Charge transport in nanochannels: a molecular theory

U. M. B. Marconi

CNISM – Universita' di Camerino
Via Madonna delle Carceri 62032 Camerino (MC), Italy

We introduce a theoretical and numerical method to investigate the flow of charged fluid mixtures under extreme confinement. We model the electrolyte solution as a ternary mixture, comprising two ionic species of opposite charge and a third uncharged component. The microscopic approach is based on the kinetic theory and is fully self-consistent. It allows determining configurational properties, such as layering near the confining walls, and the flow properties. We show that, under appropriate assumptions, the approach reproduces the phenomenological equations used to describe electrokinetic phenomena, without requiring the introduction of constitutive equations to determine the fluxes. Moreover, we model channels of arbitrary shape and nanometric roughness, features that have important repercussions on the transport properties of these systems.

Numerical simulations are obtained by solving the evolution dynamics of one-particle phase-space distributions of each species by means of the Lattice Boltzmann method for flows in straight and wedged channels. The results are presented for the microscopic density, the velocity profiles and for the volumetric and charge flow-rates. Strong departures from electroneutrality are shown to appear at the molecular level.

Electrode-electrolyte interphase in negative electrodes for rechargeable Na-ion batteries

M. A. Muñoz-Márquez[1], M. Zarrabeitia[1], E. Castillo-Martínez[1], A. Eguía-Barrio[2], T. Rojo[1,2], M. Casas-Cabanas[1]

[1] *CIC energiGUNE*
Albert Einstein 48, 01510 Miñano, Spain

[2] *Departamento de Química Inorgánica, Universidad del País Vasco UPV/EHU*
P.O. Box 644, 48080 Bilbao, Spain

Nowadays, the Li-ion battery research is focused on the development of high energy and high voltage batteries to cover the needs of the portable electronics market and the electric vehicle industry. However, in order to fulfil the continuously increasing energy demand, more efficient distribution grids and bulk energy storage systems have to be developed. For this, Na-ion batteries are becoming an attractive solution for stationary energy storage; where, despite the increase in the weight from lithium to sodium, the total price is decreased by using an aluminium current collector for anodes with the sodium being far more abundant and easier to obtain than lithium.

Recent works have shown that many lithium ion analogues are successful candidates able to operate as cathodes in sodium ion batteries [1]. Nevertheless when it comes to anodes much more deficiencies are encountered, including, the lack of sodium insertion into graphite along with the fact that a material with a stable SEI layer has not been reported to date [2]. So far, hard carbons and Sn or Sb alloys have produced the most satisfactory results.

A reversible reaction in $Na_2Ti_3O_7$ [3] has been reported at 0.3V, where a reversible phase transition is found to occur between $Na_2Ti_3O_7$ and a $Na_{12}Ti_{10}O_{28}$-like $Na_4Ti_3O_7$ phase. Two Na ions could be inserted per formula unit, leading to a specific capacity of 200 $mA{\cdot}h{\cdot}g^{-1}$. However, despite the optimum performance reported for this electrode material, no information has been gathered on the electrode surface properties as well as on the electrode/electrolyte interface.

Considering the crucial role of the electrode-electrolyte interphase in the electrochemical performance, stability and safety of the cell, a series of photoemission experiments will be presented here. X-ray photoelectron spectroscopy (XPS) being a surface specific technique, it has been found that it is the most powerful technique for probing the chemical nature of the electrochemical interface; other techniques such as surface X-ray diffraction (XRD) or Raman spectroscopy, although very relevant, are less versatile in this respect [4].

Here we present quasi in-situ XPS results that show the formation upon electrochemical cycling vs. Na of a passivating layer in $Na_2Ti_3O_7$ laminates cast on aluminium current collectors and using $NaClO_4$ in ethylene carbonate and propylene carbonate as electrolyte. The behaviour and composition of the electrode surface

was studied along with its stability at different points of the electrochemical curve (Figure 1).

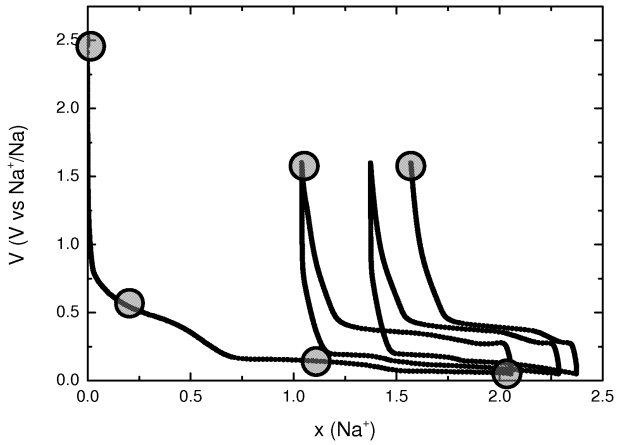

Figure 1: Galvanostatic cycling of $Na_2Ti_3O_7$ vs. Na between 2.5 and 0 V at C/10 from the first to the third oxidation/reduction cycles using 1M NaClO4 in EC:PC as electrolyte at room temperature. Spots indicate where the XPS measurements were performed

The absolute binding energies reported here are slightly different to the ones reported in the literature the reason being the non-uniform charging effects of non-conducting microdomains of salt residuals and reduction products on the surface. Internal references have been used and at the same time reference compounds were measured to corroborate the peak assignment. The majority of peaks could be assigned from relative peak positions obtained from binding energy differences [5] and after measuring the Auger parameter [6].

The XPS experiments were combined with low energy ion etching, thus a depth profile of the passivating layer was obtained. Structural information of the electrode material under study was provided by X-ray diffraction (XRD), which enabled us to have a complete picture of the factors governing the electrode stability.

Despite the formation of a passivating layer, the measured cyclability of the electrode and its specific capacity can position $Na_2Ti_3O_7$ as a cheap and competitive anode for Na-ion batteries which can certainly be further improved after optimization of different parameters of synthesis, laminate preparation and electrolyte formulation.

Acknowledgements
Financial support from the Gobierno Vasco/Eusko Jaurlaritza (ETORTEK CIC energiGUNE 10) is gratefully acknowledged.

References

[1] V. Palomares, P. Serras, I. Villaluenga, K. Hueso, J. Carretero-González, T. Rojo 2012 *Energy Envirom. Sci.* **5**, 5884; S.-W. Kim, D.-H. Seo, X. Ma, G. Ceder, K. Kang 2012 *Adv. Energy Mater.* **2**, 710

[2] Komaba, T. Ishikawa, N. Yabuuchi, W. Murata, A. Ito, Y. Ohsawa 2011 *Appl. Mat. Interf.* **3**, 4165

[3] P. Senguttuvan, G. Rousse, V. Seznec, J.-M. Tarascon, M. R. Palacín 2011 *Chem. Mater.* **23**, 4109
[4] *Lithium-Ion Batteries: Solid-Electrolyte Interphase*, ed. by P. B. Balbuena, Y. X. Wang 2004 Imperial College Press, London
[5] A. M. Andersson, A. Henningson, H. Siegbahn, U. Jansson, U. K. Edström 2003 *J. Power Sources* **119–121**, 522
[6] C. D. Wagner, A. Joshi 1988 *J. Electron Spectrosc. Relat. Phenom.* **47**, 283

Spectroscopy of potential functional materials for quantum electronics based on borate glasses

B. V. Padlyak[1,2]

[1] *Sector of Spectroscopy, Vlokh Institute of Physical Optics*
Dragomanov 23, 79005 Lviv, Ukraine

[2] *Division of Spectroscopy of Functional Materials, Institute of Physics*
University of Zielona Góra
Szafrana 4a, 65-516 Zielona Gora, Poland

A series of un-doped borate glasses with $Li_2B_4O_7$, $LiKB_4O_7$, CaB_4O_7, and $LiCaBO_3$ compositions of high optical quality and chemical purity was obtained from corresponding polycrystalline compounds using standard glass synthesis and technological conditions, described in [1]. The optically thermopoled second harmonic generation (SHG) effect in the $Li_2B_4O_7$, $LiKB_4O_7$, CaB_4O_7, and $LiCaBO_3$ glasses was investigated and analysed [2] and the perspectives of application of borate glasses for SHG were considered.

A series of Cr-doped borate glasses with $Li_2B_4O_7$:Cr, $LiKB_4O_7$:Cr, CaB_4O_4:Cr, and $LiCaBO_3$:Cr chemical compositions containing 0.4, 0.5 and 1.0 mol.% Cr_2O_3 was obtained from corresponding polycrystalline compounds using standard glass synthesis according to [3]. The X-band EPR spectroscopy showed that the Cr impurity was incorporated in the borate glass network as isolated Cr^{3+} ($3d^3$, $^4A_{2g}$) centres and Cr^{3+} pair centres coupled by magnetic dipolar and exchange interactions. All Cr-related EPR signals in the investigated Cr-doped glasses were identified and interpreted [3]. The EPR spectral parameters of both, Cr^{3+} and Cr^{3+}–Cr^{3+} centres, in glasses with $Li_2B_4O_7$:Cr, $LiKB_4O_7$:Cr, CaB_4O_7:Cr, and $LiCaBO_3$:Cr compositions were measured and analysed [3]. All transitions in optical absorption, luminescence excitation and emission spectra of the Cr-doped borate glasses were identified. The octahedral (cubic) crystal field strength ($10Dq$) and Racach parameters (B and C) for Cr^{3+} centres in the investigated glasses were calculated [3,4]. Narrow and broad emission bands in red – near infrared spectral region were assigned to the $^2E_g(F) \rightarrow {}^4A_{2g}(F)$ (R_1 line) and $^4T_{2g}(F) \rightarrow {}^4A_{2g}(F)$ (electron-vibration) transitions, which corresponded to Cr^{3+} centres in high-field and low-field sites, respectively [3]. The lifetimes of high-field and low-field Cr^{3+} centres were estimated. The excited state characteristics were measured by means of the excited state absorption (ESA), optical gain and bleaching spectra for glasses with $Li_2B_4O_7$ and $LiKB_4O_7$ compositions activated by Cr^{3+} ions [4]. It was shown that the $LiKB_4O_7$:Cr glass revealed a broadband optical gain peaking around 1050 nm, thus making this material a potential candidate for construction of a tuneable solid-state laser or a broadband amplifier operating in the near infrared spectral region.

A series of Nd-doped borate glasses with $Li_2B_4O_7$:Nd, CaB_4O_7:Nd, and $LiCaBO_3$:Nd compositions containing 0.5 and 1.0 mol.% Nd_2O_3 was obtained from correspond-

ing polycrystalline compounds using a standard glass technology [1,5]. It was shown by optical and EPR spectroscopy that the Nd impurity was incorporated in glasses with $Li_2B_4O_7$:Nd, $LiCaBO_3$:Nd, and CaB_4O_7:Nd compositions as Nd^{3+} ($4f^3$, $^4I_{9/2}$) ions. All the observed transitions of the Nd^{3+} centres in the optical absorption and luminescence spectra were identified. The oscillator strengths (f_{theor}) and phenomenological intensity parameters Ω_t ($t = 2$, 4, 6) for glasses containing 1.0 mol.% Nd_2O_3 were calculated using the standard Judd-Ofelt theory [5]. The radiative transitions rates (W_r), branching ratios (β), and radiative lifetimes (τ_{rad}) for Nd^{3+} centres in the investigated glasses were calculated and analysed in comparison with the corresponding parameters for Nd^{3+} centres in other borate glasses with different compositions. The measured lifetimes for Nd^{3+} centres in the $^4F_{3/2}$ emitting level were compared with those calculated and the quantum efficiencies (η) of the investigated glasses were estimated [5]. Perspectives of application of $Li_2B_4O_7$:Nd, $LiCaBO_3$:Nd, and CaB_4O_7:Nd glasses for Nd^{3+}- lasers ($^4F_{3/2} \rightarrow {}^4I_{11/2}$ emitting channel), particularly for LED-pumped lasers, were considered.

References

[1] B. V. Padlyak, S. I. Mudry, Y. O. Kulyk, A. Drzewiecki, V. T. Adamiv, Y. V. Burak, I. M. Teslyuk, Synthesis and X-ray Structural Investigation of Undoped Borate Glasses, *Mater. Sci. Poland* **30** (2012) 264–273

[2] B. V. Padlyak, V. T. Adamiv, Ya. V. Burak, M. Kolcun, Optical Harmonic Transformation in Borate Glasses with $Li_2B_4O_7$, $LiKB_4O_7$, CaB_4O_7, and $LiCaBO_3$ Compositions, *Physica B*, **412** (2013) 79–82

[3] B. V. Padlyak, W. Ryba-Romanowski, R. Lisiecki, V. T. Adamiv, Ya. V. Burak, I. M. Teslyuk, Synthesis, EPR and Optical Spectroscopy of the Cr-doped Tetraborate Glasses, *Opt. Mater.* **34** (2012) 2112–2119

[4] J. Mikulski, Cz. Koepke, K. Wiśniewski, B. V. Padlyak, V. T. Adamiv, Ya. V. Burak, Excited State Characteristics of the $Li_2B_4O_7$ and $KLiB_4O_7$ Glasses activated by Cr^{3+} Ions, *Opt. Mater.* (2014) submitted

[5] B.V. Padlyak, W.Ryba-Romanowski, R.Lisiecki, V.T. Adamiv, Ya. V. Burak, I. M. Teslyuk, Optical Spectroscopy of Nd-doped Borate Glasses, *Proceedings of the International Conference on Oxide Materials for Electronic Engineering (OMEE-2012)*. National University "Lviv Polytechnic" (2012) pp. 200–201

Real time quantum tunneling

G. J. Papadopoulos

Department of Physics, Solid State Physics Section, University of Athens
Panepistimiopolis, Athens 157 84 Zografos, Athens, Greece

The time evolution of the charge and current densities stemming from an initial state of a charged particle in the form of a wave packet approaching from the left hand side a square barrier is studied. In particular, the space distribution at a given time of the above densities is given. Furthermore, the evolution in time at the entrance and exit of the barrier is given. The numerical results show retrogression in the current density on the left hand side of the barrier, which means that we have reversal in the current density. However, charge entering the barrier over a long time equals the corresponding charge exiting the barrier. Owing to the fact that the wave packet expands on both of its sides, as time goes by, it is possible to have transmission even if the particle's initial momentum points away from the barrier. This effect is exemplified for the case of small initial momentum.

Band-edge BCS-BEC crossover in a two-band superconductor: physical properties and detection parameters

A. Perali[1], A. Guidini[2]

[1] *School of Pharmacy, Physics Unit, University of Camerino 62032 Camerino, Italy*

[2] *School of Science and Technology, Physics Division, University of Camerino 62032 Camerino, Italy*

Superconductivity in iron-based, magnesium diborides, and other novel superconducting materials has a strong multi-band and multi-gap character [1] and recent experimental evidence supports the possibility for a BCS-BEC crossover induced by strong-coupling and proximity of the chemical potential to the band edge of one of the bands [2,3]. Here we study the simplest theoretical model which accounts for the BCS-BEC crossover in a two-band superconductor, considering tunable interactions and different energy separations between the bands. Mean-field results for the condensate fraction, the correlation length, and the superconducting gaps are reported in typical crossover diagrams to locate the boundaries of different BCS, crossover and BEC regimes when the band edge is approached. When the superconducting gap is of the order of the local chemical potential, superconductivity is in the crossover regime of the BCS-BEC crossover and the Fermi surface of the small band is completely smeared by the gap opening. In this situation, small and large Cooper pairs coexist in the total condensate, which is the optimal condition for high-T_c superconductivity [4]. The ratio between the gap and the Fermi energy in a given band results to be the best detection parameter for experiments to locate the system in the BCS-BEC crossover. Using the available experimental data, our analysis shows that iron-based superconductors have the partial condensate of the small Fermi surface which is in the crossover regime of the BCS-BEC crossover [5], supporting in this way the recent ARPES findings [6,7].

References

[1] S. V. Borisenko et al. 2012 *Symmetry* **4**, 251; see also the videos of the MultiSuper 2014 conference in Camerino: http://www.multisuper.org

[2] D. Innocenti, N. Poccia, A. Ricci, A. Valletta, S. Caprara, A. Perali, and A. Bianconi 2010 *Phys. Rev. B* **82**, 184528

[3] A. Bianconi 2013 *Nature Phys.* **9**, 536

[4] A. Perali, C. Castellani, C. Di Castro, M. Grilli, E. Piegari, and A. A. Varlamov 2000 *Phys. Rev. B* **62**, R9295

[5] A. Guidini and A. Perali 2014 submitted to SUST special issue on Multicomponent Superconductivity; arXiv: 1407.3109

[6] Y. Lubashevsky, E. Lahoud, E. Chashka, E. Podolsky, and A. Kanigel 2012 *Nat. Phys.* **8**, 309

[7] K. Okazaki *et al.* 2013; arXiv:1307.7845, preprint

Temperature dependence of diffusion induced Ge nanowire grown by MBE

S. J. Rezvani[1,2], L. Boarino[2], L. Favre[3], F. Celegato[2], I. Berberzier[3], N. Pinto[1,4]

[1] *Scuola di Scienze e Tecnologie, Universita di Camerino Camerino, Italy*

[2] *Istituto Nazionale di Ricerca Metrologica, INRiM Torino, Italy*

[3] *IM2NP-UMR CNRS Aix Universite de Marseille Marseille, France*

[4] *INFN Sezione di Perugia, Italy*

Recently attention has been attracted to Germanium again due to its interesting properties and compatibility with the conventional CMOS technology, while having an enhanced mobility it can be used to improve the electronic and optical properties in many applications such as photovoltaics [1], electronics [2] or sensors [3]. A well studied and highly controllable method amongst various methods of semiconductor nanowire synthesis is the vapor liquid solid (VLS) method, introduced by Wagner *et al* [4]. In particular, the VLS mechanism occurs via a diffusion induced (DI) growth for NWs fabricated by MBE, since the metal droplet does not act as a catalyst but as a seed for diffused adatoms [5]. In this model the diameter of the wires is strongly dependent on the initial diameter of metal droplets which facilitates growth by nucleation in a supersaturated metal-semiconductor eutectic liquid [6]. It has been also suggested that the vertical growth rate of the wires is strongly dependent on the droplet radius with a $1/R$ relation, specially for R between 5 to 70 nm. Although, many works have been performed on the chemical deposition of nanowires [7], few studies are available on the growth mechanism and geometrical frustrations of germanium NWs grown by MBE, and in particular, the role played by the growth temperature. In fact, for the VLS method, it is reported that the growth of semiconductor NWs ceases at temperatures above 500°C [8]. It is now generally believed that this effect is mainly due to the high desorption rate of the adatomes from droplets at high temperatures which, becoming greater than the adsorption rate, stops the NW growth. However, a systematic and detailed study to clarify the mechanism behind the effect of the temperature is still lacking. In the present work, we investigated the effect of the temperature on Au mediated growth of Ge nanowires fabricated by the MBE technique. The structural and morphological properties of Ge NWs were explained in the framework of a phenomenological model based on the DI-VLS theory.

References

[1] B. Tian, X. Zheng, T. J. Kempa, Y. Fang, N. Yu, G. Yu, J. Huang, and C. M. Lieber 2007 *Nature* **449**, 885

[2] N. J. Quitoriano and T. I. Kamins 2008 *Nano Letters* **8**, 4410
[3] Y. Cui, Q. Wei, H. Park, and C. M. Lieber 2001 *Science* (New York, N.Y.) **293**, 1289
[4] R. S. Wagner and W. C. Ellis 1964 *Applied Physics Letters* **4**, 89
[5] V. G. Dubrovskii, N. V. Sibirev, J. C. Harmand, and F. Glas 2008 *Physical Review B* **78**, 235301
[6] K. Schwarz and J. Tersoff 2009 *Physical Review Letters* **102**, 206101
[7] K. Schwarz, J. Tersoff, S. Kodambaka, Y.-C. Chou, and F. Ross 2011 *Physical Review Letters* **107**, 265502
[8] J. Schmidtbauer, R. Bansen, R. Heimburger, T. Teubner, T. Boeck, and R. Fornari 2012 *Applied Physics Letters* **101**, 043105

Characterization of solid-state dye-sensitized solar cells incorporating various hole transport materials and metal free organic dyes

S. K. Shah[1,4], M. Abbas[1], T. T. Bui[3], X. Sellenave[3], J. Massin[2], C. Olivier[2], T. Toupance[2], F. Goubard[2], L. Hirsch[1]

[1] *University of Bordeaux, Laboratoire de l'Intégration du Matériau au Système (IMS) Institut Polytechnique de Bordeaux CNRS UMR 5218, ENSCBP, 16 Pey Berland, 33607 Pessac Cedex, France*

[2] *LPPI, Universite de Cergy-Pontoise 5 Mail Gay-Lussac, 95031 Cergy-Pontoise Cedex, France*

[3] *University of Bordeaux, Institut des Sciences Moléculaires (ISM) UMR 5255-CNRS, 351 cours de la Libération, 33405 Talence, France*

[4] *Department of Physics, Abdul Wali Khan Univeristy Mardan 22300 KPK, Pakistan*

Dye-sensitized solar cells (DSSCs) are based on low-cost materials [1], low temperature processing, and reel-to-reel printing [2,3] with expected power conversion efficiency up to 20% [4]. In solid state dye sensitized solar cells, liquid electrolytes have been replaced with a solid noncorrosive, nonvolatile hole-transport material to further overcome problems associated with fabrication and materials lifetime. Despite consistent improvement in the cell performance, device components such as electron-transporting anode, the light-absorbing dye sensitizers and the hole-transporting materials still require intensive studies to overcome the bottle neck in achieving high efficiency from this type of devices. In this work, we report our studies on solid-state dye-sensitized solar cells utilizing different hole-transporting materials (HTMs) and organic dyes with high molar extinction coefficients aiming at optimizing device performance and stability of ssDSSCs. The organic dye molecules synthesized are carbozole based push-pull molecules with different end groups such as OMe, tBu and thiophene for JM121, JM131, and JM164 respectively. Electrical characterization was carried out for ssDSSCs based on these dyes. JM121, JM131 perform apparently similar giving power conversion efficiencies (PCE) of 1.85% and 1.63%, while JM164 has the maximum PCE of 0.64%. Relatively stable devices were obtained the dye JM131 after 120mins of continuous operation in air without sealing with final PCE of 0.93%. The hole transport materials based on triphenylamine(TPA) moieties contains thiophene units in case BT41 or carbazole units in the case of BT58 and BT63 with different in alkyl chain length. Electrical characterization was carried out for all BT based HTMs and compared with standard hole transport material, spiro-MeOTAD. The power conversion efficiencies obtained from ss-DSSCs based on BT41, BT58 and BT63 1.2% 1.81% and 1.6% respectively as compared to 4.44% from the reference

device. However, stability tests after 120mins of continuous operation in air without sealing show a slight decrease in PCE up to 0.4%, 0.5% and 0.3%, respectively as compared to 1.17% from the reference device.

References

[1] G. Hashmi, K. Miettunen, T. Peltola, J. Halme, I. Asghar, K. Aitola, M. Toivola, P. Lund 2011 *Renewable Sustainable Energy Rev.* **15**, 3717
[2] E. Crossland, N. Noel, T. Leijtens, V. Sivaram, J. Alexander-Webber, H. Snaith 2013 *Nature* **495**, 215
[3] T. Yamaguchi, N. Tobe, D. Matsumoto, T. Nagai, H. Arakawa, *Sol. Energy Mater. Sol. Cells 2010*, **94**, 812
[4] H. Snaith 2010 *Adv. Funct. Mater.* **20**, 13
[5] M. K. Nazeeruddin, T. Bessho, L. Cevey, S. Ito, C. Klein, F. De Angelis, S. Fantacci, P. Comte, P. Liska, H. Imai, M. Graetzel 2007 *J. Photochem. Photobiol. A* **185**, 331

Heteroatom modified silica as a suitable co-dopant precursor in synthesis of silicate phosphors

K. Szczodrowski[1], J. Barzowska[1], N. Gorecka[1],
K. Anders[2], R. Piramidowicz[2], M. Grinberg[1]

[1] *Institute of Experimental Physics, University of Gdansk*
Wita Stwosza 57, 80-952 Gdansk, Poland

[2] *Institute of Microelectronics and Optoelectronics, Warsaw University of Technology*
Koszykowa 75, 00-662 Warsaw, Poland

Heteroatom (Me) modified silica is usually used as a catalyst or adsorbent in many technological processes due to higher surface acidity/reactivity compared with pure silica. The surface properties of silica depend on the type of the doped activator. Some of the frequently applied heteroatoms are aluminum and titanium. The increased surface reactivity of Al- or Ti-doped silica is attributed to the presence of additional Bronsted and/or Lewis acid sites due to aliovalent substitution of Si^{4+} with Al^{3+} in the case of Al-doped silica and changes of the charge density of Si^{4+} and thus the weakness of O-H bonds in the case of silica doped with Ti^{4+}. However, modified silica can be also successfully used as a precursor of Si^{4+} and Me^{n+} in synthesis of silicate based luminescent materials.

Ti- and also Al-modified silica was used to obtain titanium and aluminum co-doped Sr_2SiO_4:Eu^{2+} phosphor. Heteroatom doped silica in form of mesoporous SBA-15 was synthesized using the sol-gel technique whereas the synthesis of strontium orthosilicate was performed via the solid state synthesis method. Modified silica was used as one of the reagents during the phosphor synthesis. In the case of Sr_2SiO_4:Eu^{2+} co-doped with titanium, the material had strong luminescence which consisted of two partially overlapping broad bands with the maxima at 480 nm and 570 nm. The bands were attributed to the $4f65d1 > 4f7$ transitions in Eu^{2+} occupying two different Sr^{2+} sites in the Sr_2SiO_4 crystal lattice. The Sr_2SiO_4:Eu^{2+} parent phosphor undoped with Ti^{4+} exhibited also luminescence that lasted for few seconds at room temperature after stopping the excitation. The persistent luminescence was relatively weak at ambient conditions but could be easily seen in dark with the eye. The observed persistent luminescence could be significantly enhanced after introduction of titanium ions into the silicate lattice. We proved that in addition to the concentration of Eu^{2+} and Ti^{4+} it was also the form of the titanium precursor used in the synthesis that influenced the persistent luminescence phenomenon observed in the $Sr_2Si_{0.95}Ti_{0.05}O_4$:$Eu^{2+}$ phosphor. The use of the Ti-modified silica instead of titania (TiO_2) caused much more longer duration of the persistent luminescence. For all the investigated samples the persistent luminescence was dominated only by one band with the maximum at 570 nm, independently of the excitation wavelength. It led to the conclusion that traps responsible for long-lasting luminescence of Sr_2SiO_4:Eu^{2+} and Sr_2SiO_4:Eu^{2+}, Ti^{4+} observed at room temperature, deactivated directly and only

through Eu^{2+} ions occupying nine coordinated SII sites. The enhance of the luminescence duration observed in the Ti doped sample was attributed to the creation of Ti^{3+} ions after the reduction process and thus the presence of the charge compensating the defects.

The Al co-doped strontium orthosilicate was obtained using Al-modified SBA-15 to investigate the influence of the aliovalent substitution ($Al^{3+} > Si^{4+}$) on the luminescent properties of Sr_2SiO_4:Eu^{2+}. The above mentioned substitution caused the stability of part of Eu^{3+} ions under typical conditions of the europium reduction (1250°C, 5% H_2 in N_2). The negative charge created after substitution could be diminished by formation of appropriate point defects or maintenance of a higher oxidation state of europium. As the creation of defects required that energy be provided, the process of creation was not favored and the emission of Eu^{3+} could be observed even after reduction. Moreover the ratio of $[Eu^{3+}]/[Eu^{2+}]$ in the phosphor could be easily controlled via concentration of Al^{3+} ions introduced into the silicate lattice.

Acknowledgements
This work was supported by POIG.01.01.02-02-006/09 project co-funded by the European Regional Development Fund within the Innovative Economy Program. Priority I, Activity 1.1. Sub-activity 1.1.2, which is gratefully acknowledged.

Physical properties of glass with high manganese content

L. Wicikowski, L. Murawski

Department of Applied Physics and Mathematics, Faculty of Applied Physics and Mathematics, Gdansk University of Technology
Narutowicza 11/12, 80-233 Gdansk, Poland

Glasses with manganese oxide have received much attention because of their importance in technological applications such as catalysts, sensors and new magnetic materials. These materials can also be used in spintronic devices. Especially, manganese silicate, borate and phosphate glasses exhibit unique electrical and magnetic properties because they can be prepared with a high amount of MnO, even exceeding 50 mol%. The content of manganese, the valence states and distribution homogeneity in the glass network depend mainly on the properties of modifiers and glass formers, the size of glass forming ions, their field strength and mobility of modifier cations. Hence, the relation between the physical properties of the host glass and the ionic state and local structure of the manganese atoms is a crucial aspect of the design of materials for special applications.

Manganese silicate glasses exhibit interesting magnetic properties which have been investigated by several authors. It has been found that magnetic susceptibility shows Curie-Weiss behavior with a large negative paramagnetic Curie temperature indicating the presence of strong antiferromagnetic exchange interaction [1]. In addition, some anomalous behavior in specific heat has been observed [2]. These anomalies can be explained by assuming that glasses contain small (~ 5 nm) regions with an antiferromagnetical orientation. However, in the literature, there is hardly any information about their electrical properties. McMillan [3] has shown that when MnO-Al_2O_3-SiO_2 glasses are submitted to thermal treatment in air at 600°C the surface resistivity decreases about 5 orders of magnitude. This effect can be explained as a result of conversion of a part of Mn^{2+} ions to the Mn^{3+} state.

Manganese in glasses can play a role of a glass modifier (with the coordination number of six) or a network former (with tetrahedral coordination). In silicate glasses Mn^{2+} and Mn^{3+} ions occupy tetrahedral and octahedral sites and the amount of each Mn valence state can be modified by high temperature treatment in oxygen atmosphere. The presence of manganese ions in different valence states and the Mn^{2+}/Mn^{3+} ratio significantly affect the electrical conductivity of these glasses, which can be described by the small polaron hopping between Mn^{2+} and Mn^{3+}. Our experiments have shown that the electrical conductivity in borate and phosphate glasses submitted to high temperature treatment in oxygen atmosphere can also be changed in a controllable way (choosing proper treatment time and temperature). However, the electrical properties of manganese borate and phosphate glasses are different from

manganese silicate. Additionally, silicate glasses with manganese are less homogeneous and exhibit phase separation in nanoscale. For this reason, regions with high concentration of magnetic ions (monodomains) can be found in these materials.

Differences in electrical conductivity and magnetic properties of manganese glasses with different glass formers can be explained by determining the oxidation state, local environment and magnetic moments of manganese ions.

References

[1] R. A Verhelst *et al.* 1975 *Phys. Rev. B* **11** 4427
[2] G. C. Lau *et al.* 2009 *Phys. Rev. B* **89** 214414
[3] P. W. MacMillan 1962 *Adv. Glass Technology*, Plenum, New York

Highly efficient calculation method of bond order parameters

Sz. Winczewski[1,2], J. Rybicki[1,2]

[1] *Department of Solid State Physics, Faculty of Applied Physics and Mathematics Gdansk University of Technology Narutowicza 11/12, 80-233 Gdansk, Poland*

[2] *TASK Computer Center, Gdansk University of Technology Narutowicza 11/12, 80-233 Gdansk, Poland*

Bond order parameters method [1] is widely utilized throughout the physical sciences to characterize local particle structure of computer simulated materials [2–4]. The computing process of bond order parameters involves a very frequent evaluation of spherical harmonics, which makes the method computationally extremely expensive. A new computational scheme for the evaluation of bond order parameters has been proposed and implemented. The numerical experiments that have been carried out showed that the developed new algorithm increases the efficiency of bond order parameters evaluation by 60–100 times, thus making the method applicable to the characterization of the structure of large-scale atomic systems.

Acknowledgements

This work was co-financed by the European Union within European Regional Development Fund, through grant Innovative Economy (POIG.02.03.00-00-096/10), and by the Ministry of Science and Higher Education (grant IP2012 043972).

References

[1] Steinhardt P J, Nelson D R and Ronchetti M 1983 *Phys. Rev. B* **28** 784
[2] Wang Y, Teitel S and Dellago Ch 2005 *J. Chem. Phys.* **122** 214722
[3] Moroni D, ten Wolde P R and Bolhuis P G 2005 *Phys. Rev. Lett.* **94** 235703
[4] Desgranges C and Delhommelle J 2008 *Phys. Rev. B* **77** 054201

Hard X-ray absorption spectroscopy in application to ex-situ and in-situ structural analysis of close-packing metal nanoparticles

A. Witkowska[1], E. Principi[2], G. Greco[2], A. Di Cicco[2], S. Dsoke[3], R. Marassi[3]

[1] *Department of Solid State Physics, Faculty of Applied Physics and Mathematics Gdansk University of Technology Narutowicza 11/12, 80-233 Gdansk, Poland*

[2] *Physics Division, School of Science and Technology, University of Camerino Via Madonna delle Carceri 9, I-62032 Camerino (MC), Italy*

[3] *Chemistry Division, School of Science and Technology, University of Camerino Via S. Agostino 1, I-62032 Camerino (MC), Italy*

Understanding the structure and dynamics of nanomaterials as well as their physico-chemical properties is currently regarded as a challenging research activity having crucial consequences in the material design for various novel applications. Especially, nanoparticles of close-packing metals (like Pt, Cu, Au, Ag, Co, Pd, Ti, Ni and their alloys or composites) are now commonly used in our daily life (self-cleaning glasses, disinfectant tiles, filters for air purification, catalysts, photocatalysts) and still play an important role, *e.g.* in developing smart materials which can simultaneously sense and destroy harmful chemical contaminants from the environment and in simultaneous imaging (diagnostics) and therapeutic applications (magnetic nanoparticles) [1,2]. Therefore, nowadays, control of the structure of metallic nanoparticles is of really high importance and impact for the technological progress.

Our main interest has focused on materials composed of small quantities of Pt and Pt-based alloy nanoparticles (3 nm or less in diameter) embedded in some matrix, inter alia, in advanced, multicomponent electrochemically active matrices which are widely used in the fuel cell (FC) technology. Detailed studies of their micro/nanoscopic properties are still relatively difficult to perform, especially when they are under real operating conditions. X-ray absorption spectroscopy (XAS) has been recognized as a suitable probe for this kind of study [3]. In numerous papers, we have shown that XAS provides useful complementary information concerning the subtle structural and electronic changes caused by various factors, like the electrocatalyst preparation method, FC working conditions, ageing (see e.g. [4,5,6,7,8]). However, it should be underlined that high-quality X-ray absorption fine structure (XAFS) spectra collected in a wide energy range (challenging scientific task for in situ measurements) and an advanced methodology of multiple-scattering (MS) XAFS data analysis are crucial points to fully exploit this technique to the structural study of nano-systems.

In this contribution, some results of XAFS measurements performed ex-situ and in-situ for nanostructured Pt-based electrocatalysts will be presented and discussed

to demonstrate the potentiality and utility of the XAS technique (not only for the fuel cell technology). It will be shown that XAS in combination with transmission electron microscopy (TEM), X-ray diffraction (XRD) and X-ray photoemission (XPS) results can be a source of unique structural and dynamical information regarding close-packing nanoparticles (including their size and shape, composition and structure as a function of the distance from the surface, the degree of chemical and structural disorder, the role and distribution of surface atoms).

References

[1] Kamat P V, Meisel D 2003 *C. R. Chimie* **6** 999
[2] Ho D, Sun X, Sun S 2011 *Acc Chem Res.* **44** (10) 875
[3] Russell A E, Rose A 2004 *Chem. Rev.* **104** 4613
[4] Witkowska A, Principi E, Di Cicco A, Dsoke S, Marassi R, Olivi L, Centazzo M, Rossi Albertini V 2008 *J. Non-Crystalline Solids* **354** 4227
[5] Witkowska A, Dsoke S, Principi E, Marassi R, Di Cicco A, Rossi Albertini V 2008 *J. Power Sources* **178** (2) 603
[6] Principi E, Witkowska A, Dsoke S, Marassi R, Di Cicco A 2009 *Phys. Chem. Chem. Phys.* **11** (43) 9987
[7] Greco G, Witkowska A, Minicucci M, Olivi L, Principi E, Dsoke S, Moretti A, Marassi R, Di Cicco A 2012 *J. Physical Chemistry C* **116** (23) 12791
[8] Witkowska A, Greco G, Dsoke S, Marassi R, Di Cicco A 2014 *J. Non-Crystalline Solids*, doi:10.1016/j.jnoncrysol.2013.12.022

Mesoporous silica containing USPIO in ibuprofen delivery and release systems

B. Zapotoczny[1], M. R. Dudek[1], J. J. Koziol[2], G. Garbacz[3], E. Gronczewska[2], A. Defort[2]

[1] *Institute of Physics, University of Zielona Góra*
Szafrana 4a, 65-069 Zielona Gora, Poland

[2] *Faculty of Biological Sciences, University of Zielona Góra*
Szafrana 1, 65-516 Zielona Gora, Poland

[3] *Physiolution GmbH*
Walther-Rathenau-Straße 49a, 17489 Greifswald, Germany

One of the characteristics that distinguish anticancer agents from other drugs is the frequency and severity of side effects at therapeutic doses[1]. Sometimes certain side effects can have long lasting or permanent effects which do not permit further treatment. Therefore much work has been performed to synthesize a nanocapsule which would deliver the drug in a certain place in the body, reducing the side effects for the whole body. It is mesoporous silica that is often used in such systems. It has a high, reaching 1000 cm^3/g, specific surface area and a controlled pore size and volume which is the reason why these materials are perfect for storage of chemical compounds, including drugs [2–4]. Additionally, the chemical, mechanical and thermal stability of silica makes this material very suitable for further modifications. Moreover, when magnetic nanoparticles are added to silica capsules, it is possible to drag them with a magnetic field or trough an alternating high frequency magnetic field to increase their temperature, changing the local environment. The presentation will be devoted to discussing the results of the synthesis of USPIO (Ultra-small Superparamagnetic Iron Oxides) nanoparticles inside porous silica of two types: 200 nanometer silica spheres (MSS) with a pore size equal to 4 nm (Sigma-Aldrich) and Mobil Composition of Matter (MCM-41) with a pore size of 2.5 nm (Sigma Aldrich) [5,6] and the use of these materials in a delivery and release system of a drug using ibuprofen as an example.

Acknowledgements
The author is a scholar within Sub-measure 8.2.2, Regional Innovation Strategies, Measure 8.2, Transfer of knowledge, Priority VIII Regional human resources for the economy Human Capital Operational Programme co-financed by the European Social Fund and the state budget.

References

[1] Remesh A 2012 *Int. J. Basic Clin. Pharmacol.* **1** (1) 2-12
[2] Nandiyanto A B D, Kim S, Iskandar S, Okuyama K 2009 *Microporous and Mesoporous Materials* **120** 447–453

[3] Vallet-Regı Balas M F, Colilla M, Manzano M 2007 *Solid State Sciences* **9** 768–776
[4] Nandiyanto A B D, Okuyama K 2011 *Advanced Powder Technology* **22** 1–19
[5] Zapotoczny B, Dudek M R, Kozioł J J 2013 *Patent: PL406711*
[6] Zapotoczny B, Guskos N, Kozioł J J, Dudek M R, sent 8.04.2014 *Journal of Magnetism and Magnetic Materials*

POSTERS

On the mechanical properties of JOZ and other recently discovered zeolites

D. Attard[1], C. Calleja[2], R. Cauchi[1], J. N. Grima[1,2]

[1] *Metamaterials Unit, University of Malta*
Msida, MSD2080, Malta

[2] *Department of Chemistry, University of Malta*
Msida, MSD2080, Malta

Auxetic materials exhibit the unusual property of getting fatter when stretched and thinner when compressed, i.e. have a negative Poisson's ratio. This phenomenon has been reported in a number of material classes, including silicates, zeolites and aluminophospahtes such as α-cristobalite, NAT [1], THO [1] and APD [1,2], amongst others. In this study, force-field based simulations are used to predict the Poisson's ratio of the SiO_2 equivalents frameworks of five recently discovered zeolites: IRR [3], JOZ [4], JSN [5], JST [6] and LTJ [7], using different force-fields. Of these force-fields, the CVFF [8] and the Burchart [9] force-fields were found to be the most likely to offer a faithful representation of these frameworks. These two force-fields have predicted auxeticity in all three major planes of siliceous LTJ and also in the (100) plane of the siliceous JOZ framework, with maximum auxeticity occurring on axis. The studies show that in the case of siliceous JOZ, the projection of its geometry in the (100) plane is suggestive of the connected square geometry, which is very closely associated with auxetic behaviour. In fact, a study of the deformation mechanism at the nanoscale level has showed that a 'rotating semi-rigid unit' mechanism is responsible for the predicted auxeticity, with simultaneous rotations and deformations of the projected 'semi-rigid units'. The extent of rotation of the units, which is thought to be the main cause for the auxetic behaviour has been found to be more pronounced than the deformation of the units themselves. It is also being hypothesised that, given the similarity between the simulated system and the true JOZ framework, the latter may also be auxetic.

References

[1] J. N. Grima, R. Jackson, A. Alderson and K. E. Evans 2000 *Adv. Mater.*, **12** 1912.
[2] R. Cauchi, M. Zammit, D. Attard, R. Gatt, J. Rybicki, Sz. Winczewski and J. N. Grima, *10th Conference on Functional and Nanostructured Materials*, September 2013, Poros, Greece.
[3] J. Jiang, J. L. Jorda, M. J. Diaz-Cabañas, J. Yu and A. Corma 2010 *Angew. Chem. Int. Ed.*, **49** 4986
[4] J. A. Armstrong and M. T. Weller 2010 *J.Am. Chem. Soc.*, **132** 15679
[5] Z. Liu, X. Song, J. Li, Y. Li, J. Yu and R. Xu 2012 *Inorg. Chem.*, **51** 1969
[6] Y. Han, Y. Li, J. Yu and R. Xu 2011 *Angew. Chem. Int. Ed.*, **50** 3003

[7] R. W. Broach and R. M. Kirchner 2011 *Microporous Mesoporous Mat.*, **143**, 398
[8] P. Dauber-Osguthorpe, V. A. Roberts, D. J. Osguthorpe, J. Wolff, M. Genest and A. T. Hagler 1998 *Proteins: Structure, Function and Genetics*, **4** 31
[9] E. De Vos Burchart, H. Van Bekkum and B. Van de Graaf 1992 *J. Chem. Soc., Faraday Transactions*, **88** 2761

Stent geometry design

D. Attard[1], R. Gatt[1], L. Mizzi[1], A. R. Casha[1,2], K. Dudek[1], W. Wolak[1], J. N. Grima[1,3]

[1] *Metamaterials Unit, Faculty of Science, University of Malta Msida MSD 2080, Malta*

[2] *Faculty of Medicine and Surgery, University of Malta Msida MSD 2080, Malta*

[3] *Department of Chemistry, Faculty of Science, University of Malta Msida MSD 2080, Malta*

Stents are tubular expanding structures which are used to open and provide support in narrow conduits within the body and thus prevent stenosis (abnormal narrowing of a blood vessel or any other tubular organ). It is a well-known fact that the mechanical properties, which determine the suitability and effectiveness, of these devices are defined mainly by two components, the constituting material and the design pattern of the stent itself. Accordingly, in this work we investigated the properties of stent designs based on the hexagonal honeycomb geometry, a geometry which has the potential to exhibit auxeticity and thus is expected to confer superior property to the stent. This was done through 2D and 3D modelling and simulation of several honeycomb stents based on the re-entrant, non re-entrant and hybrid geometries using the Finite Element Method. The results obtained show that although some configurations are better suited for stent designs than others, none of the designs exhibit all desired properties, highlighting the difficulties encountered in finding the ideal stent design.

Acknowledgements
This work has been funded by the Malta Council for Science and Technology through the R&I-2011–024 Project (Smart Stents). The authors would like to thank the industrial partners involved in this project, Halmann Vella Group and Tek-Moulds Precision Engineering Limited. Equipment purchased through the European Regional Development Fund, Project ERDF-080 'A Supercomputing Laboratory for the University of Malta' has also been used.

EPR study of $Ni_2Fe_{1-x}In_xVO_6$ solid solutions

M. Bobrowska[1], J. Typek[1], E. Filipek[2], A. Paczesna[2]

[1] *Institute of Physics, West Pomeranian University of Technology*
Al. Piastow 48, 70-311 Szczecin, Poland.

[2] *Department of Inorganic and Analytical Chemistry*
West Pomeranian University of Technology
Al. Piastow 42, 71-065 Szczecin, Poland

This work presents the results of the EPR study of $Ni_2Fe_xIn_{1-x}VO_6$ new solid solutions, where $x = 0,\ 0.10,\ 0.25,\ 0.50,\ 0.75,\ 0.90,\ 1.00$. Monophasic samples of $Ni_2In_{1-x}Fe_xVO_6$ could be obtained by two methods. The first involves heating in air of two isostructural compounds Ni_2InVO_6 and Ni_2FeVO_6. The resulting solution has a substitutional character, i.e. it is formed by incorporation of Fe^{3+} ions at In^{3+} sites in the Ni_2InVO_6 matrix. The second method uses traditional calcination of a mixture of reagents containing V_2O_5, In_2O_3, Fe_2O_3 $2NiCO_3$ $\cdot 3Ni(OH)_2$ $\cdot 4H_2O$ in the 500°C to 1000°C temperature range. Samples were heated in several 24-hour stages and their phase composition was checked by using X-ray diffraction (XRD).

Electron Paramagnetic Resonance (EPR) study was conducted on solid solutions obtained by the calcination method. The Figure 1 shows normalized (to unit mass) EPR spectra of $Ni_2Fe_xIn_{1-x}VO_6$ registered at room temperature.

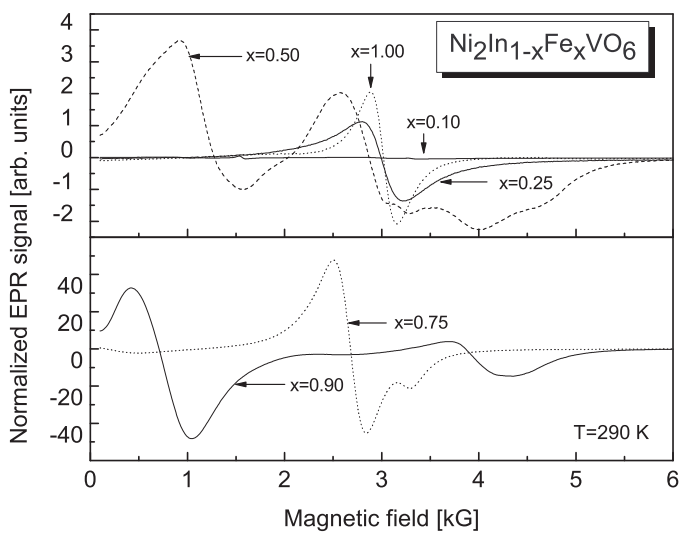

Figure 1: EPR spectra of $Ni_2Fe_xIn_{1-x}VO_6$.

The obtained spectra showed the presence of isolated high-spin Fe^{3+} ($S = 5/2$) centres for smaller concentrations of iron ions in $Ni_2In_{1-x}Fe_xVO_6$ (for $x = 0.10$ and 0.25) and enhancement of signal intensity derived from strongly coupled iron sublattices (at least two different sublattices).

Characterization of mechanical properties of (Pb,Bi)-(Si,Ge)-O oxide glasses

B. Bochentyn, J. Karczewski, M. Gazda, B. Kusz

Department of Solid State Physics, Faculty of Applied Physics and Mathematics
Gdansk University of Technology
Narutowicza 11/12, 80-233 Gdansk, Poland

Bismuth-silicate glasses are applied in low-loss fiber optic and IR-transmitting materials or as the active medium of Raman fiber optical amplifiers and oscillators [1]. They are also used in the production of electron multipliers due to their very high secondary emission coefficient and very high surface conductivity after the reduction in hydrogen [2]. It has been reported [3] that annealing in hydrogen reduces Bi^{3+} ions into neutral atoms which subsequently agglomerate into granules on the surface and inside glass. If the glass contains also lead oxide, a similar process of ionic lead reduction to neutral atoms takes place in hydrogen [4]. Then, these lead atoms subsequently agglomerate into granules on the lead-silicate glass surface and in its volume. It was observed that a thick layer was formed on the surface of oxide glass samples after reduction in hydrogen. According to the results of the EDX analysis this layer was depleted with oxygen related to the glass interior. Many homogenously distributed nano-size granules could be found on the surface of this layer. The nanoindentation investigations indicated that reduction in hydrogen prevented glass softening. Although the Young modulus of the surface layer formed after reduction was comparable to this parameter of the sample calcined in air, it was much smaller than the Young modulus of the glass interior. The aim of this work is to investigate the influence of reduction in hydrogen on the structural and mechanical properties of (Pb,Bi)-(Si,Ge)-O glass.

Acknowledgements
This work was partially supported by the National Science Center under grant No. NCN2012/05/B/ST3/02816.

References

[1] Witkowska A, Rybicki J, Di Cicco A 2005, *J. Alloys and Compounds* **401** 135
[2] Trzebiatowski K, Witkowska A, Murawski L 2000, *Mol. Phys. Rep.* **27** 115
[3] Kusz B, Trzebiatowski K, Gazda M, Murawski L 2003, *J. Non-Cryst. Solids* **328** 137
[4] Gackowska J, Gazda M, Trzebiatowski K, Kusz B 2006, *J. Non-Cryst. Solids* **352** 4242

An investigation of the effect of different solvents on the Poisson's ratio of open-cell polyurethane foam

J.-P. Brincat[1], A. Buttigieg[1], K. M. Azzopardi[1], J. N. Grima[1,2], R. Gatt[1]

[1] *Metamaterials Unit, Faculty of Science, University of Malta Msida MSD 2080, Malta*

[2] *Department of Chemistry, Faculty of Science, University of Malta Msida MSD 2080, Malta*

The aim of this work was to test the effect of different solvents on the Poisson's ratios in compression of cellular, open-cell foam. Subsequently, an attempt to understand which of the properties of the solvents are most important in bringing about the observed changes in the measured Poisson's ratios was made using multivariate statistical analysis (Principal Components Analysis). The ultimate goal was to understand how the physical and chemical characteristics of the solvents affect the foam, such that it would be possible in future to easily control, alter or tune the Poisson's ratios exhibited by the foam.

The different solvents were found to affect the different loading directions of the foam samples to different extents. It was also noted that the changes brought about by the solvents were not linear in time. Overall, the solvents which brought about the greatest decreases in Poisson's ratio were acetic acid and chloroform, and to a lesser extent cyclohexane and acetone. This indicates that the ideal solvent used should be a small molecule with an intermediate polarity and intermediate electron density. It solvent would also have a low LogP value, a low polarizability, and low steric indices. For commercial purposes, the solvent should also evaporate easily to enable fast drying of the foam and be non-toxic to life and non-hazardous to the environment.

On the thermal and compressibility properties of smart honeycombs with T-shaped joints and related systems

R. Cauchi[1], D. Attard[2], J. N. Grima[1,2]

[1] *Department of Chemistry, Faculty of Science, University of Malta Msida MSD2080, Malta*

[2] *Metamaterials Unit, Faculty of Science, University of Malta Msida MSD2080, Malta*

Most common materials usually have a positive value for thermal expansion, Poisson's ratio and compressibility; however it is not uncommon for some materials to exhibit negative values for these properties, often with added advantages in terms of applications [1–3]. In this work we elaborate further on a special case of the centro-symmetric honeycombs with T-shaped joints which has been shown to have the potential in exhibiting a non-zero, and even negative, Poisson's ratio [4]. These honeycombs have the potential to behave in a manner which results in curving of the initially straight horizontal ligaments upon uniaxial loading along their length. This property is somewhat unexpected but, may be employed in the design of novel honeycomb based systems with tuneable and also anomalous properties. Such a property arises due to uneven stretching of portions of the horizontal ligaments upon uniaxial horizontal loading as a result of the lack of compliance of the portion of surface where the vertical ligaments are attached. In this work we analyse variants of these systems, constructed from different materials to achieve a composite honeycomb system that can exhibit negative thermal expansion and/or compressibility depending on the choice of materials making up the different components of the honeycomb composite (see Figure 1).

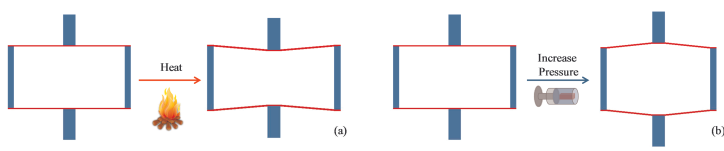

Figure 1: The proposed centro-symmetric honeycomb system, where the materials are arranged such that the one shaded in red exhibits the highest degree of deformation when subjected to an increase in (a) temperature or (b) pressure by having a higher (a) coefficient of thermal expansion or (b) compressibility respectively

Acknowledgements
This research is funded by a grant awarded to Reuben Cauchi through the Strategic Educational Pathways Scholarship (Malta). These scholarships are part-financed by

the European Union – European Social Fund (ESF) under Operational Programme II – Cohesion Policy 2007–2013, "Empowering People for More Jobs and a Better Quality of Life" and a grant from Malta Council for Science & Technology. This research has been carried out using computational facilities procured through the European Regional Development Fund, Project ERDF-080 'A Supercomputing Laboratory for the University of Malta' (http://www.um.edu.mt/research/scienceeng/erdf_080). The support of the Malta Council for Science and Technology is also gratefully acknowledged.

References

[1] R. S. Lakes and K. W. Wojciechowski 2008 *Physica Status Solidi B*, **245** 545
[2] W. Miller, C. W. Smith, D. S. Mackenzie and K. E. Evans 2009 *Journal of Materials Science*, **44** 5441
[3] A. Alderson 1999 *Chemistry and Industry* 384
[4] R. Cauchi, D. Attard, J. N. Grima 2013 *Phys. Status Solidi B* **250**, 2002

Thermo-mechanical properties of APC and APD aluminophosphates

R. Cauchi[1], D. Attard[1], J. Rybicki[2], Sz. Winczewski[2], R. Gatt[1], J. N. Grima[1,3]

[1] *Metamaterials Unit, Faculty of Science, University of Malta Msida MSD 2080, Malta*

[2] *Faculty of Applied Physics and Mathematics, Gdansk University of Technology Narutowicza 11/12, 80-233 Gdansk, Poland*

[3] *Department of Chemistry, Faculty of Science, University of Malta Msida MSD2080, Malta*

The Poisson's ratios, isothermal compressibilities and thermal expansion coefficients are quantities that describe the behaviour of a system when it is uniaxially loaded, hydrostatically compressed and subjected to temperature changes respectively. For many existing materials these properties assume a positive value. However, in some systems, one of these properties may assume negative values. A number of studies performed on zeolite systems have shown that these frameworks have the potential to exhibit such anomalous thermo-mechanical properties. In this work, the frameworks of two closely related aluminophosphates, APD and APC, are investigated through molecular dynamics simulations which suggest that these frameworks have the potential to exhibit negative thermo-mechanical properties, and that topotactical transformation of the frameworks have an effect on the properties such systems exhibit. It is also shown that the APC framework system is highly anisotropic and may indeed exhibit a combination of negative Poisson's ratios, negative compressibility as well as negative thermal expansion.

Acknowledgements
This research was funded by a grant awarded to Reuben Cauchi through the Strategic Educational Pathways Scholarship (Malta). These scholarships are part-financed by the European Union – European Social Fund (ESF) under Operational Programme II – Cohesion Policy 2007–2013, "Empowering People for More Jobs and a Better Quality of Life" and a grant from Malta Council for Science & Technology. This research was also supported in part by PL-Grid Infrastructure. The authors gratefully acknowledge the TASK Academic Computer Centre in Gdansk (CI TASK) for providing the computer time and the facilities. Equipment procured through the European Regional Development Fund, Project ERDF-080 'A Supercomputing Laboratory for the University of Malta' was also used. The support of the Malta Council for Science and Technology is also gratefully acknowledged.

Phase diagram of asymmetric multiblock copolymer melt

M. Dziecielski[1], P. Knychala[1,2], M. Banaszak[1]

[1] *Department of Physics, Adam Mickiewicz University Umultowska 85, 61-614 Poznan, Poland*

[2] *The President Stanislaw Wojciechowski Higher Vocational State School Lodzka 149-153, 62-800 Kalisz, Poland*

Block copolymers are a class of materials of practical importance [1] because of an intriguing ability to self-organize into a variety of spatially ordered nanostructures or nanophases. The phase diagram of asymmetric multiblockcopolymers SASAS-B is calculated using the self-consistent field theory [2] in spherical unit cells of various dimensionalities [3,4]. A simple model without long-range interactions was used to examine the self-assembly process in poly(styrenesulfonate)-b-poly(methyl butylene) block copolymer melts. The copolymer was modeled by a linear chain consisting of N segments of type A, S, and B, corresponding to styrene, sulfonated styrene, and methylbutylene, respectively. The experimentally defined Flory-Huggins interaction parameters are used to describe intermonomer interactions [5]. The results of experiments [6,7] and the Monte-Carlo simulations for the same multiblock copolymers are also presented.

Acknowledgements
Grant 2012/07/N/ST4/00293 of the Polish NCN is gratefully acknowledged. A significant part of the simulations was performed at the Poznan Supercomputing and Networking Center (PCSS).

References

[1] Hamley I W 2005 *Developments in Block Copolymer Science and Technology*, John Wiley and Sons, New York
[2] Matsen M W and Schick M 1994 *Phys. Rev. Lett.* **72** 2660
[3] Banaszak M, Koper A, Knychala P and Lewandowski K 2012 *Acta Physica Polonica A* **121** (3) 703
[4] Dziecielski M, Lewandowski K and Banaszak M 2011 *Computational Methods in Science and Technology* **17** 17
[5] Knychala P, Dziecielski M, Banaszak M and Balsara N P 2013 *Macromolecules* **46** 5724
[6] Park M J and Balsara N P 2008 *Macromolecules* **41** 3678
[7] Wang X, Yakovlev S, Beers K M, Park M J, Mullin S A, Downing K H and Balsara N P 2010 *Macromolecules* **43** 5306

Linear-scaling Hartree-Fock exchange and hybrid exchange-correlation functionals with plane-wave basis set accuracy

J. Dziedzic[1,2], C.-K. Skylaris[1]

[1] *School of Chemistry, University of Southampton*
Southampton, United Kingdom

[2] *Department of Solid State Physics, Faculty of Applied Physics and Mathematics*
Gdansk University of Technology
Narutowicza 11/12, 80-952 Gdansk, Poland

Local and semilocal functionals used in density functional theory (DFT) calculations have long been known to underestimate band gaps and to incorrectly describe the energetics of small molecules, among other deficiencies [1]. The hybrid functional approach, where Hartree-Fock exchange is included into the exchange-correlation functional offers a more accurate description of geometries and of several properties, such as bond energies and band gaps, particularly for metal oxides [2].

We present a resolution-of-identity-based approach [3] for evaluating the Hartree-Fock exchange energy and various hybrid exchange-correlation functionals with a computational cost that scales linearly with the number of atoms. We discuss the conditions that need to be satisfied to ensure the proposed technique is stable and accurate. We describe the implementation of this approach in the linear-scaling DFT code ONETEP [4], which can perform such calculations with near-complete basis set accuracy.

We validate the method against energies, forces and equilibrium bondlengths [2,5] computed with conventional, cubic-scaling DFT codes, demonstrating excellent agreement, even with approaches using an all-electron description and Gaussian basis sets. We show qualitative agreement between B3LYP calculations performed with our technique and the predictions [6] of DFT+U for the binding of O_2 and CO to a simplified model of myoglobin.

We conclude with a description of a hybrid (MPI+OpenMP) parallelisation strategy for the proposed implementation, which offers excellent scaling up to hundreds of CPU cores. Benchmarks for larger systems, demonstrating the linear-scaling of the computational time with the size of the system and strong scaling will also be presented.

Acknowledgements
J. D. acknowledges the support of the Engineering and Physical Sciences Research Council (EPSRC grant No. EP/J015059/1), of the Polish National Science Centre and the Ministry of Science and Higher Education (grants N N519 577838 and

IP2012 043972) and of the Human Capital Operational Programme (POKL04.03.00–00–238/12).

C.-K. S. would like to thank the Royal Society for a University Research Fellowship. We would like to thank the University of Southampton for the Iridis3 and Iridis4 supercomputers that were used in this work and to the TASK Academic Computer Centre for access to the Galera cluster.

References

[1] M. Marsman, J. Paier, A. Stroppa and G. Kresse 2008 *J. Phys. Cond. Matt.* **20**, 064201
[2] V. N. Staroverov, G. E. Scuseria, J. Tao and J. P. Perdew 2003 *J. Chem. Phys.* **23**, 12129
[3] J. Dziedzic, Q. Hill, C.-K. Skylaris 2013 *J. Chem. Phys.* **139**, 214103
[4] C. -K. Skylaris, P. D. Haynes, A. A. Mostofi and M. C. Payne 2005 *J. Chem. Phys.* **122**, 084119
[5] N. D. M. Hine, M. Robinson, P. D. Haynes, C.-K. Skylaris, M. C. Payne and A. A. Mostofi 2011 *Phys. Rev. B* **83**, 195102
[6] D. J. Cole, D. D. O'Regan and M.C. Payne 2012 *J. Phys. Chem. Lett.* **3**, 1448

Minimal-parameter implicit solvent model for large-scale DFT calculations

J. Dziedzic[1,2], C.-K. Skylaris[1]

[1] *School of Chemistry, University of Southampton Southampton, United Kingdom*

[2] *Department of Solid State Physics, Faculty of Applied Physics and Mathematics Gdansk University of Technology Narutowicza 11/12, 80-233 Gdansk, Poland*

Accurate studies of important biochemical processes, such as protein folding or protein-ligand binding, require that their solvent environment is taken into account in the computation [1]. Explicit inclusion of the solvent with full atomic detail proves to be computationally unfeasible, not only because it substantially increases the number of atoms in the system, but also because it necessitates extensive averaging over the solvent degrees of freedom. The implicit solvent (IS) approach introduces an unstructured continuum dielectric to represent the solvent, which seeks to address this difficulty. This averaging property makes IS the prime candidate for use within density functional theory (DFT) calculations on biological systems. Owing to the low directionality and low specificity of most of the solvent's effects, this simplified description is often sufficient to capture the relevant phenomena and provides solvation energies in good agreement with experiment.

A multitude of IS models of differing sophistication have been proposed to date (see [2] for a review). One of the approaches for determining the electrostatic component of solvation involves solving the nonhomogeneous Poisson equation (NPE) for a system where the solute is placed in a suitably defined cavity, with the dielectric placed outside of the cavity. The exact shape of the cavity usually depends on a number of parameters. The iso-density formulation of Fattebert and Gygi (FG) [3] instead defines the cavity naturally in terms of the electronic density, which eliminates the need to carefully tune the many cavity parameters present in most other models.

In this work [4,5] we present an implementation of NPE-based solvation models in the ONETEP [6] linear-scaling density functional theory program. ONETEP achieves CPU and memory requirements that increase linearly with the number of atoms by employing a density matrix formulation of DFT using localized functions (Non-orthogonal Generalized Wannier Functions or NGWFs) [7]. We employ the FG formulation and extend it by using consistent open boundary conditions, approximately including dispersion-repulsion interactions and reducing the computational overhead. In so doing, we obtain a fully self-consistent approach, where the electronic density is optimized in the presence of the implicit solvent. Solutions to the NPE are obtained using a high-order defect-corrected multigrid method [8] which we demonstrate is efficient and accurate. We show how the proposed approach consistently gives

predictions in excellent agreement with experiment on a test set of 100+ molecules and demonstrate how it can be used to obtain binding energies in solvent for entire proteins with thousands of atoms, while maintaining good parallel scalability.

Acknowledgements

J. D. acknowledges the support of the Engineering and Physical Sciences Research Council (EPSRC grant No. EP/J015059/1), of the Polish National Science Centre and the Ministry of Science and Higher Education (grants N N519 577838 and IP2012 043972)

C.-K.S. would like to thank the Royal Society for a University Research Fellowship. We would like to thank the University of Southampton for the Iridis3 and Iridis4 supercomputers that were used in this work and to the TASK Academic Computer Centre for access to the Galera cluster.

References

[1] N. A. Baker 2005 *Current Opinion in Structural Biology* **15**, 137
[2] J. Tomasi, B. Mennucci and R. Cammi 2005 *Chem. Rev.* **105**, 2999
[3] J.-L. Fattebert and F. Gygi 2003 *Int. J. Quantum Chem.* **93**, 139
[4] J. Dziedzic, H. Helal, C.-K. Skylaris, A. A. Mostofi and M. C. Payne 2011 *Europhys. Lett.* **95** 43001
[5] J. Dziedzic, S. J. Fox, T. Fox, C. S. Tauterman and C.-K. Skylaris 2013 *Int. J. Quantum Chem.* **113** 771
[6] C.-K. Skylaris, P. D. Haynes, A. A. Mostofi and M. C. Payne 2005 *J. Chem. Phys.* **122**, 084119
[7] C.-K. Skylaris, A. A. Mostofi, P. D. Haynes, O. Dieguez and M. Payne 2002 *Phys. Rev. B* **66**, 035119
[8] S. Schaffer 1984 *Math. of Comp.* **43**, 89–115

Lucifer Yellow fluorescence spectrum effected by external electric and magnetic fields

T. P. Firoozabadi[1], A. Izadi[2]

[1] *Department of Physics, Varamin-Pishva Branch, Islamic Azad University Varamin, Iran*

[2] *Department of Physics, K. N. Toosi University of Technology Tehran, Iran*

The fluorescent dye Lucifer Yellow (LY) has been extremely useful in studying the cell structure and communications for labeling cells in biological studies, specifically in electroporation and magnetopermeablization studies. The changes of external field-induced-LY fluorescence spectrum have been investigated in a different range of magnetic and electric fields. Electric fields, applied by the ECT-SBDC electric system, in the range of 10–150 V/cm with the frequency range of 1–6 kHz, based on the low voltage electroporation protocol, caused the quenching effects in our steady state studies. Furthermore the changes of the magnetic field-induced-LY fluorescence spectrum were investigated in the range of 0.6–3.2 Tesla strength, which were applied by the TMS magnetic system. Three different numbers of pulses (28, 56, and 112) and different frequencies (0.25, 1, and 10 Hz) were chosen based on the magnetopermeablization protocol. Our results showed an enhancement in the intensity of the spectra. In addition, the effects of electric and magnetic fields being simultaneously induced were examined. Experiments showed that the magnitude of the electric-field-induced quenching became smaller in the presence of the magnetic field. The results of our research indicate that using Lucifer Yellow as an accepted candidate marker in electroporation and magnetopermeabilization is highly questionable. In fact the validity of previous permeability studies based on the LY spectrum changes becomes unreliable in the presence of external electric and magnetic fields.

An investigation on the Poisson's ratios of ceramic type frameworks

D. Gambin[1], J. N. Grima[1,2], R. Gatt[1]

[1] *Metamaterials Unit, Faculty of Science, University of Malta Msida MSD 2080, Malta*

[2] *Department of Chemistry, Faculty of Science, University of Malta Msida MSD 2080, Malta*

Auxetic materials are materials which exhibit the anomalous behaviour of getting fatter rather than thinner when stretched i.e. they exhibit a negative Poisson's ratio. This anomalous behaviour has been reported in various material classes, including metals, nano- and micro-structured polymers and inorganic non-metallic solids i.e. ceramics. In this study, the Poisson's ratio of six SiO_2 equivalents of the frameworks of the previously unstudied ceramics AEN, BOF, cordierite, danburite, caesium aluminium titanate and gallium phosphate were investigated though force-field based simulations. Energy expressions for these systems were constructed using COMPASS, CVFF, BKS and Burchart force-fields, where it was shown that the best representation, in terms of similarity between the simulated crystalline structure and that obtained experimentally, is given by the COMPASS and CVFF force-fields with worst results being given by the BKS force-field which gave an inadequate representation of these systems.

Of the six ceramic frameworks studied, three where shown to have the potential of exhibiting a negative Poisson's ratio, namely danburite, BOF and gallium phosphate. In particular it was shown that the SiO_2 equivalent framework of danburite exhibits auxetic behaviour in all the three major planes with maximum auxeticity being exhibited for loading at 45° off-axis, in the case of the SiO_2 equivalent framework of BOF maximum auxetic behaviour was exhibited in the (001) plane for loading on-axis, whilst in the case of the SiO_2 equivalent of the $GaPO_4$ framework, auxetic behaviour was exhibited in the (010) and (100) planes with its maximum value exhibited for loading at 45° off-axis.

On the mechanical properties of the SiO_2 framework of gallium phosphate

D. Gambin[1], J. N. Grima[1,2], R. Gatt[1]

[1] *Metamaterials Unit, Faculty of Science, University of Malta Msida MSD 2080, Malta*

[2] *Department of Chemistry, Faculty of Science, University of Malta Msida MSD 2080, Malta*

Auxetic materials are materials which exhibit the anomalous behaviour of getting fatter rather than thinner when stretched i.e. they exhibit a negative Poisson's ratio. Several material classes have been studied for their potential to exhibit auxetic behaviour, particularly ceramic materials such as α-cristobalite and β-cristobalite, NAT, THO and EDI. In view of this, the work carried out in this studied aimed to enhance the corpus of knowledge available on ceramic species. In particular the SiO_2 equivalent framework of $GaPO_4$ was studied for its potential to exhibit auxetic behaviour through force-field based simulations.

The results obtained suggest that this species exhibits auxetic behaviour in the (010) and (100) planes with its maximum value exhibited for loading at 45° off-axis. Furthermore, a study on the deformation mechanism of the SiO_2 equivalent of the $GaPO_4$ framework has shown that the auxetic behaviour can be explained via a combined tetrahedral model where rotation and deformation of the tetrahedra occur concurrently. This is very significant as it further confirms that relative rotation of semi-rigid units, in this case semi-rigid tetrahedra, is an important mechanism for the generation of auxetic behaviour.

An investigation into the different heat conversion methods of conventional foam into auxetic foam

R. Gatt[1], A. Buttigieg[1], J.-P. Brincat[1], K. M. Azzopardi[1], J. N. Grima[1,2]

[1] *Metamaterials Unit, Faculty of Science, University of Malta Msida MSD 2080, Malta*

[2] *Department of Chemistry, Faculty of Science, University of Malta Msida MSD 2080, Malta*

The thermal activity in the production of auxetic foam through the method proposed by Lakes will be investigated in an attempt to understand the process better. The same analysis will then be carried out for a novel method based on heated air flow. These two methods will then be compared in order to determine which production process heats the sample most efficiently and uniformly.

Auxetic foam samples will then be produced using both methods and then mechanically tested in order to determine their Poisson's ratio and Young's modulus with the aim of investigating whether the new heated air flow method is more effective than the old convection heating method. The results of these tests show that air-flow heating, including stretching of the foam sample between two intervals of intense heat, is a superior method to the conventional convection heating method for converting regular foams into auxetic foams. The foams produced using air-flow heating are more auxetic, and the time required for the conversion process is less. The main reason for this is that air-flow heating, while reducing the difference in temperature between the exterior and interior segments of the foam cuboid greatly, also heats the foam more quickly, thus increasing the exposure time of the interior part of the foam to the desired temperature with respect to conventional heating. Furthermore, it has been shown that scaling up of the size of the foam sample being treated should not increase the Poisson's ratio or time required to complete the treatment significantly, as long as the air-flow is kept high enough. This is an important consideration for the eventual industrial conversion of conventional to auxetic foam. Air-flow heating would not only be faster when scaled up, but it would also produce a higher quality product for a reduced cost, especially if the heated air is recycled into the system once passed through the foam.

Characterization and environmental application of polypropylene coated nano-TiO_2 in wastewater depuration

R. Giovannetti, C. A. D'Amato, E. Rommozzi, M. Zannotti, M. Minicucci, R. Gunnella

School of Environmental Science, Chemistry Division, University of Camerino
Via S. Agostino 1, 62032 Camerino (MC), Italy

Ground water contamination causes degradation of water quality and is likely to be the primary contact of humans with toxic chemicals. Organic dyes, originating from different sources such as textile, paper and pulp, pharmaceutical industries, tannery, etc, undesirable in water even in very small amounts, can affect the integrity of ecosystems [1]. Residual dyes from these sources are considered as a wide variety of organic pollutants introduced into the natural water resources that represent an environmental hazard. The discharge of dyes into water environment is disagreeable, not only by reason of their color, but also due to the fact that many released dyes and their breakdown products are toxic, carcinogenic or mutagenic to life forms [2]. In addition, only partial degradation of dyes is possible since they are intentionally chosen to be resistant to light and aerobic oxidation by microorganisms [3].

Alizarin Red S (sodium salt of 1,2-dihydroxyanthraquinone-3-sulfoacid, ARS) represents a durable dye because it cannot be completely degraded by general chemical, physical and biological processes. In recent years a great progress has been observed in the field of photocatalytic studies [4] and heterogeneous photocatalysis has gained attention as a promising technique that can be used as an alternative or as complementation to conventional wastewater treatment using UV or visible light. The most used photocatalyst is TiO_2 and its applications show advantages such as chemical and biological resistance, low price, non-toxicity, expensive recycling and recovery [5].

In this study Polypropylene-coated nano-TiO_2 photocatalysts (PP@TiO_2) were successfully prepared. The optimization of TiO_2 pastes preparation using two commercial TiO_2 (Degussa P-25 and Anatase) was performed and a green, low-cost dip-coating procedure was developed. The study was conducted in four steps. In the first step, Electron Diffraction, Scanning Electron Microscopy and Atomic Force Microscopy were used in order to obtain crystallographic and morphological information of TiO_2 on the support material. In the second step, ARS was spectrophotometrically characterized at different pH conditions showing that at acid pH, dyes favorably bound on the TiO_2 surface through the sulfo group. In the third step, equilibrium and kinetic data of ARS adsorption process were obtained showing a difference in the absorption capacity, isotherm model and kinetic constants between two types of TiO_2. Finally, in the fourth step, adsorption/photodegradation processes of ARS were studied simultaneously and as a separated process under the action of visible light,

obtaining kinetic data for the two types of TiO_2. According to all the obtained results a kinetic model for the adsorption/photodegradation process was proposed confirming that the use of PP@TiO_2 in the visible light photodegradation of ARS permitted to efficiently obtain dye degradation, suggesting application for environmental treatment of wastewaters.

Acknowledgements
We gratefully acknowledge the support of co-organizers and all our sponsors.

References

[1] Guillard C, Lachheb H, Houas A, Ksibi M, Elalou E, Herrmann J 2003 *Journal of Photochemistry and Photobiology* **158** 27
[2] Teh C M, Mohamed A R, Herrmann J 2011 *Journal of Alloys and Compounds* **509** 1648
[3] Kant R 2012 *Natural Science* **4** 22
[4] Czecha B, Pasieczna-Patkowska S, Wójcik G 2013 *Journal of Photochemistry and Photobiology* **260** 14
[5] Bhatkhande D S, Pangarkar V G, Beenackers A C M 2001 *Journal of Chemical Technology and Biotechnology* **77** 102

Porphyrin funtionalized multiwall carbon nanotubes and their interaction with TiO_2 nanoparticle surface

R. Giovannetti, M. Zannotti, C. A. D'Amato,
E. Rommozzi, S. Ferraro

School of Environmental Science, Chemistry Division, University of Camerino
Via S. Agostino 1, 62032 Camerino (MC), Italy

Porphyrins are light-absorbing chromophores that play a central role in photosynthesis. They are particularly interesting as photosensitizers for the Dye Sensitized Solar Cell (DSSC) for the absorption in the 400–450 nm region of the Soret band and in the 500–700 nm region of Q-bands and also for the appropriate LUMO and HOMO energy levels; this makes them promising candidates as substitutes for ruthenium dyes in DSSC applications [1].

In the last decade carbon nanotubes (CNTs) have been one of the most studied nanomaterials in nanoscience and nanotechnology for their excellent electronic and mechanical properties with extraordinary thermal and electrical conductivity. The external wall of CNTs can interact with aromatic molecules, such as porphyrin, pyrene and their derivatives by means of unreadible stacking interactions [2]. A variety of spectroscopic studies performed in a solution indicate [3,4] that there occurs a photoinduced electron transfer (PET) from porphyrin to carbon-based species.

Cu(II) and Zn(II) complexes of Coproporphyrin-I (2,7,12,17-tetrapropionic acid of 3,8,13,18-tetramethyl-21H,23H porphyrin or CPI) were synthesized in our laboratory and tested as sensitizers in DSSC [5]. In this study we report the UV-vis and fluorescence investigations of the interaction of multi wall CNTs (MWCNTs) with CPI, ZnCPI and CuCPI (MCPIs) in ethanolic solutions and the equilibrium and kinetic aspects in the sensitization of monolayer transparent TiO_2 thin films.

The obtained results demonstrate that CPI and CPI metal complexes presented noncovalently interaction with MWCNTs and their functionalization permits efficient adsorption on a TiO_2 monolayer. MWCNT-(CPI-dyes) concentrations and adsorption times affected the adsorption on TiO_2 surfaces. The equilibrium and kinetic data obtained permitted to establish the best experimental conditions according to the Langmuir and pseudo first-order kinetic models.

After chemisorptions of MWCNT-(CPI-dyes), the TiO_2 monolayer was characterized with Scanning Electron Microscopy (SEM). The obtained results suggest their potential application in DSSC.

Acknowledgements
We gratefully acknowledge the support of co-organizers and all our sponsors.

References

[1] Panda M K, Ladomenou K, Coutsolelos A G 2012 *Coord. Chem. Revs* **256** (21) 2601
[2] Zaho Y-L, Stoddart J F 2009 *Acc. Chem. Res.* **42** 1161

[3] Baskaran D, Mays J W, Zhang X P, Bratcher M S 2005 *J. Am. Chem. Soc.* **127** 6916
[4] Luo C, Guld D M, Imahori H, Tamaki K, Sakata K 2000 *J. Am. Chem. Soc.* **122** 6525
[5] Alibabaei L, Wang M, Giovannetti R, Teuscher J, Moser J-E, Compte P, Pucciarelli F, Zakeeruddin S M, Graetzel M 2010 *En. Env. Sci.* **3** 956

Auxetic Polyphenylacetylene Nanosheets and Nanotubes

J. N. Grima[1,2], J. Xuereb[1], R. Cauchi[1]

[1] *Department of Chemistry, Faculty of Science, University of Malta Msida MSD2080, Malta*

[2] *Metamaterials Unit, Faculty of Science, University of Malta Msida MSD2080, Malta*

Auxetic materials, materials with a negative Poisson's ratio, undergo lateral expansion when stretched as well as lateral compression when compressed. Polyphenylacetylene networks, are made from acetyl chains connected together through tetra substituted phenyl rings to form a structure that can be described in terms of the rotating triangles model. This study examines various forms of these polyphenylacetylene systems designed such that their geometry resembles the rotating triangles model studied by Grima *et al.* [1,2].

In this work we have used static molecular simulations to simulate single layer systems of these sheets in an attempt to estimate the structural and mechanical properties of the graphene equivalent of these systems. It was found that the Poisson's ratio compared well with the crystalline counterparts, reaching values of -1. Furthermore, nanotubes made from a polyphenylacetylene network were also modelled as so as to estimate the properties of the carbon-nanotube equivalent of these systems. The Poisson's ratios for small tensile deformations were estimated using PCFF and COMPASS force-field based simulations and it was found that auxeticity is also conserved in these systems, again reaching high auxetic values of -1.

Acknowledgements

This research is funded by a grant awarded to Reuben Cauchi through the Strategic Educational Pathways Scholarship (Malta). These scholarships are part-financed by the European Union – European Social Fund (ESF) under Operational Programme II – Cohesion Policy 2007–2013, "Empowering People for More Jobs and a Better Quality of Life" and a grant from Malta Council for Science & Technology. This research has been carried out using computational facilities procured through the European Regional Development Fund, Project ERDF-080 'A Supercomputing Laboratory for the University of Malta' (http://www.um.edu.mt/research/scienceeng/erdf_080). The support of the Malta Council for Science and Technology is also gratefully acknowledged.

References

[1] Grima J N, Evans K E 2000 *Chem. Comm.* **16**, 1531

[2] Grima J N, Attard D, Cassar R N, Farrugia L, Trapani L, Gatt R 2008 *Molec. Sim.*, **34**, 1149

Structural characterisation of borate glasses with high manganese content

T. Lewandowski, L. Wicikowski

Department of Solid State Physics, Gdansk University of Technology
Narutowicza 11/12, 80-233 Gdansk, Poland

MnO addition to borate glass has influence on the structure and thermal properties of the modified material. It has been proven that manganese oxide has a negative effect on the thermal stability of the manganese-borate glass in the considered compositional range. Some influence of the addition of this oxide was noticed in the results of FT-IR measurements that showed a modification in band intensities, peak positions and areas. It was concluded that gradual addition of MnO was causing a decrease in the number of tri- and pentaborate groups. On the other hand, an increase in the number of diborate groups was noticed. In addition the number of orthoborate groups decreased. Peak positions varied in function of the manganese oxide amount. These peak shifts could be due to bond length modifications upon MnO addition and due to the influence of Mn atoms on their strength.

References

[1] Ramesh Babu A. et al. 2012 *J. Non-Cryst. Solids* **358** 1391
[2] Winterstein-Beckman A. et al. 2013 *J. Non-Cryst. Solids* **376** 165
[3] Hruby A. 1972 *Physica B* **22** 1187

Surface nanostructration by diblock copolymers

F. F. Lupi[3], N. De Leo[1], G. Aprile[1], M. Laus[2], K. Sparnacci[2], D. Antonioli[2], G. Seguini[3], M. Perego[3], L. Boarino[1]

[1] *NanoFacility Piemonte, Electromagnetism Division*
Istituto Nazionale di Ricerca Metrologica
Strada delle Cacce 91, 10135 Torino, Italy

[2] *Dipartimento di Scienze dell'Ambiente e della Vita*
Università del Piemonte Orientale Amedeo Avogadro
Viale Teresa Michel 11, 15121 Alessandria, Italy

[3] *Laboratorio MDM, IMM-CNR*
Via C. Olivetti 2, 20864 Agrate Brianza, Italy

In recent years an increasing interest has been devoted by the scientific and industrial community to self-assembly processes at the nanoscale. Polymer spherical nano-particles, where repulsive forces generate typically hexagonal structures [1], as well as block copolymer thin films, in which the incompatible block components segregate into a wide range of microphases, have been demonstrated to be a viable solution for the fabrication of nanostructured templates below 50 nm in size. The International Technology Roadmap of Semiconductors [http://www.itrs.net] indicates directed self-assembly based on diblock copolymers (BCP) as a consistent low cost alternative to immersion extreme UV lithography for the 32 nanometer node and for large area nanostructuration. Coupling diblock copolymer self-assembly with dry etching, it is possible to propagate the ordered microphase to any large area substrates, in particular silicon and silicon dioxide (Figures 1, 2). The perfect control of the morphology of block copolymer (BCP) thin films deposited on pre-patterned surfaces is another mandatory step in view of their application in nanoelectronics [2]. At this purpose, we analyze the morphological evolution as a function of the annealing time of BCP films (forming both lamellar and cylindrical features), when confined inside periodic topographical structures. The width of these structures ranges from 90 to 240 nm. Very fast annealing rates at a high temperature and short annealing times were employed. Remarkable slowing down of the direct self-assembly (DSA) process of the BCPs arranged inside the trenches, with respect to the same process performed on a flat surface, was observed. In addition, a different degree of organization as a function of annealing time was observed (Figure 3). These results point out the influence of the boundary conditions, including the lateral confinement and matching of the trench size with the BCP periodicity, on the kinetic of the DSA process [3]. Reactive Ion Etching (RIE) is a straightforward technique industrially compatible, and preliminary results of cylinders and lamellas propagation will be shown in the framework of this work, as a part of a wider European Metrology Project devoted to the realization of probe microscopy standards (EMRP s17 CRYSTAL).

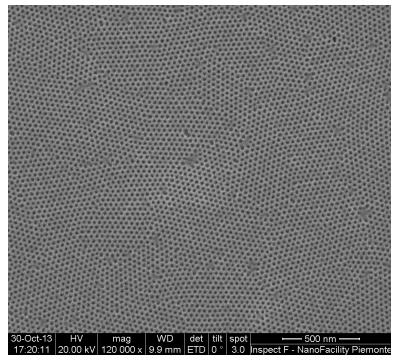

Figure 1: Diblock copolymer mask (PS-b-PMMA) after PMMA removal. The vertical cylinders are around 17 nm

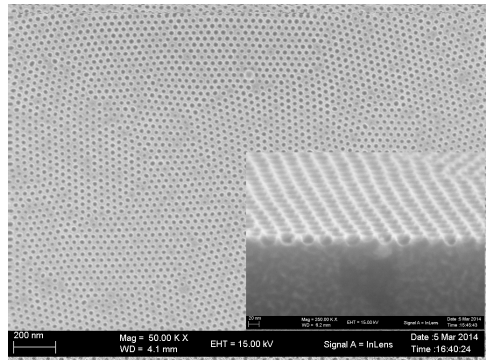

Figure 2: BC mask and propagated cylindrical morphology onto silicon substrate after SF_6 RIE

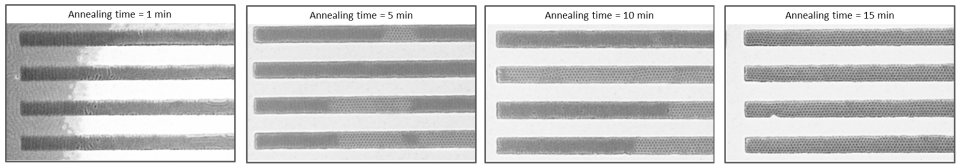

Figure 3: Temporal evolution of morphology in cylinder forming PS-b-PMMA film

References

[1] E. Giani, K. Sparnacci, M. Laus, G. Palamone, V. Kapeliouchko, V. Arcella 2003 *Macromol.* **36**, 4360

[2] The International Technology Roadmap for Semiconductors (ITRS) 2011

[3] F. Ferrarese Lupi, T. J. Giammaria, G. Seguini, M. Laus, E. Enrico, N. De Leo, L. Boarino, C. K. Ober, M. Perego 2014 *J. Mater. Chem. C* **2**, 2175; doi: 10.1039/C3TC32283A

An analysis of the mechanical properties of perforated sheets

L. Mizzi[1], K. M. Azzopardi[1], D. Attard[1], J. N. Grima[1,2], R. Gatt[1]

[1] *Metamaterials Unit, Faculty of Science, University of Malta Msida MSD 2080, Malta*

[2] *Department of Chemistry, Faculty of Science, University of Malta Msida MSD 2080, Malta*

It is widely known that the introduction of perforations into a system can have a significant effect on its mechanical properties, including a change from a positive to a negative Poisson's ratio. In this study the effect of a class of perforation patterns, namely diamond (or rhombic)-shaped perforations, on the mechanical properties of a planar 2D material were investigated using the Finite Element Method and experimental models. It was found that simply by altering the parameters and orientation relative to each other of the diamond perforations one could obtain a vast spectrum of Poisson's ratios, ranging from positive Poisson's ratios to extremely negative ones. From the results obtained, it was found that altering the tilt of the diamond shaped perforation has a significant effect on the Poisson's ratio, On the other hand, the effect of the separation between perforations was less significant. It should also be noted that structures are not isotropic and the Poisson's ratios are highly direction dependent. This is due to the fact that the resultant system deforms in a mechanism similar to the rotating parallelograms mechanism, a deformation mechanism which is known to exhibit the potential for auxetic behaviour.

Following an evaluation of the results obtained, the most promising structures with regards to a negative Poisson's ratio were constructed as models for experimental testing. The structures were built using Artidee® Formalate Latex Molding Emulsion, which was poured into a mold based on the Finite Element model and built using a Makerbot Replicator 3D Printer. The Latex models were then stretched using a Testometric Tensile tester distributed by Messphysik® Materials and the Poisson's ratio was recorded using a Video Extensiometer. The experimental results obtained showed agreement with the simulation data.

Acknowledgements
This work is part of the Project R&I-2012-061 financed by the Malta Council for Science and Technology through the National Research and Innovation Programme 2012.

X-ray diffraction studies of structural relaxation in $Fe_{75}Mo_5Si_6B_{14}$ amorphous alloy

S. Mudry, Yu. Kulyk, S. Zhovneruk

Physics of Metals Department, Ivan Franko National University of Lviv
Kyrylo and Mephodii 8, 79005 Lviv, Ukraine

Interest in materials fabricated under conditions which are far from equilibrium has been increasing due to their unique properties. These properties can be improved by various methods among which the thermal treatment is most widely used. Transition from the metastable thermodynamic state of an alloy to a more stable one which is known as a relaxation process is accompanied by variation of the atomic arrangement. Such a change of the structure in turn is the reason for changes in the physical and chemical properties. A rearrangement of atoms and atomic groups (clusters) is related to the topologic and chemical ordering and suggests its high sensitivity to temperature and other thermodynamic parameters. In the last years many interesting results have been obtained by means of electroresistance measurements, Mössbauer spectroscopy, acoustic emission and DSC methods. Unfortunately, the data on X-ray diffraction studies and small angle X-ray scattering are scarce.

We studied the relaxation process in the $Fe_{75}Mo_5Si_6B_{14}$ amorphous alloy by means of the X-ray diffraction method. Scattered intensities were analyzed for amorphous alloys, annealed at different temperatures and used for calculation of pair correlation functions. Most attention at the interpretation of these functions was paid to second maxima, consisting of two subsidiary peaks. The analytical expressions were chosen to fit these two maxima for different annealing temperatures. It follows from the obtained results that the relaxation process is accompanied by a decrease in the cluster size and formation of a more stable amorphous structure. Certainly the cluster size reduction can be related to changes in properties allowing the relaxation process to be controlled and an advanced amorphous and nanocrystalline materials to be produced as a result.

Structure and thermal expansion of liquid bismuth

S. Mudry, I. Shtablavyi, U. Liudkevych

Physics of Metals Department, Ivan Franko National University of Lviv
Kyrylo and Mephodii 8, 79005 Lviv, Ukraine

The thermal behavior of liquid metals over a wide temperature range was studied by experimental methods. Most of them were obtained by means of dilatometers and density measurements. Unfortunately the relation between the variation of the most probable interatomic distance r_1 and the number of neighbors N with the thermal expansion coefficient still remains unclear. It was particularly interesting to study the thermal behavior of melts suggesting their cluster structure. We attempted also to compare the thermal behavior of equilibrium and superheated liquids.

The aim of this work was to study the thermal properties of liquid bismuth by analysis of structure parameters obtained using the X-ray diffraction method. The structure of this metal was well studied resulting in the temperature dependences of structure factors (SF) and pair correlation functions (PCF), from which the main structure parameters were derived. Unfortunately, the current understanding of the anomalous change of structure parameters of this metal upon melting and further heating is not fully clear. Such behavior occurs because the melting process in liquid Bi is accompanied by a significant atomic rearrangement. A similar feature is observed also in other semimetals (Sn, Ga, Sb), which as well as Bi, reveal shoulders on right hand sides of structure factors.

The structure studies were carried out at different temperatures above the melting point and at a superheated range. Main structure parameters r_1, N were obtained for few temperature points that allowed us to obtain the temperature dependences of these parameters. PCF were used also to calculate the mean interatomic distances $\langle r_1 \rangle$, and the size of the first coordination sphere r_{1min}.

The temperature dependences of these parameters showed negative thermal expansion in a wide temperature range above the equilibrium melting temperature as well as at temperatures corresponding to supercooled state. It is important that such behavior is observed within the first coordination shell that may be related with transformation of the cluster structure of the melt with temperature.

Production and structural features of $Al(Al_{0.85}Zn_{0.15})$-$CoFe_2O_4$ composites prepared by stir-casting technique

S. Mudry[1], I. Shtablavyi[1], M. Lytvyn[1], T. Talako[2]

[1] *Physycs of Metals Department, Ivan Franko National University of Lviv Kyrylo and Mephodii 8, 79005 Lviv, Ukraine*

[2] *Laboratory of New Materials and Technologies State Scientific Institution "Powder Metallurgy Institute" Platonov 41, 220005 Minsk, Belarus*

Improvement of the existing and development of new materials is currently one of the priorities of modern materials science. Particularly noteworthy are materials that combine different or, in some cases, opposite properties. Such materials include paramagnetic matrix composites with ferromagnetic fillers. By changing the contents of the paramagnetic and ferromagnetic phases we can control the magnetic properties of the composite as a whole.

For that reason the structure changes upon mixingof $CoFe_2O_4$ particles with Al were investigated in this work.

Composites were prepared by the stir-casting method, followed by heat treatment at different temperatures and duration. The phase analysis was performed on the X-ray diffraction data collected on an STOE STADI P automatic diffractometer ($CuK_{\alpha 1}$ radiation, $\lambda = 1.5406$ Å, in the angular range $6 \leq 2\Theta \leq 100°$ with scan step 0.015° and scan time 250 s).

Our investigations revealed that no chemical interaction between the matrix and the filler as well as reduced iron or cobalt was found in the composite, which may appear as a result of reducing the magnetite by aluminum. Increasing the magnetite content in the composite led to inhibition of diffusion processes resulting in an increase in the zinc content in the Al(Zn) solution. As a result, the microhardness of the investigated composites increased.

Acknowledgements
This work was supported by a grant from the Fundamental Researches State Fund of Ukraine (No 0113U002789).

Partially auxetic behavior in static systems of soft binary dimers

J. W. Narojczyk, K. W. Wojciechowski, M. Kowalik

Institute of Molecular Physics Polish Academy of Sciences
Smoluchowskiego 17, 60-179 Poznan, Poland

This work presents the results of basic research, on the influence of the atomic size polydispersity on elastic properties and Poisson's ratio [1] of cubic systems of di-atomic molecules (dimers). Particles are arranged such, that the positions of their centres of mass and their orientations are random, but the constituting atoms form a perfect (or slightly disrupted) f.c.c. lattice. Such a phase is called the *Degenerate Crystalline* (DC) phase [2]. Size polydispersity was imposed on all atoms in the model system, by assigning diameters generated according to binary distribution. The distribution implies that there are only two possible diameter values: $\sigma \pm \delta$, where σ is the reduced unit of length and δ is the standard deviation (further referenced as the polydispersion parameter). Figure 1 shows an example of a vast set of possible realizations of the binary DC phase. Short-ranged interactions are assumed and restricted only to atoms sharing a side of the Voronoi polyhedron. Particles interact with soft, repulsive n-inverse-power potential. Studies were performed by computer simulations in the NVT ensemble, with additional assumption that the temperature is equal to zero ($T = 0$ K).

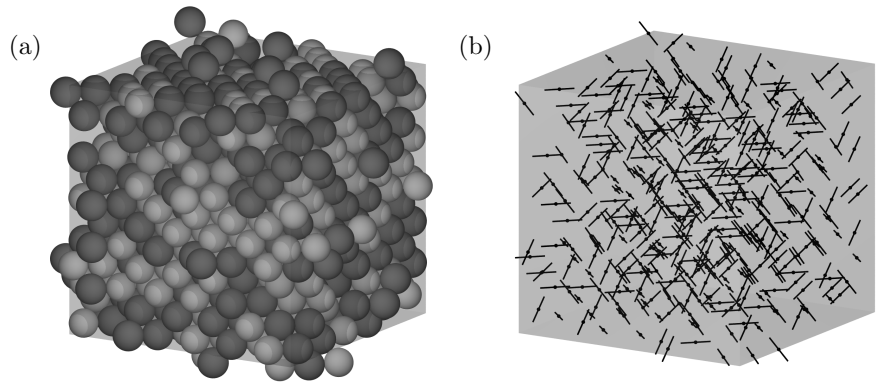

Figure 1: Example of microscopic structure of binary DC dimer system. The structure shown consists of 432 dimers and has the polydispersity parameter δ equal to 3%. In (a) the atoms are drawn in two colors, indicating their size. The darker color indicates the larger atomic diameter. The gray cube indicates the periodic box. In (b) dimer center positions and orientations for the structure in (a) are represented by points and line segments connecting the atomic centers

Poisson's ratio is the negative ratio of the relative change in the transverse dimension to the relative change in the longitudinal dimension when infinitesimal change of the longitudinal strain is applied [1]. In the case of anisotropic materials, the Poisson's ratio ($\nu_{\alpha\beta}$) may depend on both the longitudinal (α) and transversal (β) direction. It is known, that in general, the disorder of crystalline lattice leads to the increase of average Poisson's ratio, both in the case of isotropic [3–6] and anisotropic [7–9] systems. However, in the case of cubic systems a direction exists ($\beta = [1\bar{1}0]$) for which, atomic size dispersion has an opposite effect, when the sample is deformed in $\alpha = [110]$. In this case it has been found, that increasing polydispersity parameter leads to a *decrease* in the Poisson's ratio [8,9], even down to *negative* values. For unconstrained, binary and polydisperse cubic system (f.c.c. spheres), the decrease was insignificant [8], and negligible in the limit of hard interactions. Negative Poisson's ratio was observed for the range of soft interactions. For f.c.c. dimers, increasing polydispersity significantly decreases the value of $\nu_{[110][1\bar{1}0]}$ in the range of hard interactions [9] in the polydisperse dimer system. However, the practical application of the model studied in [9] may be difficult, thus two binary models were proposed in this work.

The comparison of the elastic properties and Poisson's ratio for all dimer models was done. It has been found that all binary models exhibit similar *partial auxetic* properties. The most negative value observed was $\nu_{[110][1\bar{1}0]} = -0.81$. Thus, the binary models can be of interest from the practical applications perspective, as they seem to be easier to manufacture, compared to polydisperse models.

Acknowledgements
Part of the simulations was performed at Poznań Supercomputing and Networking Center (PCSS)

References

[1] L. D. Landau and E. M. Lifshitz 1986 *Theory of Elasticity*, Pergamon Press, London
[2] K. W. Wojciechowski 1991 Degenerate crystalline phase in a two-dimensional system of hard dimers, *Modern Physics Letters B*, **5** 1843
[3] K. W. Wojciechowski and J. Narojczyk 2006 Influence of disorder on the Poisson's ratio of static solids in two dimensions, *Reviews on Advanced Materials Science*, **12** 120
[4] J. W. Narojczyk and K. W. Wojciechowski 2006 Computer simulation of the Poisson's ratio of soft polydisperse discs at zero temperature, *Materials Science (Poland)*, **24** 921
[5] J. W. Narojczyk and K. W. Wojciechowski 2006 Elastic properties of two-dimensional soft discs of various diameters at zero temperature, *Journal of Non-Crystalline Solids*, **352** 4292
[6] J. W. Narojczyk and K. W. Wojciechowski 2008 Elasticity of periodic and aperiodic structures of polydisperse dimers in two dimensions at zero temperature, *Physica Status Solidi (b)*, **245** 2463
[7] J. W. Narojczyk, A. Alderson, A. R. Imre, F. Scarpa, and K. W. Wojciechowski 2008 Negative Poisson's ratio behavior in the planar model of asymmetric trimers at zero temperature, *Journal of Non-Crystalline Solids*, **354** 4242
[8] J. W. Narojczyk and K. W. Wojciechowski 2008 Elastic properties of the fcc crystals of soft spheres with size dispersion at zero temperature, *Physica Status Solidi (b)*, **245** 606
[9] J. W. Narojczyk and K. W. Wojciechowski 2010 Elastic properties of degenerate f.c.c. crystal of polydisperse soft dimers at zero temperature, *Journal of Non-Crystalline Solids*, **356** 2026

Surprising behaviour of the temperature in shock waves

P. M. Pigłowski, K. W. Wojciechowski

Institute of Molecular Physics, Polish Academy of Sciences
Smoluchowskiego 17, 60-179 Poznan, Poland

Temperature profiles at fronts of shock waves were determined by using Non-Equilibrium Molecular Dynamics (NEMD) simulations. Various microscopic definitions of the temperature were tested and compared. Interesting results at the fronts of the shock waves were observed.

1. In strong shock waves the temperature is no more a scalar, but becomes a second-rank tensor. This means, e.g., that the kinetic energy is not equally distributed over different degrees of freedom.

2. The temperature changes non-monotonically along its profile.

3. In contrast to the situation at equilibrium, various definitions of the temperature are not equivalent near the front of the shock wave.

Vanadium oxide nanostructures prepared by sol-gel method

M. Prześniak-Welenc, M. Łapiński, B. Kościelska, W. Sadowski

Department of Solid State Physics, Faculty of Applied Physics and Mathematics
Gdansk University of Technology
Narutowicza 11/12, 80-952 Gdansk, Poland

Introduction

For the last decade one dimensional (1D) nanostructures have been intensively studied due to their remarkable physical and chemical properties which may predispose them to potential applications in highly functional devices [1]. Vanadium oxides, owing to their fascinating physical and chemical properties, seem to be particularly interesting. These properties consist in various metal oxidation states (from +II to +V) and different V-O coordination geometries what makes them suitable for many commercial applications in optical, electrical, electrochemical and thermochromic devices [2–6].

In the present work, we focused on the synthesis and characterization of different vanadium oxides using the sol-gel method.

Experimental

The starting solution was prepared by mixing a vanadium (V) oxytripropoxide in anhydrous ethyl alcohol as the solvent and in acetic acid. The sol transformed via gel into xerogel powder by drying at 50°C for 48 h. Next, the precursor powder was pressed into a disk-shaped pellet 12 mm in diameter. Different atmospheres and calcination temperatures were used to obtain different vanadium oxides. V_2O_5 was achieved by calcining the pellet at 650°C for 10 h under air atmosphere. The pellet was thermally treated at 1000°C under nitrogen atmosphere to obtain VO_2 and V_2O_3 composites.

The crystal structure of the samples was identified by the powder X-Ray diffraction method (XRD) with the Philips X'Pert diffractometer system using the CuKα radiation in the range of 10°–80° of 2θ. The surface morphology of the samples was studied with a scanning electron microscope (SEM) using FEI Company Quanta FEG 250. The thermal gravimetric analysis was performed under synthetic air and nitrogen using Netzsch STA 449 F1.

Results and Conclusion

The XRD results (not presented here) show that high purity of V_2O_5 products was obtained under air atmosphere while a mixture of VO_2 and V_2O_3 crystallized under nitrogen atmosphere. The SEM image of the sample calcined under air atmosphere is presented in Figure 1. A densely packed rod-like nanostructure was obtained. The SEM images of the pellet calcined under nitrogen atmosphere are presented in Figure 2. A core-shell structure was obtained after calcination (Figure 2 a). One of

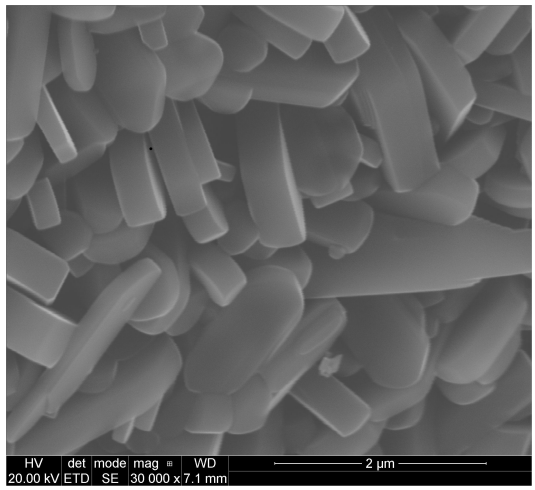

Figure 1: SEM image of V_2O_5 nanorods

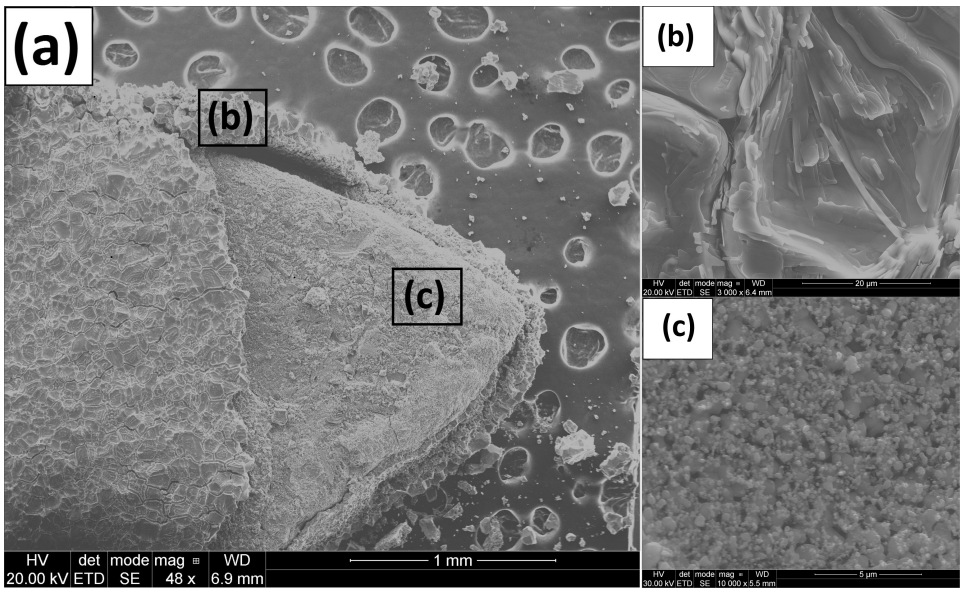

Figure 2: SEM images of the pellet after calcination under nitrogen atmosphere, (a) core-shell structure of mixtures VO_2 and V_2O_3, (b) shell structure and (c) core structure

the most significant properties of vanadium oxides is that compounds can be characterized by different colors. The principal vanadium oxides are V_2O_5, VO_2, V_2O_3 and VO. Orthorhombic vanadium pentoxide (V_2O_5) is orange-red and it is the most stable of the vanadium oxides. The dark blue VO_2 oxide has a rutile-like structure distorted by the presence of pairs of vanadium atoms bonded together. Black V_2O_3

has a corundum structure. The grey-colored VO or V_2O_2 has somewhat metallic behavior and possesses a defect rock-salt structure [7]. On the basis of the sample color it was deduced that VO_2 accumulated mostly in the shell (dark blue color), while V_2O_3 was present in the core (black color). The shell consists of fused rod-like nanocrystals (Figure 2 b), while the core is composed of nanospherical crystals (Figure 2 c).

In summary, we can obtain different vanadium oxides of different nanostructures from one powder precursor by varying atmospheres and calcination temperatures.

References

[1] Da Silva D, Viegas A C, Acuna J and Pasa A 2012 *Mater Lett* **68** (1) 267
[2] Cui J, Da D, and Jiang A 2012 *Appl Surf Sc* **133** (3) 225
[3] Chen S, Ma H, Wang S, Schen N, Xiao J, Zhou H, Zhao X, Li Y and Yi X 2006 *Thin Solid Films* **497** (1–2) 267
[4] Kaid M A 2006 *Egypt J Solids* **29** (2) 273
[5] Chab S H S, W T Y, Juan J H and Teh C Y 2011 *J Chem Technol Biotechnol* **86** (9) 1130
[6] Ozer N 1997 *Thin Solid Films* **305** (1–2) 80
[7] Weckhuysen B M and Keller D E 2003 *Catal Today* **73** (3–4) 80

Layer-thinning transitions in freely suspended smectic films in water – the mean field approach

I. Śliwa[1], A. V. Zakharov[2]

[1] *Institute of Molecular Physics, Polish Academy of Sciences*
Smoluchowskiego 17, 60-179 Poznan, Poland

[2] *Saint Petersburg Institute for Machine Sciences, Russian Academy of Sciences*
Saint Petersburg 199178, Russia

Understanding how surface boundaries influence the structural and thermodynamic properties of liquid crystals (LCs), both with relatively weak and strong surface anchoring interactions, has relevance for several different areas of applied chemistry, physics, and material science. Using the extended McMillan's mean field approach with anisotropic forces we have carried out a numerical study of both the structural and thermodynamic properties of free-standing smectic film (FSSF) in water under heating to the isotropic temperature. By solving the self-consistent nonlinear equations for the order parameters, we observed that the smectic-A-isotropic (AI) transition occurs through the series of layer-thinning transitions causing the films to thin in the stepwise manner as the temperature is increased above the bulk smectic-A-isotropic temperature T_{AI}(bulk). With enhanced pair interactions in the bounding layers, the smectic-isotropic transition corresponds to smectic melting of the central layers. This is in accord with the well established scenario of melting in such quasi-two-dimensional systems, where the melting originates in the interior of the smectic film and penetrates towards the surface. The layer-thinning transition has been modeled as the successive melting and subsequent removal of the interior layers of the films as the films temperature is increased in the range $T > T_{\mathrm{AI}}$(bulk). The effects of surface "enhanced" pair interactions in the bounding layers and of film thickness on the orientational and translational order parameters, the Helmholtz free energy and entropy of FSSFs have also been investigated. Reasonable agreement between the theoretically predicted and the experimentally obtained – by means of optical microscopy and ellipsometry techniques – data of the temperature when the thin decylcyanobiphenyl (10CB) smectic film immersing in water ruptures has been obtained.

Optical and electronic properties of ssDNA self assembly monolayers on gold

I. Solano[1], P. Parisse[2], O. Cavalleri[1], M. Castronovo[3], L. Casalis[2], M. Canepa[1]

[1] *Department of Physics, University of Genoa*
Via Dodecaneso 33,16146 Genova, Italy

[2] *Sincrotrone Trieste SCpA*
I-34149 Trieste, Italy

[3] *University of Udine, Dept Biol & Med Sci*
I-33100 Udine, Italy

The development of label-free biosensors for medical diagnostics based on detection of single strand DNA (ssDNA) hybridization prompts an in-deep investigation of the optical and electronic properties of self-assembled single and double strand DNA (dsDNA) layers.

Here we present a work in progress investigation devoted to detect the hybridization of gold-immobilized thiolated ssDNA (22 base pair) SAMs with their complementary strands. Single stranded DNA SAMs on gold were characterized from the optical point of view by using Spectroscopic Ellipsometry (SE). The evolution of the thickness and the optical properties of the sample during SAM deposition were characterized through in-situ (buffer) and ex-situ SE (245–1700 nm) whereas transmission and absorbtion spectra (193–1100 nm) were determined from a diluted ssDNA buffer solution.

Differential SE data analysis of highly compact ssDNA SAMs allowed us to clearly distinguish the optical spectral features related to the DNA molecules: in particular a strong DNA absorption in the UV range (260–270 nm) could be clearly observed in both in-situ and ex-situ data. An optical model was developed in order to describe the ssDNA SAM properties: properly chosen oscillators in the UV range were used in order to specifically describe the optical absorption of the four different DNA bases (Adenine (A), Thymine (T), Guanine (G) and Cytosine (C)).

Further data analysis is in progress to address the ssDNA/gold interfacial properties with particular attention paid to the SAM density and the S-Au bond.

We also present preliminary results on the adsorption of Yeast Cytochrome c (YCC) on ssDNA SAMs. YCC is a heme protein presenting strong Soret bands in the UV-VIS region. Using differential SE analysis [1,2] we are able to point out the aspecific submonolayer adsorption of YCC on ssDNA.

References

[1] M. Prato et al. 2008 *Phys. Chem. C* **112** 3899
[2] C. Toccafondi et al. 2011 *J. Colloid Interf. Sci* **364** 125

Influence of preparation method on microstructure and dielectric properties of strontium-borate glasses containing bismuth vanadate

N. A. Szreder, J. Karczewski, M. Gazda, R. J. Barczyński

Department of Solid State Physics, Faculty of Applied Physics and Mathematics
Gdansk University of Technology
Narutowicza 11/12, 80-233 Gdansk, Poland

The $Bi_2VO_{5.5}$ ceramic is ferroelectric below 725K and exhibits high ionic conductivity which is attributed to the presence of oxide ion vacancies [1–4]. The vanadium oxide is a transition metal oxide which in a glass structure may play a role of both the glass former and the glass network modifier. Glasses containing large amounts of transition metal oxides exhibit electronic conductivity usually described by the mechanism of polaron hopping [5–8]. Strontium tetraborate glass, SrB_4O_7 has good dielectric, thermal and optical properties, hence, it may be an ideal host matrix for dispersing crystallites. It has a relatively low melting point and can easily be prepared by the traditional melting method [1–4].

Two sets of glass samples with the same stoichiometric chemical composition were prepared from different reagents. The first group of samples were prepared from pre-prepared strontium-borate glass and bismuth and vanadium oxides. In the second group, oxides were replaced by pre-prepared $Bi_2VO_{5.5}$ ceramic, synthesised via a conventional solid state reaction route.

The topography, microstructure and electrical properties were studied. The topography was observed with the use of the XRD, EDS, SEM, AFM, and confocal microscopy methods. The obtained results showed that both sets of samples were amorphous regardless of the used reagents (Figure 1). However, microscopy pictures (Figures 2 a, b) confirmed that replacement of [Bi_2O_3, $0.5V_2O_5$] on $Bi_2VO_{5.5}$ had significant influence on the glass microstructure. It can be seen that only glasses prepared with $Bi_2VO_{5.5}$ (Figure 2 b) exhibit a specific nanostructure which is not visible in the XRD spectrum (Figure 1). A subset of samples were crystallized to obtain glass-ceramics. The XRD measurements (Figure 1) determined the presence of crystalline phases in heat-treated samples which mainly consisted of bismuth vanadate $Bi_2VO_{5.5}$. It is showed that a change of [Bi_2O_3, $0.5V_2O_5$] on $Bi_2VO_{5.5}$ increases the amount and intensity of the observed maxima.

The a.c. complex conductivity was investigated as a function of temperature and frequency. The influence of the change of glass compounds on the electrical properties of glasses is discussed. The effect of the crystallization process on the dielectric behavior is analyzed. The obtained results confirmed that $50SrB_4O_7$-$50(Bi_2O_3$-$0.5V_2O_5)$ glasses and glass-ceramics did not show any ferroelectric behavior, contrary

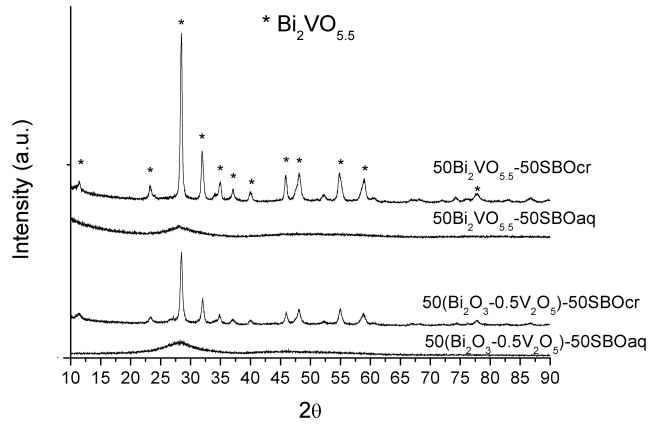

Figure 1: XRD spectrum

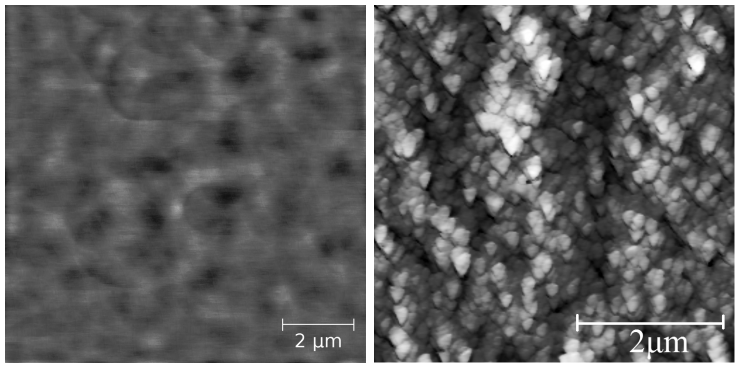

Figure 2: Microscopic pictures

to the $50SrB_4O_7$-$50Bi_2VO_{5.5}$ samples. We suspect that in the first group of samples, some part of vanadium and bismuth ions do not form a crystalline phase after heat-treatment but are still incorporated in the glass network. Therefore, the sizes of crystallites are too small to exhibit any ferroelectric properties.

References

[1] Prasad N. Syam, Varma K. B. R., Lang Sidney B. 2001 *J. Phys. Chem. Solids* **62** 1299
[2] Shankar M. V., Varma K. B. R. 1997 *J. Non-Cryst. Solids* **226** 145
[3] Varma K. B. R., Shankar M. V., Subbanna G. N. 1996 *Mater. Research Bulletin* **31** 475
[4] Kumari N., Krupanidhi S. B., Varma K. B. R. 2007 *Mater. Scie. Engineer.* **B 138** 22
[5] Murawski L., Chung C. H., Mackenzie J. D. 1979 *J. Non-Cryst. Solids* **32** 91
[6] Murawski L., Chung C. H., Mackenzie J. D. 1979 *Revue de Chimie Minerale* **16** 308
[7] Murawski L. 1982 *J. Mater. Scie.* **17** 2155
[8] Mott N. F. 1968 *J. Non-Cryst. Solids* **1** 1

Elastic constants by the minimum image neighbors

K. V. Tretiakov, K. W. Wojciechowski

Institute of Molecular Physics, Polish Academy of Sciences
Smoluchowskiego 17/19, 60-179 Poznan, Poland

A simple and efficient approach for determining the elastic properties of solids is proposed. The approach, using the minimum image method (MIM)[1], is tested on a model system of particles interacting by the Lennard-Jones (LJ) potential [2]. The elastic constants of this model are computed in the thermodynamic limit (both in the NVT and NPT ensembles [3,4]) using the standard MC simulations and using the MC simulation with the MIM. The simulation results show that in the case of the elastic constants, the contribution of long-range interactions cannot be ignored. In addition, the simulations reveal that by including interactions of each particle with all its minimum image neighbors leads to results which are very close to the values of elastic constants in the thermodynamic limit [5] even in case of small systems. This enables one for a quick and accurate estimation of the elastic constants using very small samples. It should be also noticed that to achieve the same relative error of the elastic constants using the MC simulation with MIM, shorter times of calculation are required than using the standard MC scheme [5].

Acknowledgements

This work was supported by the grant DEC-2012/05/B/ST3/03255 of the Polish National Science Center. Part of the calculations was performed at the Poznań Supercomputing and Networking Center (PCSS).

References

[1] A. C. Ladd 1977 *Mol. Phys.* **33** 1039; A. C. Ladd 1978 *Mol. Phys.* **36** 463
[2] J.-P. Hansen, I. R. McDonald 2006 *Theory of Simple Liquids*, Amsterdam
[3] D. R. Squire, A. C. Holt, W. G. Hoover 1968 *Physica* **42** 388
[4] M. Parrinello, A. Rahman 1982 *J. Chem. Phys.* **76** 2662
[5] K. V. Tretiakov, K. W. Wojciechowski *Comput. Phys. Commun.* (submitted)

FMR study of samples obtained by nitriding and nitride reduction of nanocrystalline iron

J. Typek[1], N. Guskos[1,2], G. Zolnierkiewicz[1], A. Guskos[1], A. Kielbasa[3], W. Arabczyk[3]

[1] *Institute of Physics, West Pomeranian University of Technology Al. Piastow 48, 70-311 Szczecin, Poland*

[2] *Department of Solid State, Faculty of Physics, University of Athens Panepistimiopolis, 15 784, Athens, Greece*

[3] *Institute of Inorganic Chemical Technology and Environmental Engineering West Pomeranian University of Technology Pulaskiego 10, 70-322 Szczecin, Poland*

Samples obtained by nitriding of promoted nanocrystalline iron and nitride reduction at various nitriding potentials in terms of thermodynamic parameters were investigated by the ferromagnetic resonance (FMR) technique at room temperature. Experimental FMR spectra were fitted by the Callen-type lineshape resonance lines arising from the presence of different Fe-N phases. The obtained FMR parameters allowed identifying the component phases and determining their magnetic properties. In general, the proposed simple method of decomposition of the FMR spectra produces results concerning the phases content of the investigated samples that are consistent with XRD measurements and additionally provides magnetic characteristics of the studied nanomagnets.

Magnetic study of $ZnFe_2O_3$ nanopowder in different diamagnetic matrices

K. Wardal[1], J. Typek[1], G. Zolnierkiewicz[1], N. Guskos[1,2], U. Narkiewicz[3], E. Piesowicz[4]

[1] *Institute of Physics, West Pomeranian University of Technology Al. Piastow 48, 70-311 Szczecin, Poland*

[2] *Solid State Physics, Department of Physics, University of Athens Panepistimiopolis, 15 784 Zografos, Athens, Greece*

[3] *Institute of Chemical and Environment Engineering West Pomeranian University of Technology K. Pulaskiego 10, 70-322 Szczecin, Poland*

[4] *Institute of Material Engineering, West Pomeranian University of Technology Al. Piastow 19, 70-310 Szczecin, Poland*

Nanopowders $0.7(Fe_2O_3)/0.3(ZnO)$ obtained by the traditional wet chemistry method followed by a calcination process in concentrated form and embedded at a concentration of 0.1 wt.% in a PEN-b-PTMO polymer were studied by dc magnetization and ferromagnetic resonance (FMR) measurements. One magnetic phase only in all the investigated samples was observed: $ZnFe_2O_3$.

Magnetic resonance measurements were performed on a conventional X-band ($\nu =$ 9.4 GHz) Bruker E 500 spectrometer with 100 kHz magnetic filed modulation. The temperature measurements of FMR spectra were performed in the temperature range of 4–290 K using an Oxford helium-flow cryostat (Figs. 1 a and c). Magnetic measurements in the temperature range of 293–443 K were performed on a Radiopan SE/X 2544-M spectrometer (Figs. 1 b and c). The FMR spectra were dominated by a single, intense, broad and asymmetrical line. The apparent amplitude of the line decreased with the temperature from 260 K for pure nanopowder (Fig. 1 a) and from 240 K for nanopowder in the polymer (Fig. 1 c).

The line shifts towards lower magnetic fields with the decreasing temperature and the linewidth increases with the temperature decrease. Below 200 K these changes are larger for the polymer sample than for concentrated $ZnFe_2O_3$ (Fig. 2).

The resonance field starts to decrease with the temperature decrease from 350 K for concentrated nanopowder, but for the polymer sample it is constant down to 220 K. It decreases significantly with the temperature decreasing below 70 K for both types of samples (Figure 3). Smaller interparticle exchange and greater importance of magnetic anisotropy might be the reason for the constant resonance field in the polymer sample in the high temperature range. It might be taken as a proof of good dispersion of nanopowder in the polymer. Smaller magnetic susceptibility for the polymer sample is obsereved from the temperature dependence of integrated intensity which could be

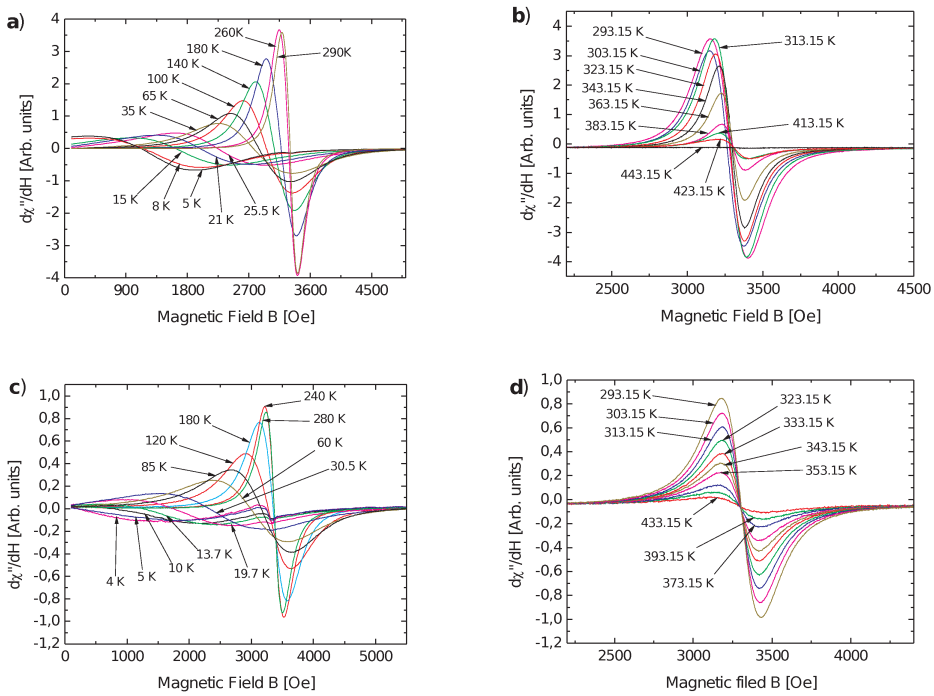

Figure 1: FMR spectra of concentrated $ZnFe_2O_3$ (a,b) and dispersed in polymer (c,d) recorded at different temperatures

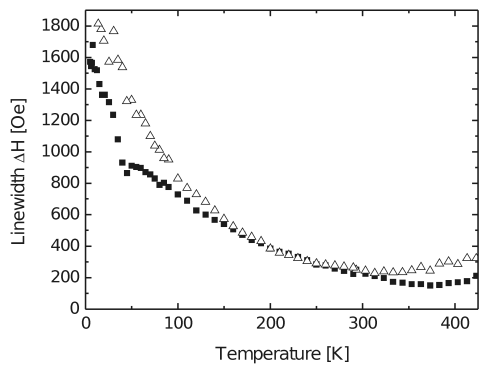

Figure 2: Temperature dependence of apparent linewidth of $ZnFe_2O_3$ in concentrated form (squares) and dispersed in polymer (triangles)

explained by smaller dipole-dipole interaction. The integrated intensity maximum is almost the same for both sample types and it is about 50 K. It could be interpreted as the FMR blocking temperature.

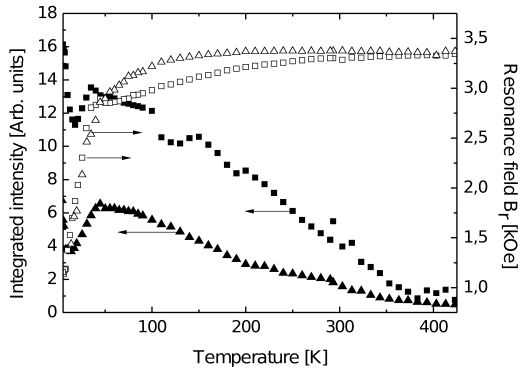

Figure 3: Temperature dependence of apparent resonance filed of concentrated $ZnFe_2O_3$ (squares) and dispersed in polymer (triangles) (left axis) and integrated intensity (right axis)

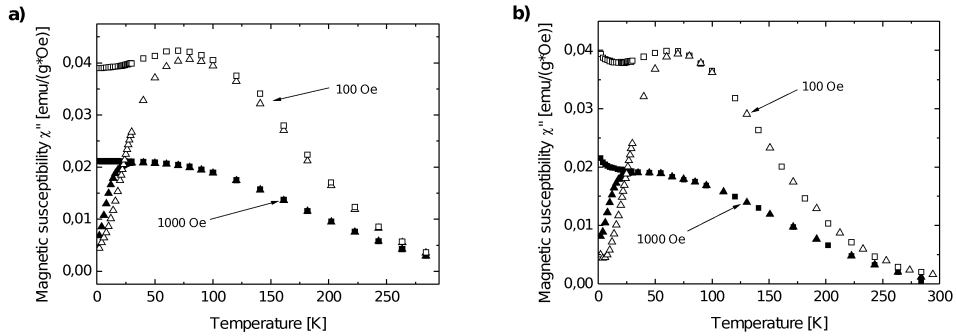

Figure 4: Magnetic susceptibility of concentrated $ZnFe_2O_3$ (a) and dispersed in polymer (b) measured in two different magnetic fields (100 Oe and 1000 Oe)

The results of dc magnetization show typical superparamagnetic behavior in high temperatures with the blocking temperature of about 46 K for concentrated $ZnFe_2O_3$ (Fig. 4 a) and 49 K for $ZnFe_2O_3$ dispersed in the polymer (Fig. 4 b).

INDEX OF AUTHORS